

11176-H508-RO-00

N7024300



TRW NOTE NO. 70-FMT-819

PROJECT APOLLO  
TASK MSC/TRW A-50

---

APOLLO MISSION 11, TRAJECTORY  
RECONSTRUCTION AND POSTFLIGHT ANALYSIS  
VOLUME 1

---

16 MARCH 1970

N 7 0 - 2 4 3 0 0		(ACCESSION NUMBER)	(THRU)
FACILITY FORM 603	137	(PAGES)	/
	1	(CODE)	
NASA CR 108 349		(NASA CR OR TMX OR AD NUMBER)	31
		(CATEGORY)	

Prepared for  
MISSION PLANNING AND ANALYSIS DIVISION  
NATIONAL AERONAUTICS AND SPACE ADMINISTRATION  
MANNED SPACECRAFT CENTER  
HOUSTON, TEXAS  
NAS 9-8166

TRW NOTE NO. 70-FMT-819

PROJECT APOLLO  
TASK MSC/TRW A-50

---

APOLLO MISSION 11, TRAJECTORY  
RECONSTRUCTION AND POSTFLIGHT ANALYSIS  
VOLUME 1

---

16 MARCH 1970

Prepared for  
MISSION PLANNING AND ANALYSIS DIVISION  
NATIONAL AERONAUTICS AND SPACE ADMINISTRATION  
MANNED SPACECRAFT CENTER  
NAS 9-8166

Approved by W. P. Girod

W. P. Girod, Manager  
MSC/TRW Task A-50

Approved by

J. E. Alexander  
J. E. Alexander, Manager  
Guidance and Control  
Systems Department

Approved by

H. L. Moore  
H. L. Moore, Manager  
MSC/TRW Task A-50

Approved by

D. G. Saile  
D. G. Saile, Assistant  
Project Manager  
Guidance and Performance  
Mission Trajectory Control Program

Approved by

R. K. Petersburg  
R. K. Petersburg, Manager  
Systems Evaluation  
Department

Approved by

T. R. Parten  
R. P. Parten, Chief  
Mission Planning Support  
Office  
NASA Manned Spacecraft  
Center

## FOREWORD

This report is submitted to the NASA Manned Spacecraft Center in accordance with MSC/TRW Task A-50 Contract NAS 9-8166. This report contains the postflight analysis performed in conjunction with the Apollo 11 mission and is issued as supplement one to the Apollo 11 Mission Report (NASA/MSC Report MSC-00171, Nov. 1969).

The report is issued in two volumes. Volume I contains details of the analysis and results obtained, including appendixes. Volume II contains a listing of the 45-day best estimated trajectory (BET) for the Apollo 11 mission in the NASA Apollo Trajectory (NAT) format. The listing is not generally distributed but is available from NASA/MSC upon request. Requests should be made to:

NASA/MSC Computations and Analysis Division  
Central Metric Data File  
Code ED-5, Building 12, Room 133  
Houston, Texas 77058

**Page Intentionally Left Blank**

## TABLE OF CONTENTS

	<u>Page</u>
7.1 INTRODUCTION AND SUMMARY	7-1
7.1.1 Apollo 11 Mission	7-1
7.1.2 Postflight Analysis	7-1
7.2 ORBIT ANALYSIS	7-7
7.2.1 Methods of Reconstruction	7-7
7.2.2 CSM Best Estimate of Trajectory	7-8
7.2.3 LM Best Estimate of Trajectory	7-9
7.2.3.1 Descent Phase Trajectories	7-9
7.2.3.2 Rendezvous Trajectories	7-10
7.3 ONBOARD TRACKING DATA ANALYSIS	7-15
7.3.1 Introduction	7-15
7.3.2 Onboard Measurements	7-16
7.3.3 Evaluation of Onboard Tracking Data	7-16
7.4 LANDING RADAR DATA ANALYSIS	7-63
7.4.1 Descent Trajectories	7-63
7.4.2 Landing Radar Velocity Residuals	7-65
7.4.3 Lunar Surface Altitude Along Groundtrack	7-75
REFERENCES	R-1
APPENDIX A	A-1
APPENDIX B	B-1
APPENDIX C	C-1
APPENDIX D	D-1

**Page Intentionally Left Blank**

## LIST OF TABLES

	<u>Page</u>
7.1 Apollo 11 Sequence of Events	7-3
7.2 Descent and Rendezvous Maneuver Summary for Apollo 11	7-4
7.3 Matchpoint Comparisons of Trajectories Produced with the R2 and L1 Lunar Potential Models	7-12
7.4 Apollo Mission 11 BET Summary	7-14
7.5 Summary of Rendezvous Radar Residual Statistics	7-18
7.6 Rendezvous Radar Only Solution Residual Statistics	7-28
7.7 Summary of VHF Ranging Residual Statistics	7-33
7.8 Summary of Sextant Residual Statistics	7-39
7.9 Comparison of Rendezvous Radar Noise Estimates with Specification Requirements	7-61
7.10 Comparison of VHF Ranging and Sextant Noise Estimates with Specification Requirements	7-61
7.11 LM Landing Site Coordinates	7-67
7.12 Landing Radar Velocity Residual Statistics	7-68

**Page Intentionally Left Blank**

## LIST OF ILLUSTRATIONS

	<u>Page</u>
7-1a Relative Motion of the LM for Apollo 11 Descent - DOI to Landing (CSM Centered)	7-5
7-1b Relative Motion of the LM for Apollo 11 Rendezvous - Ascent to Docking (CSM Centered)	7-6
7-2 Tracking Data (Onboard and Ground Based) Timeline for Apollo 11 Descent and Rendezvous	7-13
7-3a Rendezvous Radar Angle Residual Statistics	7-19
7-3b Rendezvous Radar Range and Range Rate Residual Statistics	7-20
7-4 Rendezvous Radar Residuals (Insertion to CSI)	7-21
7-5 Rendezvous Radar Residuals (CSI to CDH)	7-23
7-6 Rendezvous Radar Residuals (CDH to TPI)	7-25
7-7 Rendezvous Radar Shaft Noise as a Function of Average Range	7-30
7-8 Rendezvous Radar Trunnion Noise as a Function of Average Range	7-31
7-9 Rendezvous Radar Range Noise as a Function of Average Range	7-32
7-10 VHF Ranging Residuals (DOI to PDI)	7-34
7-11 VHF Ranging Residuals (CSI to CDH)	7-35
7-12 VHF Ranging Residuals (CDH to TPI)	7-36
7-13 VHF Ranging Noise as a Function of Average Range	7-37
7-14 VHF Ranging Residual Statistics	7-38
7-15 Sextant Residuals (DOI to PDI)	7-41
7-16 Sextant Residuals (Insertion to CSI)	7-42
7-17 Sextant Residuals (CSI to CDH)	7-43
7-18 Sextant Residuals (CDH to TPI)	7-44
7-19 Sextant Angular Random Noise as a Function of Average Range	7-45
7-20 Sextant Residual Statistics	7-46
7-21 Out-of-Plane Component of LM Position Relative to CSM (DOI to PDI)	7-47
7-22 Differences Between Position Components of Relative Trajectories (DOI to PDI)	7-48

## LIST OF TABLES

	<u>Page</u>
7.1 Apollo 11 Sequence of Events	7-3
7.2 Descent and Rendezvous Maneuver Summary for Apollo 11	7-4
7.3 Matchpoint Comparisons of Trajectories Produced with the R2 and L1 Lunar Potential Models	7-12
7.4 Apollo Mission 11 BET Summary	7-14
7.5 Summary of Rendezvous Radar Residual Statistics	7-18
7.6 Rendezvous Radar Only Solution Residual Statistics	7-28
7.7 Summary of VHF Ranging Residual Statistics	7-33
7.8 Summary of Sextant Residual Statistics	7-39
7.9 Comparison of Rendezvous Radar Noise Estimates with Specification Requirements	7-61
7.10 Comparison of VHF Ranging and Sextant Noise Estimates with Specification Requirements	7-61
7.11 LM Landing Site Coordinates	7-67
7.12 Landing Radar Velocity Residual Statistics	7-68

LIST OF ILLUSTRATIONS  
(Cont)

	<u>Page</u>
7-23 Differences Between Velocity Components of Relative Trajectories (DOI to PDI)	7-49
7-24 Differences Between Position Components of Relative Trajectories (Insertion to CSI)	7-51
7-25 Differences Between Velocity Components of Relative Trajectories (Insertion to CSI)	7-52
7-26 Out-of-Plane Component of LM Position Relative to CSM (Insertion to CSI)	7-53
7-27 Out-of-Plane Component of LM Position Relative to CSM (CSI to TPF)	7-54
7-28 Differences Between Position Components of Relative Trajectories (CSI to TPF)	7-55
7-29 Differences Between Velocity Components of Relative Trajectories (CSI to TPF)	7-58
7-30 LM Landing Site Coordinates	7-66
7-31 Landing Radar X-Antenna Velocity Residuals (BET #3)	7-69
7-32 Landing Radar Y-Antenna Velocity Residuals (BET #3)	7-70
7-33 Landing Radar Z-Antenna Velocity Residuals (BET #3)	7-71
7-34 Landing Radar X-Antenna Velocity Residuals (Onboard/MSFN H-S)	7-72
7-35 Landing Radar Y-Antenna Velocity Residuals (Onboard/MSFN H-S)	7-73
7-36 Landing Radar Z-Antenna Velocity Residuals (Onboard/MSFN H-S)	7-74
7-37 Surface Altitude Along Ground Track	7-77
7-38.1	7-79
7-38.2 } Groundtrack of LR Range Beam Piercepoint	7-81
7-38.3 }	7-83
7-39 Altitude of LM During LR Range Sampling	7-85

## 7.0 APOLLO MISSION 11 TRAJECTORY RECONSTRUCTION AND POSTFLIGHT ANALYSIS

### 7.1 INTRODUCTION AND SUMMARY

#### 7.1.1 Apollo 11 Mission

The Apollo 11 mission was launched from the Kennedy Space Center at 13:32:00 (hrs:min:sec) Greenwich Mean Time on 16 July 1969. Apollo 11 was the third manned lunar mission and the first to attempt and accomplish a landing on the lunar surface. A summary of the major events is presented in Table 7.1.

The descent phase of the mission was initiated during the thirteenth revolution of the moon at approximately  $100^{\text{h}}\ 07^{\text{m}}$  Ground Elapsed Time (GET). The lunar module (LM) successfully landed on the lunar surface at approximately  $102^{\text{h}}45^{\text{m}}$  GET.

The rendezvous phase began with ascent ignition during the 25<sup>th</sup> CSM revolution and ended with docking at  $128^{\text{h}}03^{\text{m}}$  GET. A summary of the CSM and LM maneuvers performed during descent and rendezvous is presented in Table 7.2 and a graphical representation of these phases of the mission which depicts the motion of the LM relative to the CSM is shown in Figures 7-1a and 7-1b.

#### 7.1.2 Postflight Analysis

The objective of the postflight analysis task was, in general, to generate trajectory parameters and data for the command and service modules (CSM) and LM from S-IVB/CSM separation to the end of mission. As in the Apollo missions 9 and 10, a preliminary trajectory was generated from the best available RTCC vectors. The bulk of the postflight analysis effort was then concentrated on reconstruction of the two periods of flight from LM/CSM undocking to LM touchdown (descent phase) and from LM ascent to LM/CSM docking (rendezvous).

The RTCC vectors used to generate the preliminary NAT (NASA Apollo Trajectory) are summarized in Appendix A. Most of the lunar trajectories were generated using RTCC SS2 (inclination constrained) solution vectors rather than SS1 (no a priori) solution vectors. Unlike the Apollo 10

SS2 vectors which were constrained to the pre-LOI1, rev 18, and rev 29 planes, the Apollo 11 SS2 vectors were constrained on a rev to rev basis. Each SS2 vector contained two revs of data and was constrained to the SS1 solution plane of one of these two revs (exceptions existed at maneuvers). This technique prevented the accumulation of a large error in the out-of-plane component of position. The lunar potential model used in the generation of the preliminary NAT and for propagation of RTCC vectors was the Boeing R2 model defined in Appendix B.

The final NAT was produced by updating the preliminary NAT to include reconstructions of critical maneuvers for which telemetered acceleration data was available and to reflect the results of the trajectory reconstruction efforts performed on the descent and rendezvous periods of the mission. These reconstructions will be discussed in detail in the following sections.

In general, the postflight analysis was accomplished without difficulty. Coincident with the trajectory reconstruction activities, analyses were performed to determine the quality of the onboard tracking data (LM rendezvous radar, CSM sextant, CSM VHF ranging, and LM landing radar). The results of these analyses are also included in this report.

Table 7.I Apollo 11 Sequence of Events

	CET h:m:s	GMT d:h:m:s
Range Zero	00:00:00	16:13:32:00
Insertion	00:11:49.3	16:13:43:49.3
Translunar Injection Ignition	02:44:16.2	16:16:16:16.2
S-IVB/CSM Separation	03:17:04.6	16:16:49:04.6
First Docking	03:24:03.1	16:16:56:03.1
Spacecraft Ejection	04:16:59.1	16:17:48:59.1
Midcourse Correction #1	26:44:58.7	17:16:16:58.7
Lunar Orbit Insertion #1	75:49:50.4	19:17:21:50.4
Lunar Orbit Insertion #2	80:11:36.8	19:21:43:36.8
Undocking	100:12:00	20:17:44:00
CSM Separation	100:39:52.9	20:18:11:52.9
Descent Orbit Insertion	101:36:14	20:19:08:14
Powered Descent Initiation	102:33:05.2	20:20:05:05.2
Touchdown	102:45:39.9	20:20:17:39.9
Liftoff	124:22:00.8	21:17:54:00.8
Coelliptic Sequence Initiation	125:19:36	21:18:51:36
Constant Differential Height	126:17:49.6	21:19:49:49.6
Terminal Phase Initiation	127:03:51.8	21:20:35:51.8
Terminal Phase Finalization	127:46:09.8	21:21:18:09.8
Second Docking	128:03:00	21:21:35:00
Final Separation	130:30:01	22:00:02:01
Transearth Injection	135:23:42.3	22:04:55:42.3
Midcourse Correction #2	150:29:57.4	22:20:01:57.4
CM/SM Separation	194:49:12.7	24:16:21:12.7
Entry Interface	195:03:05.7	25:02:35:05.7

**Table 7.2 Descent and Rendezvous Maneuver Summary for Apollo 11**

Maneuver	Type of Maneuver	Ignition Time (h:m:s) GET	Cutoff Time (h:m:s) GET	T/M Coverage	ΔV (FPS)
SEPARATION	CSM/RCS	100:39:52.9	100:40:01.9	Yes	2.6
DOI	LM/DPS	101:36:14.0	101:36:44.0	No	76.4
PDI	LM/DPS	102:33:05.0	102:45:42.2	Yes	6775.8
ASCENT	LM/APS	124:22:00.8	124:29:15.7	Yes	6070.1
CSI	LM/RCS	125:19:36	125:20:23	No	51.5
CDH	LM/RCS	126:17:49.6	126:18:07.4	Yes	19.9
TPI	LM/RCS	127:03:51.8	127:04:14.5	Yes	25.3
TPF	LM/RCS	127:46:09.8	127:46:38.1	No	31.4

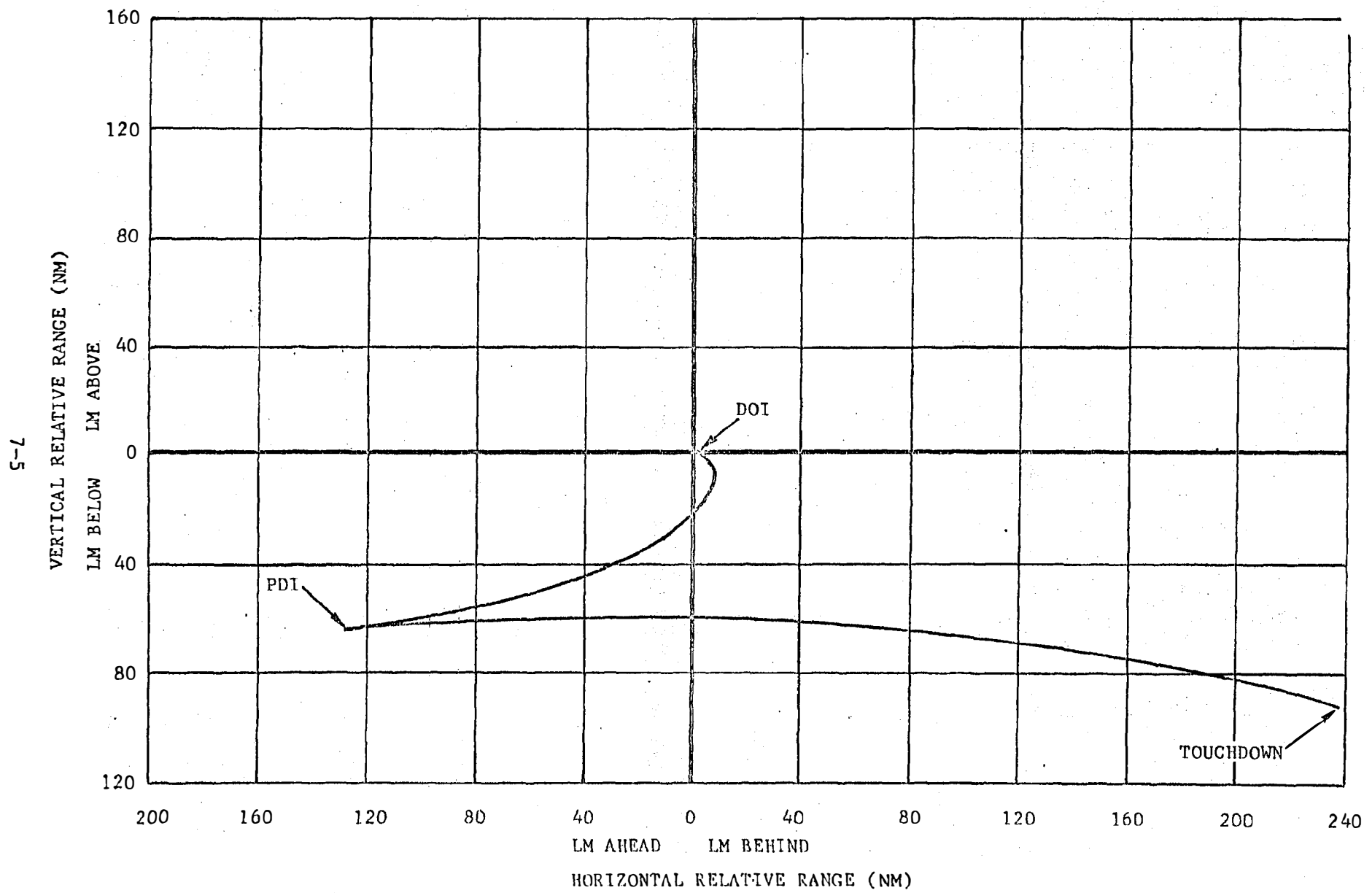


Figure 7-1a Relative Motion of the LM for Apollo 11 Descent - DOI to Landing (CSM Centered)

9-L

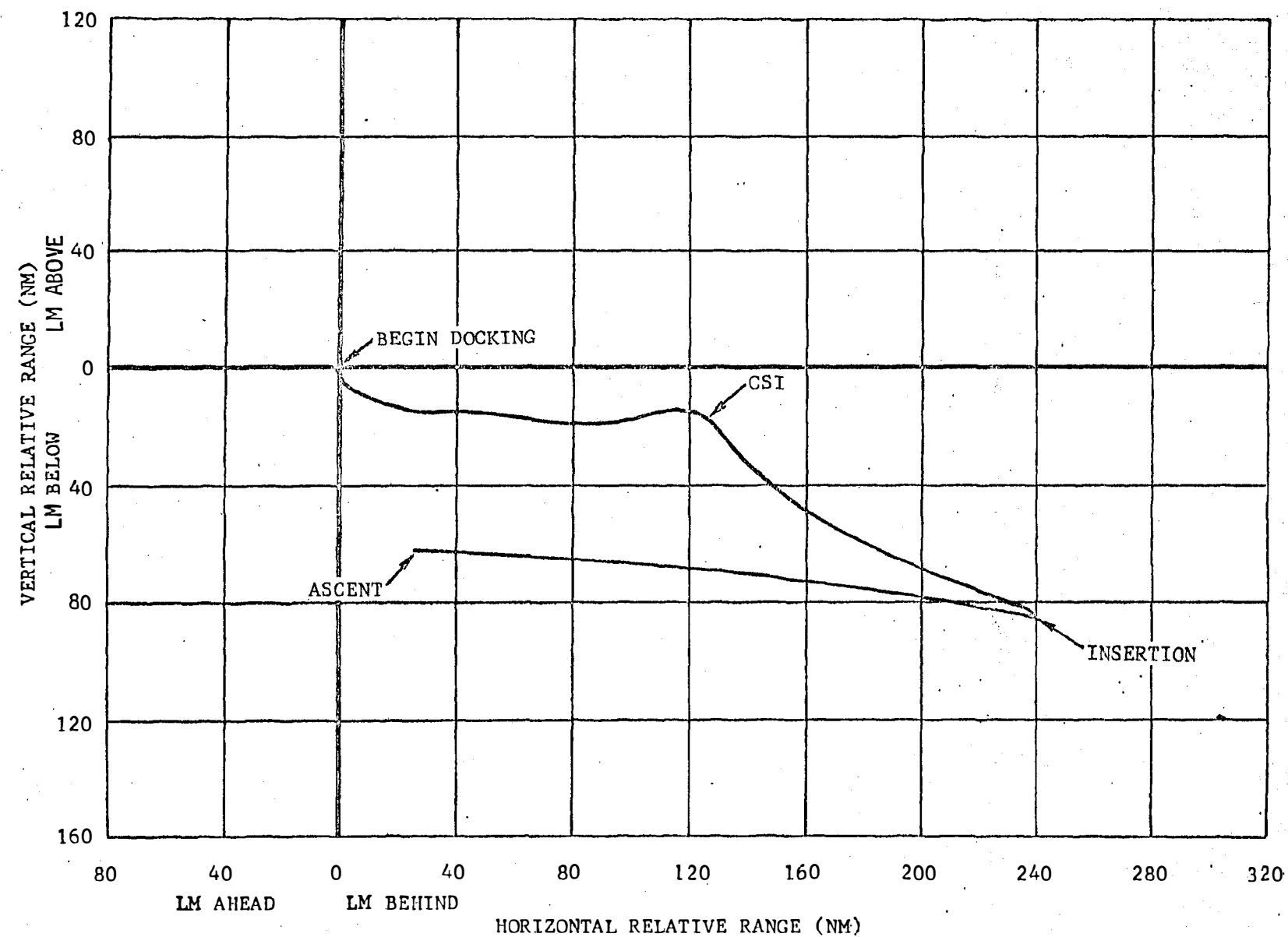


Figure 7-1b Relative Motion of the LM for Apollo 11 Rendezvous - Ascent to Docking (CSM Centered)

## 7.2 ORBIT ANALYSIS

### 7.2.1 Methods of Reconstruction

The HOPE Program was used as the basic orbit determination tool. The program utilizes a weighted least squares differential correction technique to regress on a large set of parameters. It is capable of handling two vehicles, and can use both ground based and onboard tracking data. An additional capability is the IGS (Inertial Guidance System) burn option which models the Apollo inertial measurement unit and uses telemetered acceleration data to reconstruct maneuvers.

The orbit determination was accomplished using four basic fit techniques. These techniques are described as follows:

- a) MSFN free flight - regression on the state vector over free flight intervals as defined by spacecraft maneuvers using MSFN data.
- b) MSFN IGS - regression on the state vector using, at maximum, one revolution of MSFN data and incorporating the spacecraft maneuvers which had telemetry coverage by means of the HOPE IGS burn model.
- c) Onboard free flight - regression on the state vector over free flight intervals using available onboard tracking data to correct the LM trajectory with respect to a fixed CSM trajectory (MSFN fits).
- d) Onboard IGS - regression on the state vector using available onboard data to correct the LM trajectory with respect to a fixed CSM trajectory and incorporation of the LM maneuver (which had telemetry coverage) by means of the HOPE IGS burn model.

More accurate trajectories are usually produced with techniques (b) and (d) since they take advantage of longer tracking data arcs. This factor is important in descent and rendezvous trajectory reconstruction since the tracking intervals between some maneuvers are too short to produce a representative trajectory over the whole segment.

As a result of the analysis of various lunar potential models contained in Reference 7, and on the basis of improved observation residuals and propagation characteristics, the L1 model (Langley Model 1) was used

in the orbit analysis. This model is basically the Boeing R2 model augmented by a C33 term. Table 7.3 shows improvements in propagation characteristics of the L1 over the R2 model. Both models are defined in Appendix B.

The trajectories for both Apollo 11 vehicles during descent and rendezvous were reconstructed using the methods summarized above. The data used in these reconstruction activities primarily included low speed MSFN, high speed MSFN, rendezvous radar, VHF ranging, and sextant data. Telemetered acceleration data were used to reconstruct maneuvers where available and applicable. Table 7.2 lists the maneuvers performed during the descent and rendezvous periods. Figure 7-2 shows the tracking data arcs (which were available over the periods of interest) as a function of ground elapsed time. In Figure 7-2, the solid bars represent the transmitting (two-way) MSFN station and the numbers represent the number of observations upon which final fits were based. Note that some stations operated in the dual mode (simultaneous tracking of both the CSM and the LM).

The following paragraphs describe the trajectories which were used as the final BET for both vehicles.

#### 7.2.2 CSM Best Estimate of Trajectory

The trajectories for the CSM lunar revolutions 13, 14, 25 and 26 were reconstructed from low speed MSFN tracking data compacted to a rate of two samples per minute or, in the case of stations operating in the dual mode, one sample every 36 seconds. The data used are summarized in Figure 7-2. The quantity of data obtained for revolutions 13 and 26 was good. Because of the partial data arcs from some stations on revolutions 14 and 25, the data quantity in these revs could only be rated as fair. Inclusion of data from a southern hemisphere station (Ascension) enhanced the geometry of the active tracking network configuration and contributed to the quality of all the fits.

Two reconstruction techniques were used to obtain the CSM BET's. The MSFN IGS fit technique was used on revolution 13 because of the presence of telemetered acceleration data from the CSM separation burn performed

in the MSFN data arc. BET's for the remaining orbits of interest (14, 25 and 26) were obtained from MSFN free flight fits.

In general, the CSM BET's were of good quality. This is illustrated to some extent by the good position and velocity comparisons between revolutions (Table 7.4) and by the residual statistics listed for each fit in Appendix B. These statistics (standard deviation of .1 to .25 cycles per second) compare very well with Apollo 8 (standard deviations between .3 and .6 cycles per second) and Apollo 10 (standard deviations between .2 and .4 cycles per second). A portion of this improvement may be attributed to the better fit produced by the L1 lunar potential model.

Table 7.4 contains a summary of the final BET's giving fit type (technique), data interval, NAT trajectory interval, and position and velocity differences at matchpoints between segments.

### 7.2.3 LM Best Estimate of Trajectory

A major portion of the postflight analysis effort was directed towards reconstruction of the LM trajectories from undocking to landing and from liftoff through rendezvous. A discussion of the origin and quality of the final trajectories is included in the following paragraphs.

#### 7.2.3.1 Descent Phase Trajectories

The descent phase was reconstructed in three segments; undocking to DOI, DOI to PDI, and PDI to Touchdown. The BET for undocking to DOI was obtained from a MSFN free flight fit based upon the entire data arc from revolution 13. The quantity of data was considerably better than for the CSM since five stations were tracking the LM. Residual statistics (summarized in Appendix B) compare well with the MSFN residual statistics obtained from the CSM fits. Note from Figure 7-2, which shows the tracking history, that the tracking station geometry was good.

The BET for the period from DOI to PDI was obtained from an onboard free flight fit based on CSM sextant and VHF ranging data taken prior to PDI. As can be seen in Figure 7-2 the data quantity was good, with 18 VHF ranging observations and 13 sextant sightings. Data quality is discussed more thoroughly in Section 7.3. The CSM trajectory which was used as the reference trajectory was the revolution 14 BET discussed in paragraph 7.2.2.

The BET for the powered descent segment of the flight was originally based on a fit obtained from low speed MSFN data taken from revolution 14 acquisition of signal to touchdown. The trajectory obtained from this fit was modified to force the landing point to coincide with the current best estimate of landing site location. Landing site parameters obtained from this descent trajectory (BET #3) were  $.6358^{\circ}$  latitude,  $23.4938^{\circ}$  longitude, and -8557 feet altitude (referenced to the mean lunar radius). These figures compare well with the value published in Reference 10 as the best estimate (latitude  $.647^{\circ}$  and longitude  $23.505^{\circ}$ , determined from postflight photo reduction).

Since the BET #3 was constrained to impact a desired landing site, the quality of the trajectory at PDI is not the best available. A subsequent reconstruction using a combination of onboard plus high speed MSFN data is discussed in Section 7.4 of this report. This combination of high speed data from acquisition of signal to landing and relative tracking data obtained prior to PDI produces a consistent and continuous representation of the LM trajectory from DOI to touchdown.

#### 7.2.3.2 Rendezvous Trajectories

The BET for LM ascent was initialized with landing site coordinates of  $.6357^{\circ}$  latitude,  $23.4701^{\circ}$  longitude, and a height of -8607 feet above the mean lunar radius. These initial conditions were then propagated to insertion using accelerometer data to model the ascent burn.

The LM BET for the period from insertion to TPF was reconstructed in two segments; insertion to CSI and CSI to TPF. The trajectory for the insertion to CSI segment was obtained from a MSFN free flight fit. The data arc and trajectory interval are described in Table 7.4. The MSFN data was good both quantitatively and qualitatively as can be seen in Figure 7-2. The residual statistics, summarized in Appendix B, show that the standard deviations of the doppler residuals are larger in this segment than in segments which have a less severe orbital geometry. This characteristic also existed in the Apollo 10 postflight results.

The second rendezvous segment covered the period from CSI to TPF. The BET chosen was obtained from an onboard data, IGS fit. The data used in the fit included LM rendezvous radar, CSM sextant, and CSM VHF ranging observations. In addition, telemetered acceleration data was used in the IGS burn option of HOPE to reconstruct the CDH and TPI burns. The data arcs are shown in Figure 7-2, and the residual statistics are summarized in Appendix B. Data quality was good, and the resulting BET produced an accurate relative trajectory. The CSM trajectory chosen as the reference for the relative observations was the revolution 26 trajectory described in paragraph 7.2.2. (The quality of the data and the reconstruction are discussed in more detail in Section 7.3 of this report.)

Table 7.3 Matchpoint Comparisons of Trajectories Produced  
with R2 and L1 Lunar Potential Models

Revolutions Compared	R2		L1	
	POS RSS (ft)	VEL RSS (ft/sec)	POS RSS (ft)	VEL RSS (ft/sec)
11-12	10,637	7.187	7544	5.756
12-13	9,936	8.178	4817	3.046
13-14	8,643	8.723	1555	2.53
25-26	9.595	9.139	2147	3.173

RSS = Square root of the sum of the squares of the differences  
between position (POS) or velocity (VEL) components.

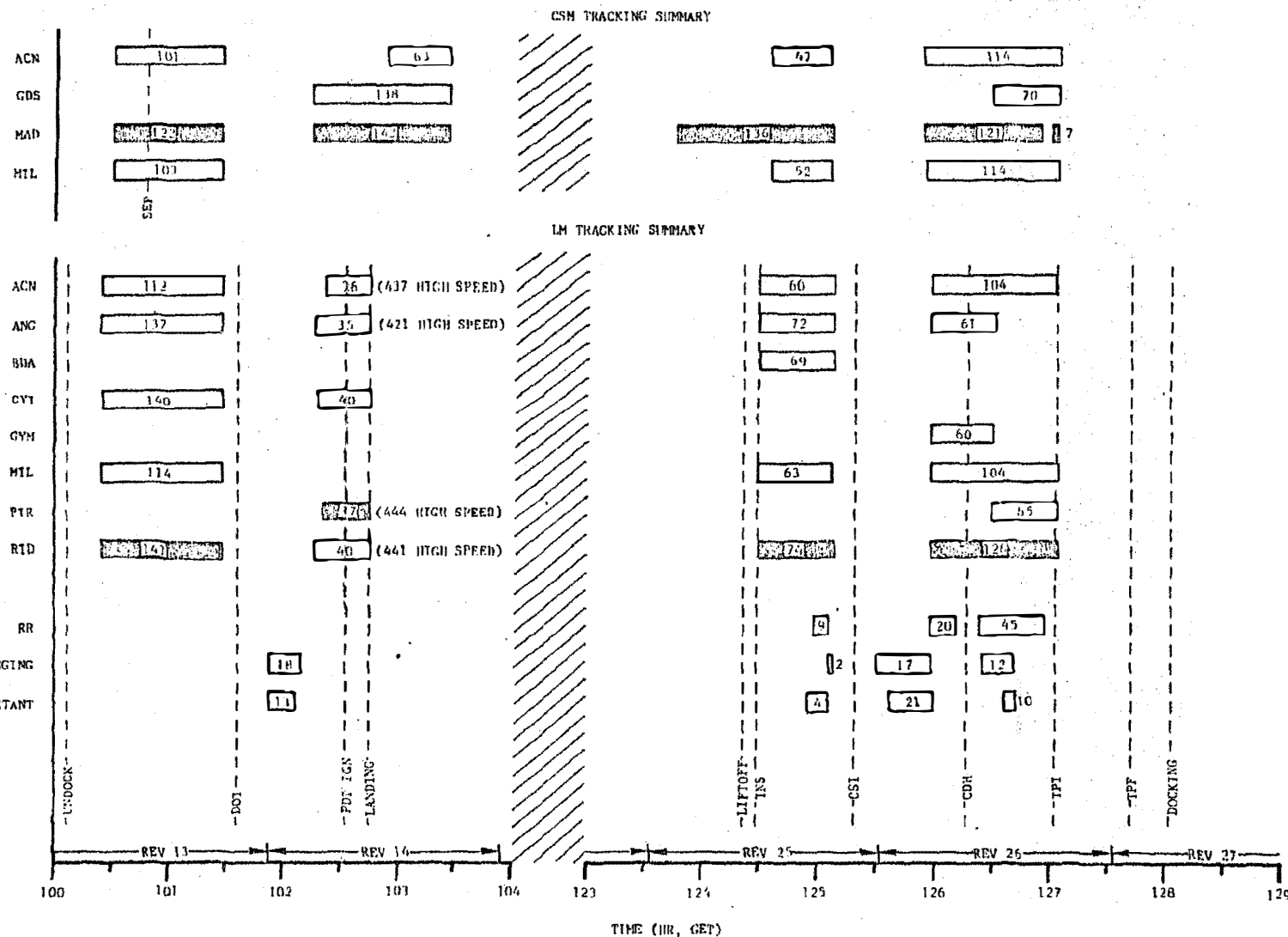


Figure 7-2 Tracking Data (Onboard and Ground Based) Timeline for Apollo 11 Descent and Rendezvous

Table 7.4 - Apollo Mission 11 BET Summary

7-14

Vehicle	Flight Segment	Fit Type	Data Interval		Trajectory Interval		$\Delta R$ ft	$\Delta V$ ft/sec
			(d:h:m:s)	GMT	(d:h:m:s)	GMT		
LM	Undock to DOI	MSFN F.F.	20:17:48:45	20:18:59:57	20:17:39:00	20:19:08:14.7	--	--
LM	DOI to PDI	O/B, F.F.	20:19:25:03	20:19:43:56	20:19:08:44.5	20:20:04:00	2007.	75.9*
LM	Powered Descent	Modified MSFN IGS	20:19:48:51	20:20:17:45	20:20:04:37.2	20:20:17:45.2	N/A	N/A
LM	Ascent	IMU only	---	---	21:17:53:58.9	21:18:03:08.9	--	--
LM	Insertion to CSI	MSFN F.F.	21:18:03:03	21:18:40:15	21:18:01:21	21:18:51:36	N/A	N/A
LM	CSI to POST TPI	O/B IGS	21:19:02:17	21:20:29:38	21:18:52:00	21:21:15:08	4253.	50.8**
CSM	Revolution 13	MSFN IGS	20:17:54:24	20:18:59:36	20:17:22:00	20:19:22:00	--	--
CSM	Revolution 14	MSFN F.F.	20:19:47:27	20:20:58:21	20:19:22:00	20:21:17:00	1555.	2.5
CSM	Revolution 25	MSFN F.F.	21:17:27:51	21:18:38:33	21:16:57:00	21:18:57:00	--	--
CSM	Revolution 25	MSFN F.F.	21:19:26:15	21:20:36:51	21:18:57:00	21:20:57:00	2147.	3.2

\*DOI Burn  $\Delta V = 76.4$  ft/sec\*\*CSI Burn  $\Delta V = 51.5$  ft/sec

### 7.3 ONBOARD TRACKING DATA ANALYSIS

#### 7.3.1 Introduction

Analysis of the LM rendezvous radar data from Apollo missions 9 and 10 and CSM VHF ranging data from Apollo 10 resulted in the conclusions that both data types were of high quality and, in general, produced trajectories consistent with those obtained from ground based tracking data (References 1 and 5).

A similar analysis of the onboard tracking data obtained during the Apollo 11 mission was performed with the following objectives:

- a) Determine the consistency of the LM rendezvous radar data and the CSM VHF ranging data with similar data from Apollo missions 9 and 10.
- b) Using these data as a standard of comparison, evaluate the LM sightings made with the CSM sextant.
- c) Determine the consistency of all onboard data with the ground based data.
- d) Use the onboard data to construct a more accurate LM rendezvous trajectory.

The onboard tracking data were obtained from the downlink telemetry tapes by a special purpose computer program designed to read the tape, and output the desired observations and associated information on punched cards. The format of the punched cards was the specified input to the HOPE Program. Editing of bad data was performed manually.

Onboard tracking data yields a measure of the position and velocity of one vehicle relative to another. It is necessary, therefore, to obtain a good, independent estimate of the trajectory of one vehicle and fix this as a reference trajectory. Since the LM trajectory is perturbed by several maneuvers during the descent and rendezvous mission periods, it is logical to fix the trajectory of the relatively quiescent CSM as the reference.

As discussed in Section 7.2, the CSM trajectory was reconstructed in four single revolution fits from MSFN tracking data. The three segments of interest here were MSFN free flight fits on revolutions 14, 25, and 26.

Trajectories for the LM free flight segments were also reconstructed from MSFN tracking data. The ground based MSFN tracking available for use during the periods of interest are summarized in timeline form in Figure 7-2.

The CSM trajectory was fixed as the reference, and the LM MSFN free flight trajectories were then used to initialize fits based on onboard data in the four segments where relative data were available. A priori confidence values of 10,000 feet were placed on each component of position and 10 feet per second on each component of velocity in the initial conditions.

The reconstruction activities will be discussed in more detail in the following sections. In addition, various tables and figures are included which serve to describe the operations performed and show the accuracy and validity of the data.

### 7.3.2 Onboard Measurements

Rendezvous radar data were obtained during three periods of the Apollo 11 mission; these were Insertion to CSI (9 observations), CSI to CDH (20 observations), and CDH to TPI (45 observations). As in previous missions, the amount of rendezvous radar data obtained was limited to those periods when telemetry coverage was available.

VHF ranging data were obtained from the CSM during four segments of the flight; these were DOI to PDI (18 observations), insertion to CSI (2 observations), CSI to CDH (17 observations), and CDH to TPI (12 observations). Since only two observations were obtained from Insertion to CSI, no meaningful statistics could be obtained.

Sextant data were obtained during the same periods of flight as were VHF ranging data; 13 observations between DOI and PDI, 4 observations from insertion to CSI, 21 observations from CSI to CDH, and 10 observations between CDH and TPI. Listings of all the data are included in Appendix D.

### 7.3.3 Evaluation of Onboard Tracking Data

#### Rendezvous Radar Data

In order to determine the quality of the rendezvous radar data, the residuals (differences between the actual measured value and a measurement

value computed from given CSM and LM trajectories) were examined. The CSM trajectories used in obtaining these residuals were the BET's discussed in Section 7.2 of this report (one rev MSFN free flight fits). The LM trajectories were obtained by using technique (c) described in paragraph 7.2.1 (onboard free flight fits). All available onboard data were used in these fits.

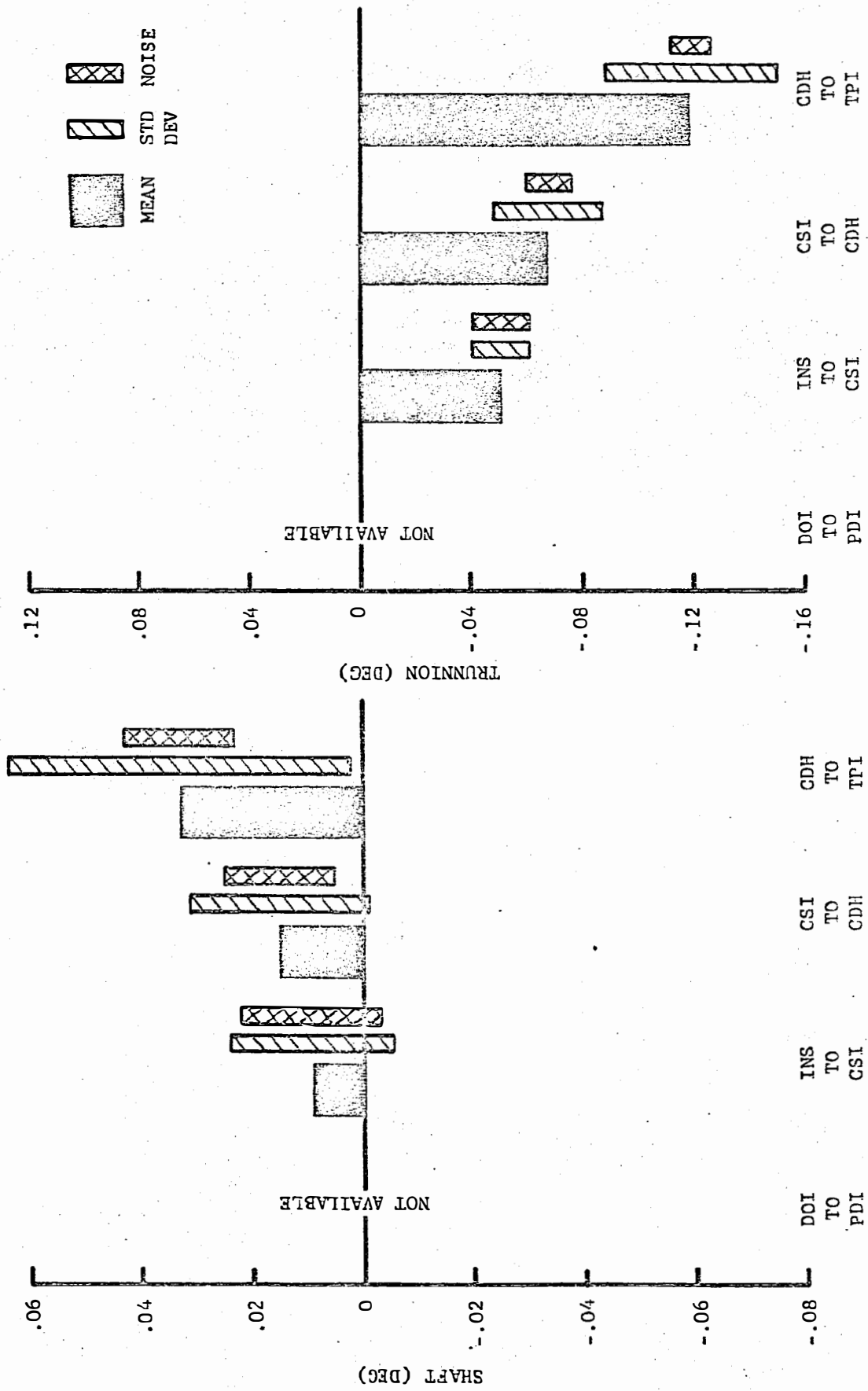
Table 7.5 lists residual statistics (mean, standard deviation, one-sigma noise estimate) computed from the onboard free flight fits of each segment and Figures 7-3a and 7-3b illustrate the results graphically. The data were generally well behaved as can be seen in the residual plots (Figures 7-4 through 7-6). The relatively large differences between the standard deviation and noise computed for shaft and trunnion in the CSI to CDH and CDH to TPI periods can partly be attributed to the fact that both rendezvous radar and sextant data were used in the fit. As the two data sets become more equal in size (weighted effect) or the sampling arcs more coincident, residual statistics deteriorate. This effect is demonstrated by the statistics listed in Table 7.6 which were obtained from fits made with only rendezvous radar data included. Note that when sextant data is eliminated, the RR shaft and trunnion means and deviations decrease in all segments. The shaft statistics are still relatively high (especially in the CDH and TPI period), indicating that a systematic error is still present in the shaft measurement. It should also be noted that the rendezvous radar residual statistics from Apollo 10 exhibited a similar characteristic (Reference 1). In Apollo 10, the standard deviations for both shaft and trunnion measurement are relatively large in the CDH to TPI period (no sextant data were included in Apollo 10 solutions). The large mean values seen in Table 7.5 are also a result of the inclusion of sextant data in the solution data sets. When only rendezvous radar data was included, the mean values decreased to near zero values.

The range residual statistics exhibited characteristics similar to the Apollo 10 data. When VHF ranging data is removed from the solution data set, standard deviations decrease and become, in two segments, almost equal to noise estimates. The mean values also approach zero, indicating that no bias is present.

Table 7.5 Summary of Rendezvous Radar Residual Statistics

	Insertion To CSI	CSI To CDH	CDH To TPI	
Shaft (deg)	.009	.015	.033	Mean
	.015	.016	.031	S. Dev.
	.013	.010	.010	Noise
Trunnion (deg)	-.051	-.068	-.119	Mean
	.010	.019	.031	S. Dev.
	.010	.008	.007	Noise
Range (feet)	79.	75.	55.	Mean
	144.	63.	92.	S. Dev.
	39.	37.	27.	Noise
Range Rate (fps)	.604	-.243	-.305	Mean
	.173	.339	.277	S. Dev.
	.6278	.6278	.6278	Q. E.*

\* Quantization Error.



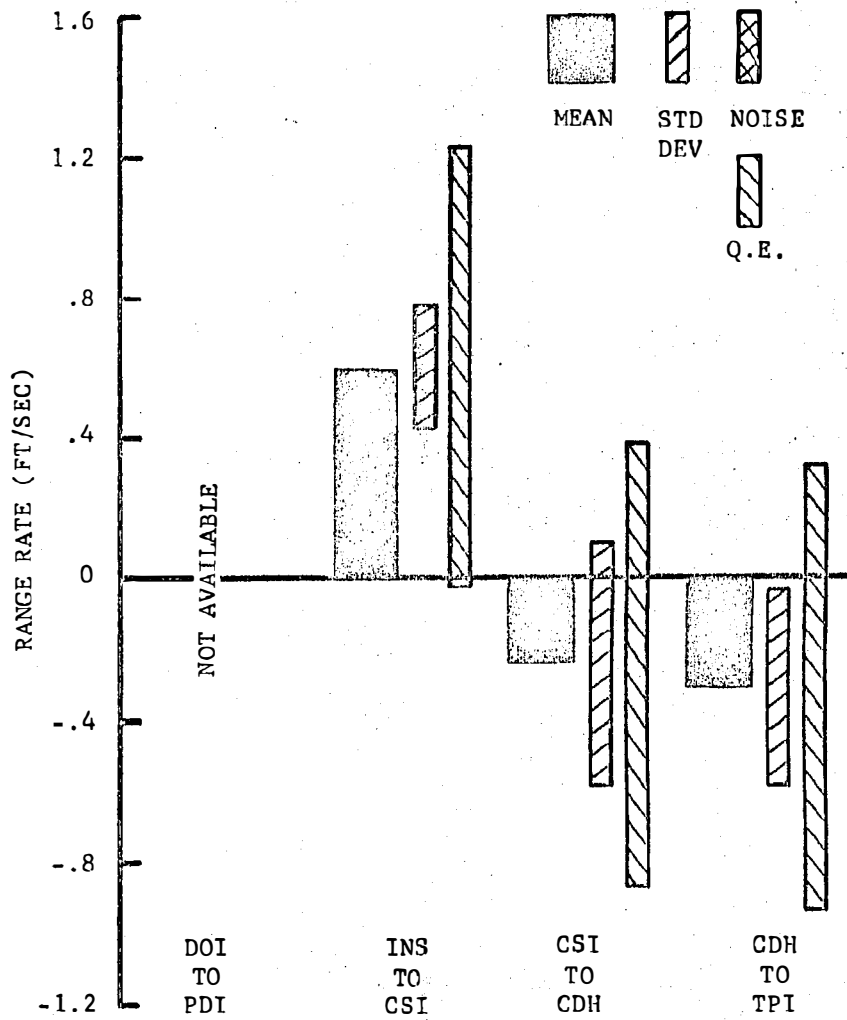
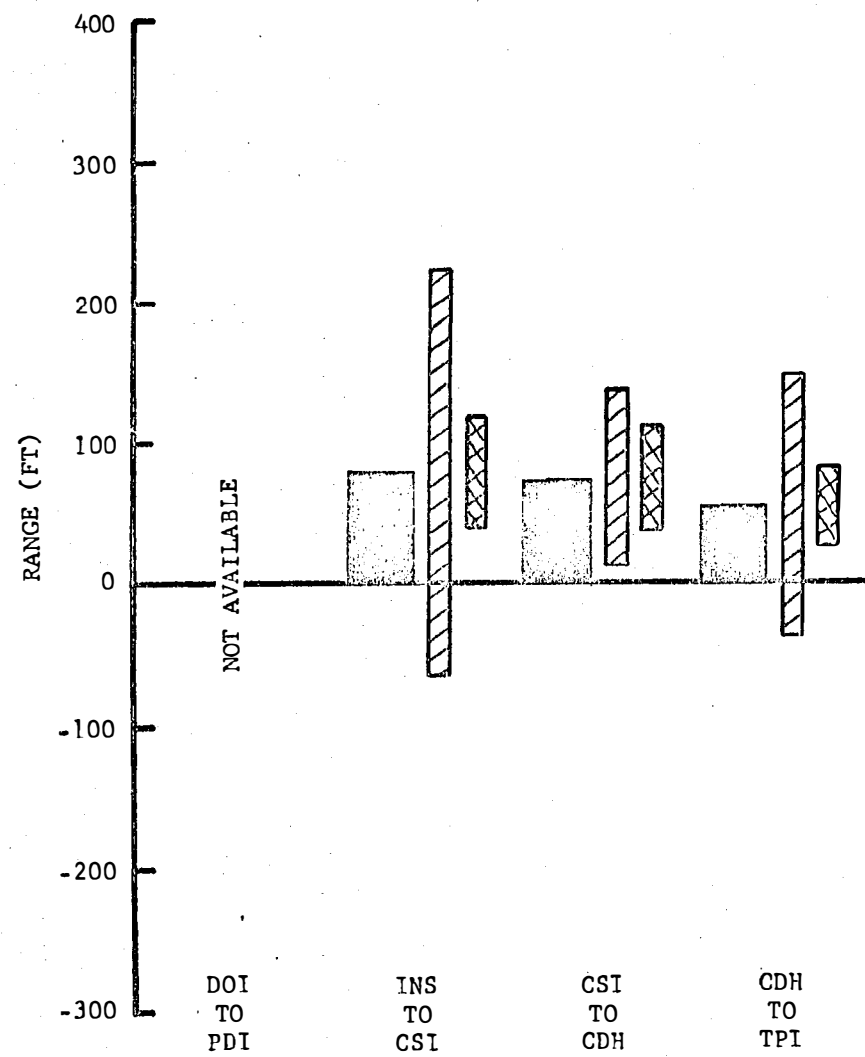


Figure 7-3b Rendezvous Radar Range and Range Rate Residual Statistics

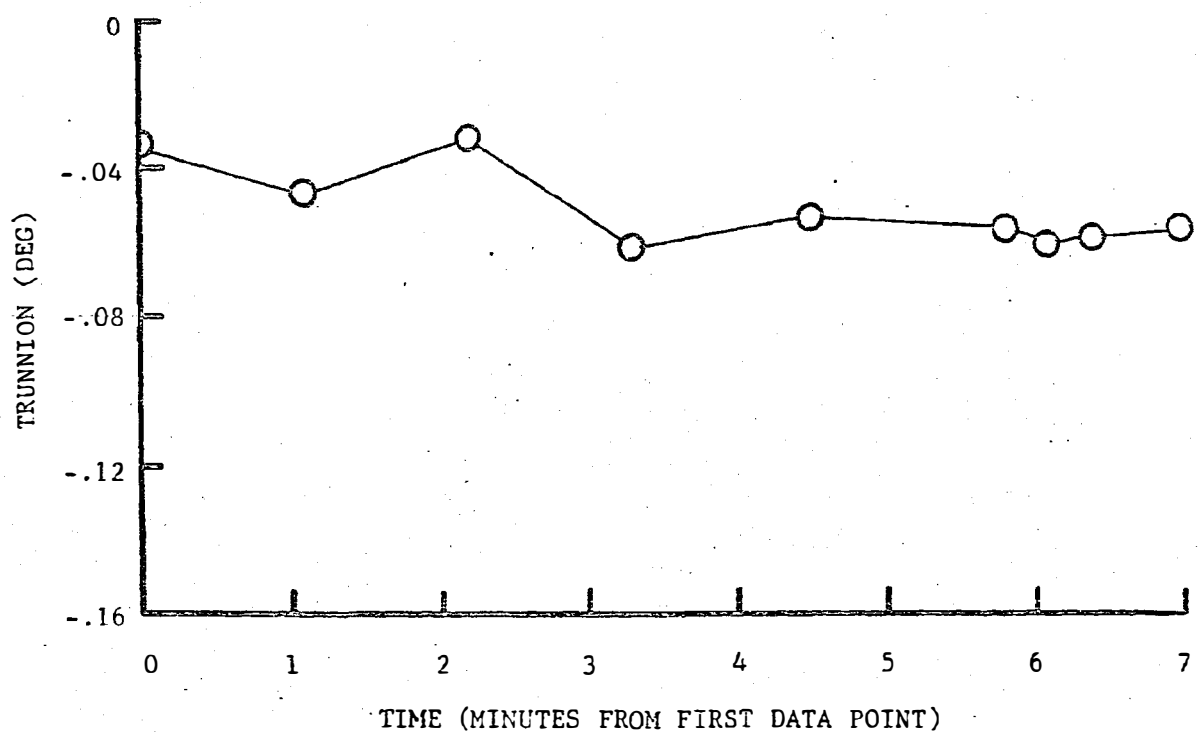
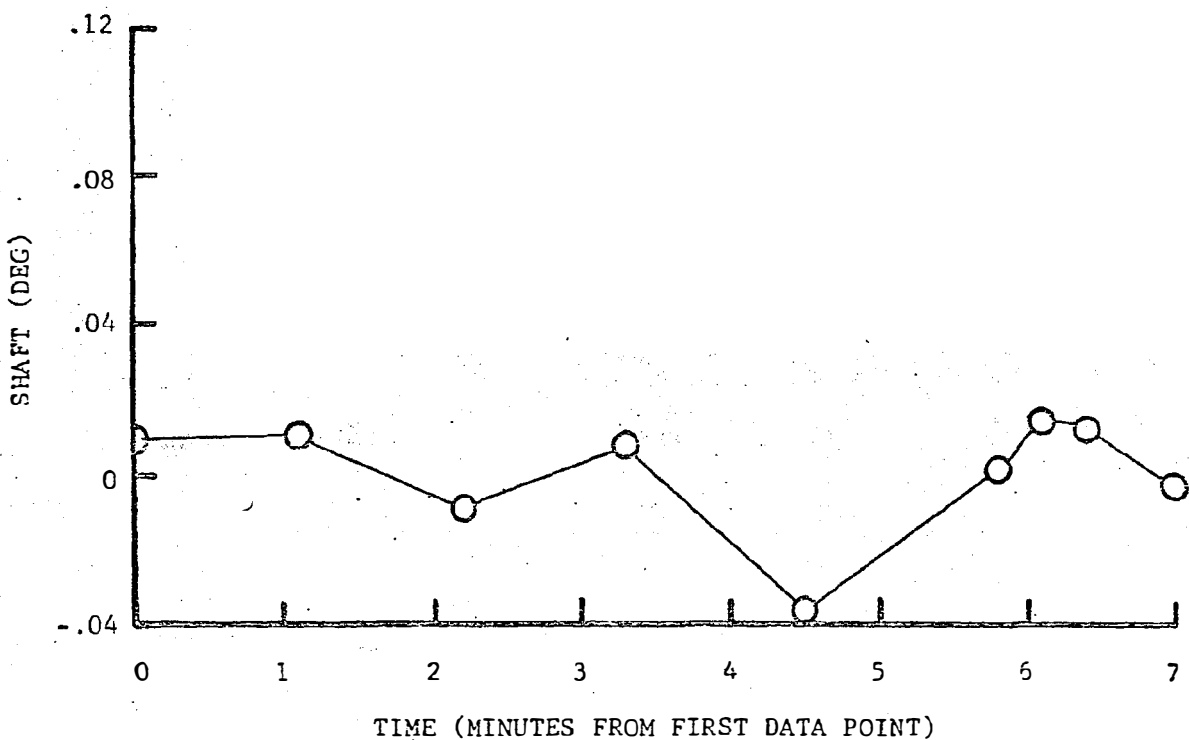


Figure 7-4 Rendezvous Radar Residuals (Insertion to CSI)

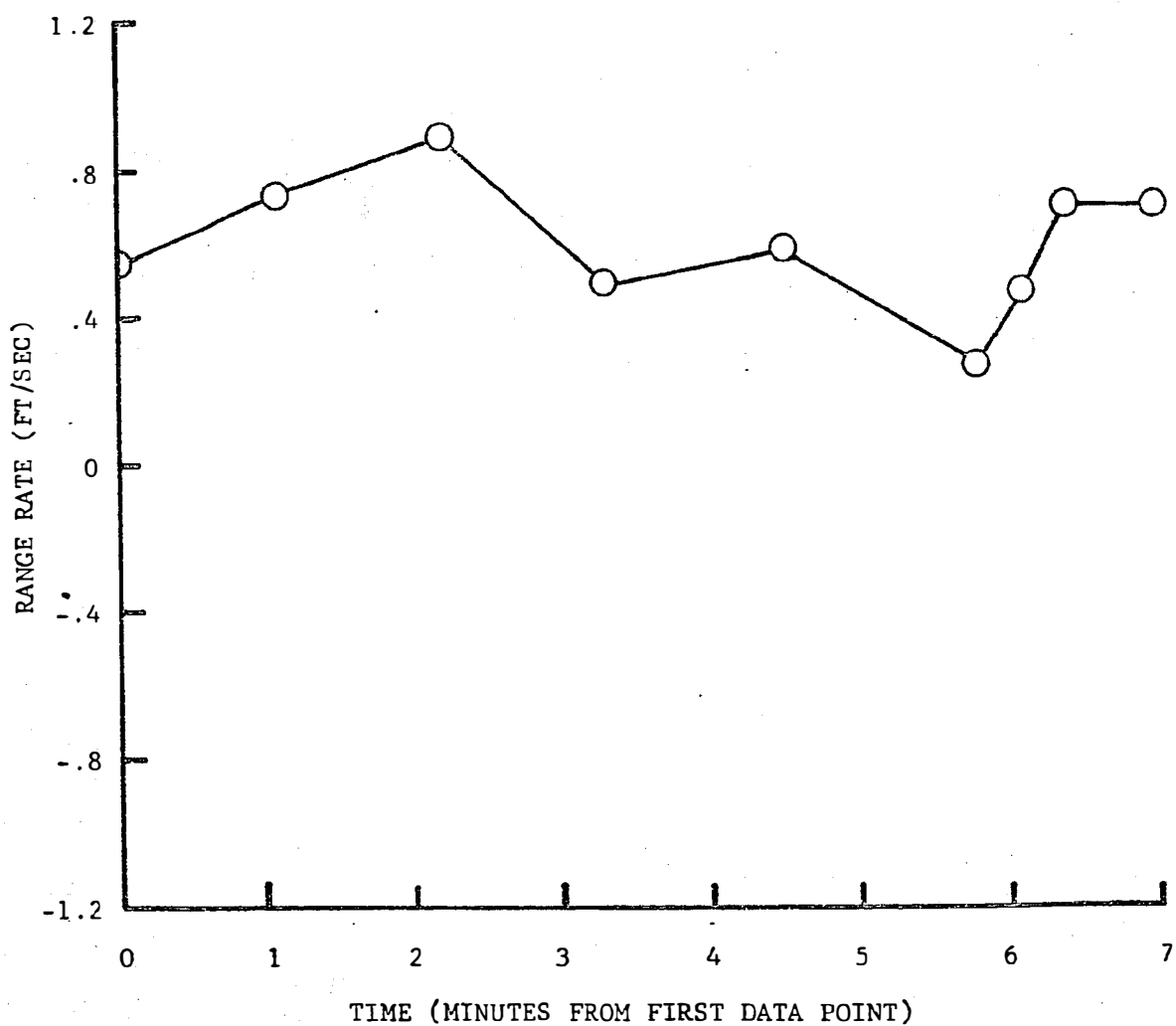
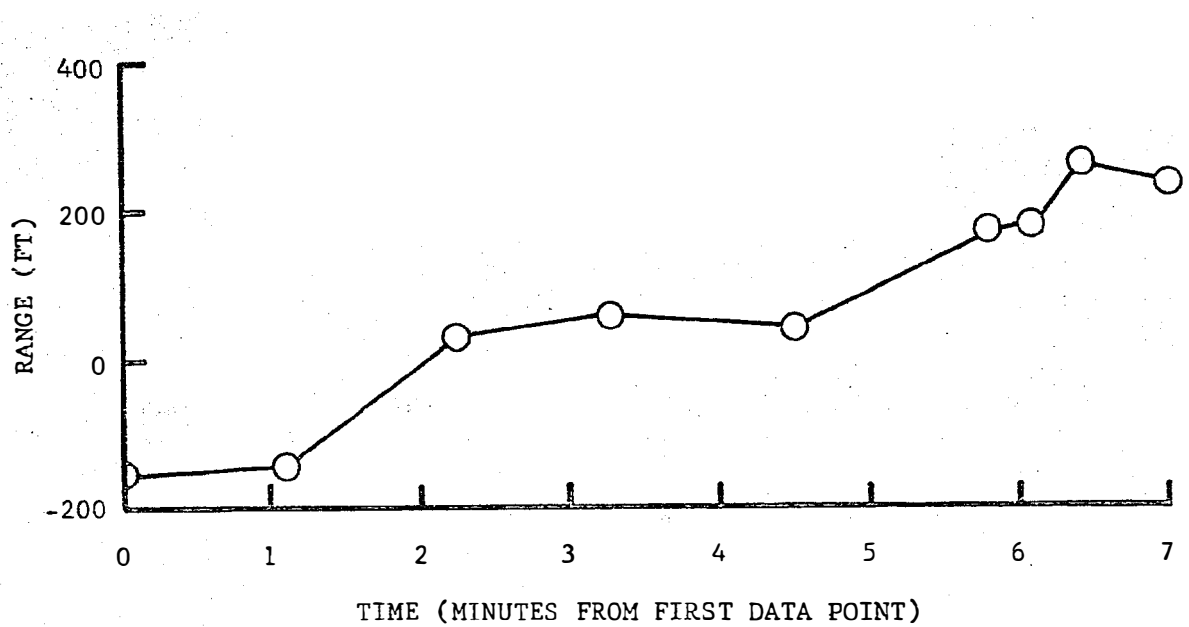


Figure 7-4 Concluded

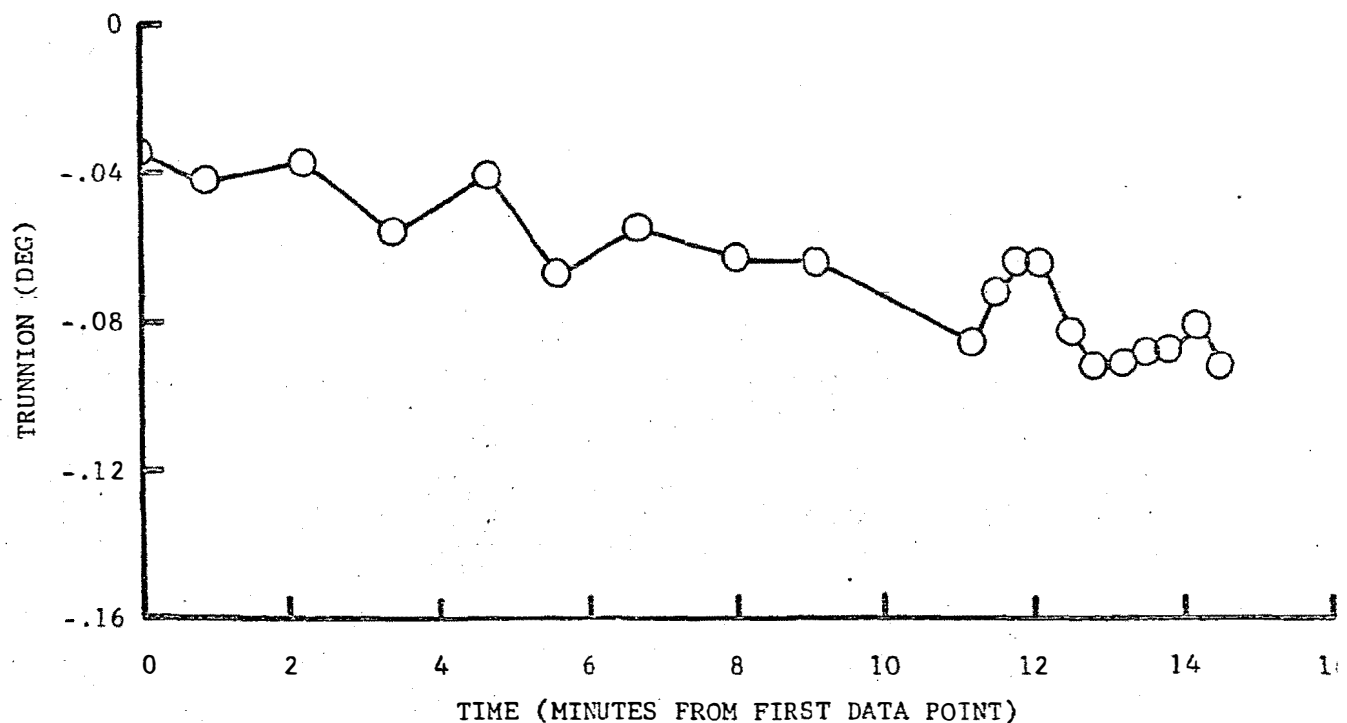
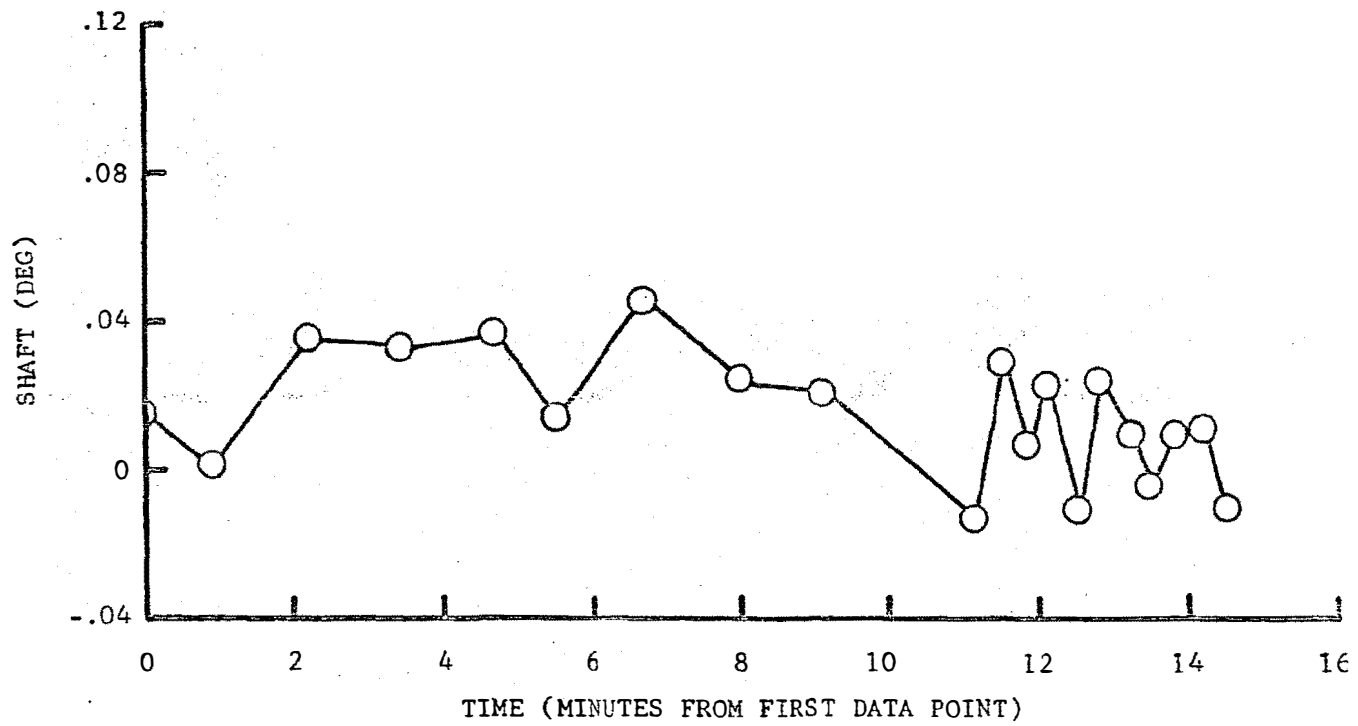


Figure 7-5 Rendezvous Radar Residuals (CSI to CDH)

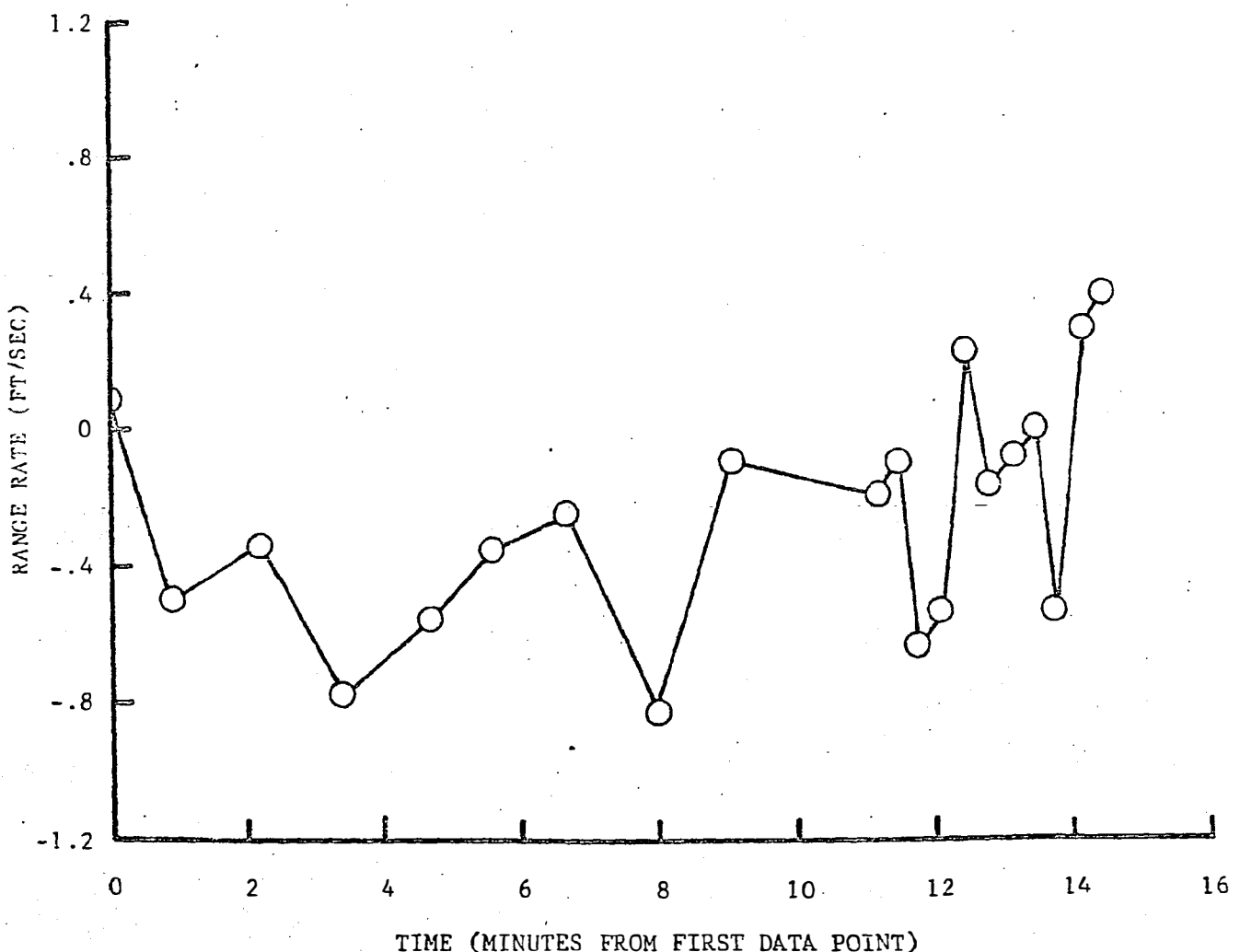
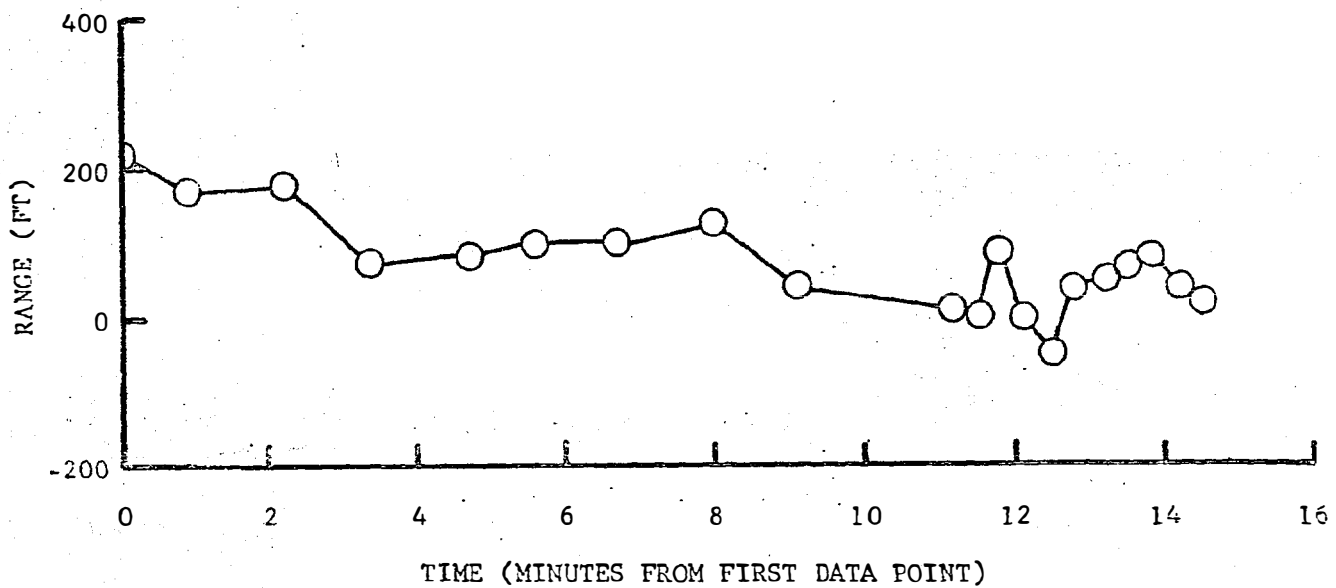


Figure 7-5. Concluded

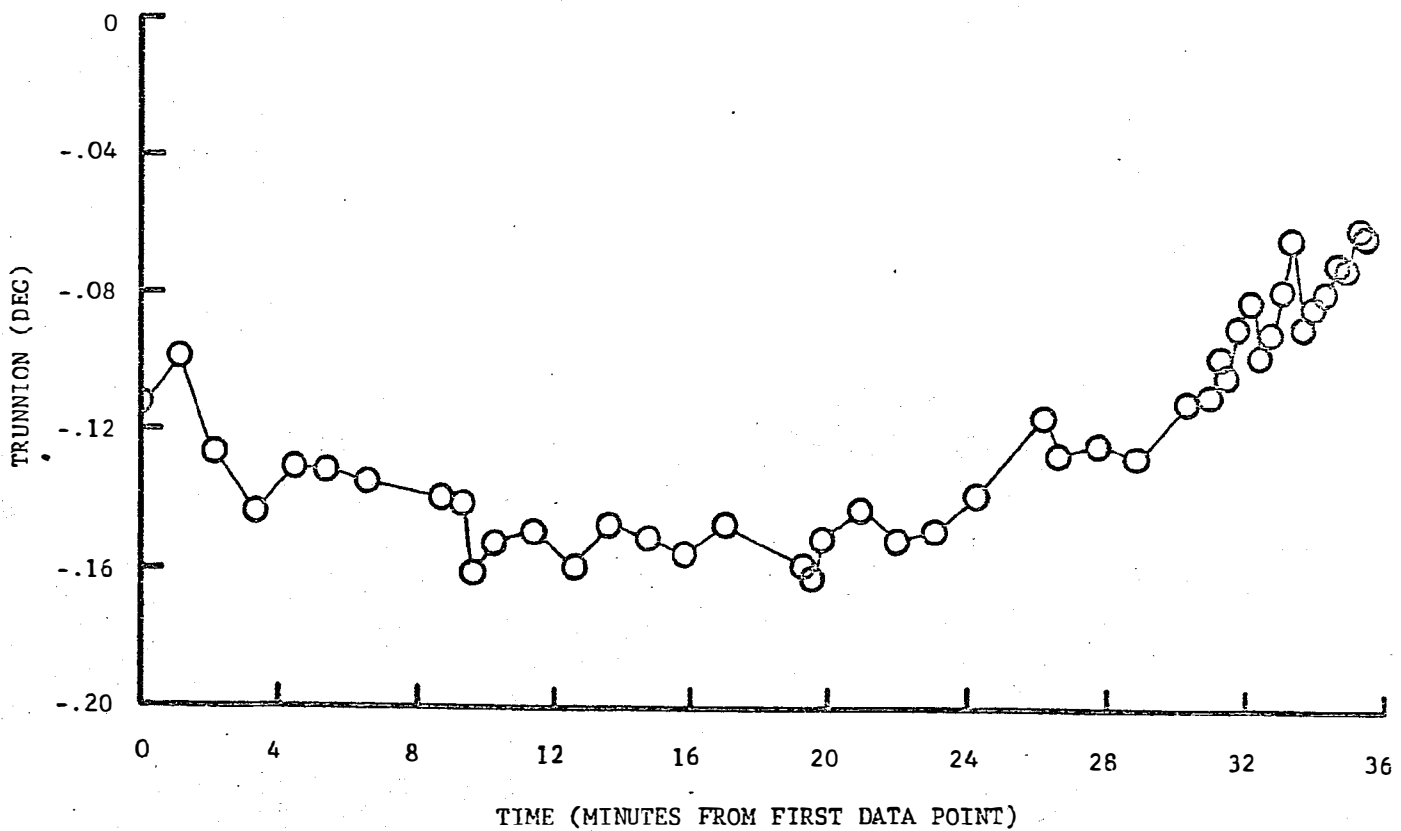
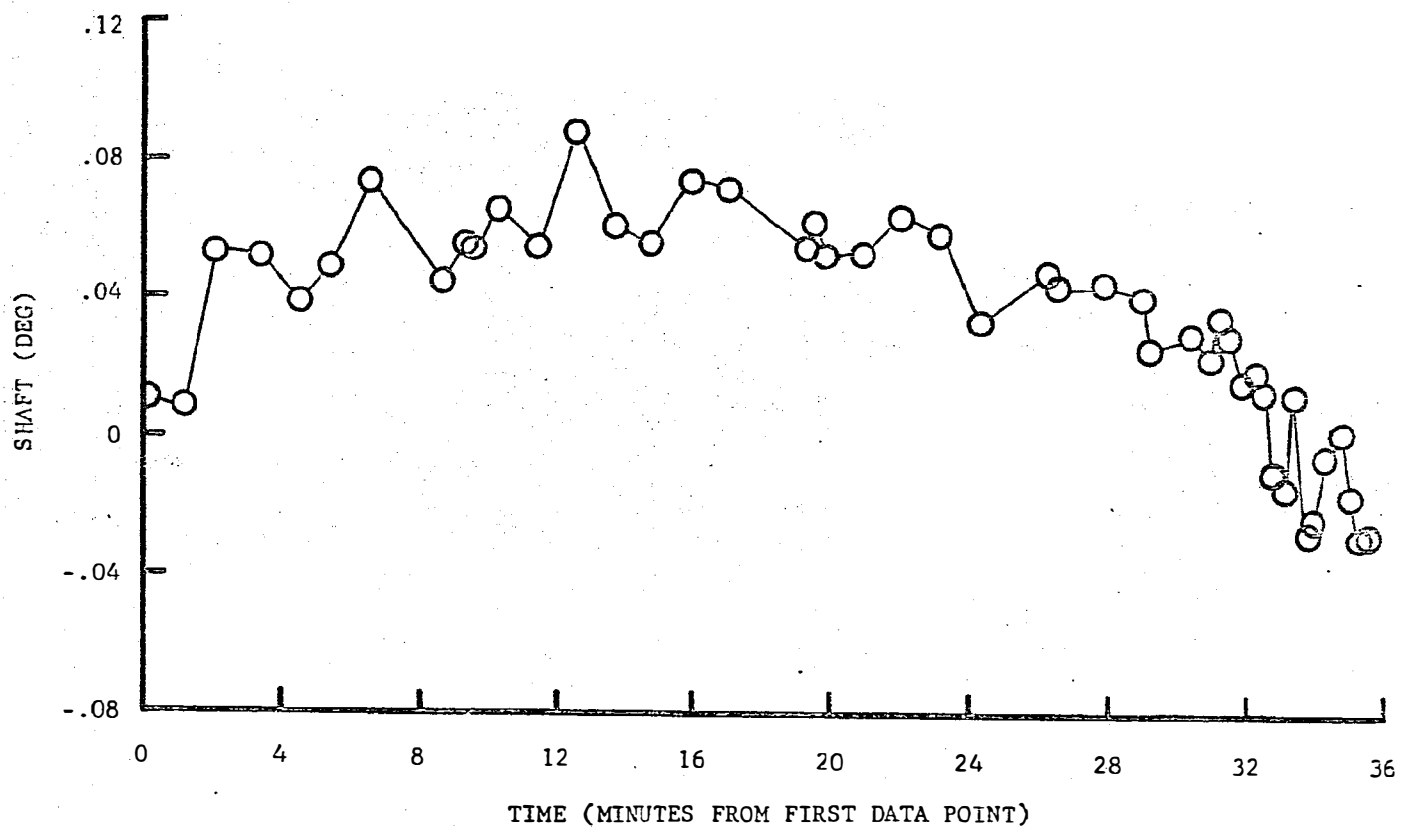


Figure 7-6 Rendezvous Radar Residuals (CDH to TPI)

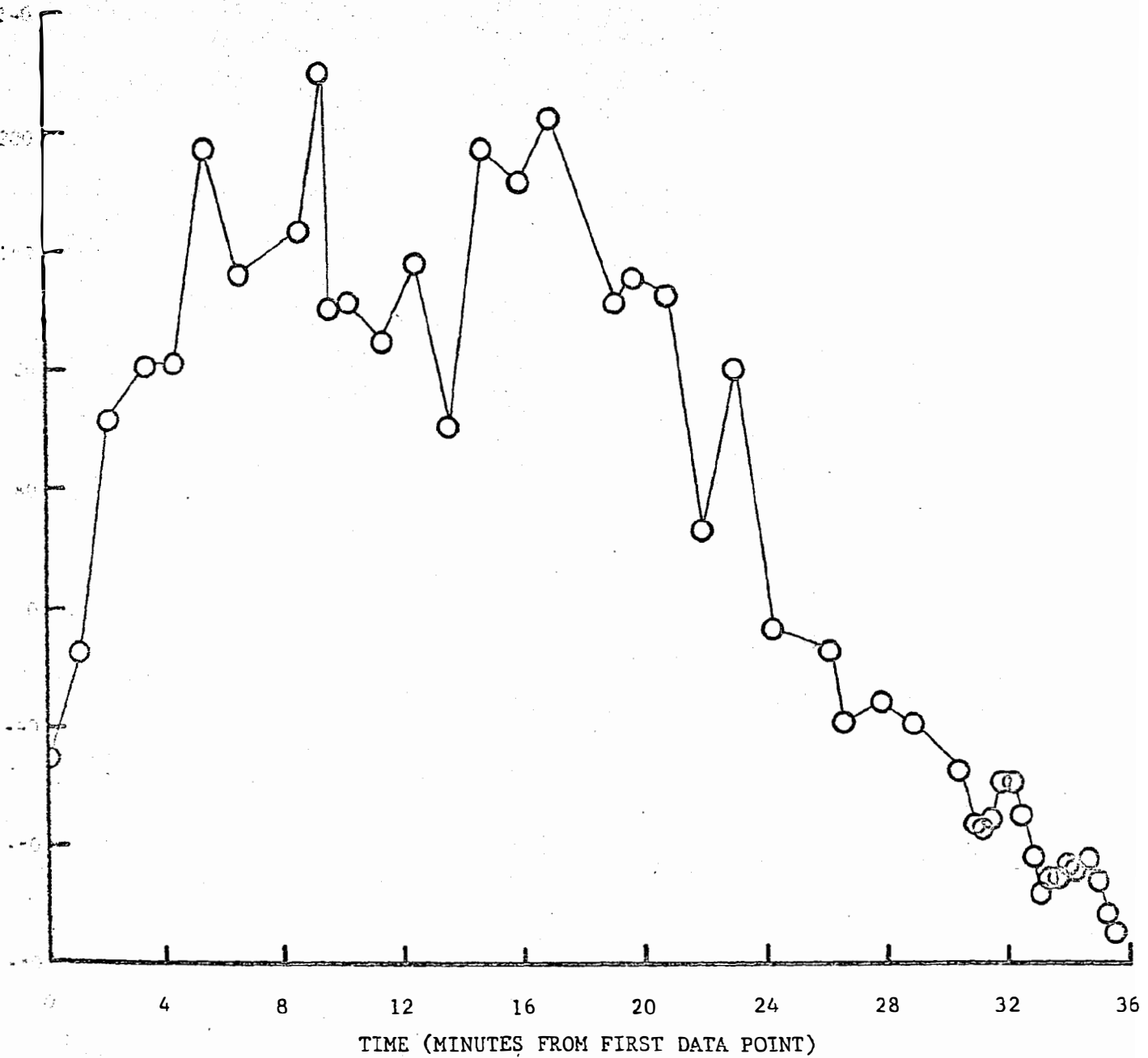


Figure 7-6 Continued

Reproduced from  
best available copy

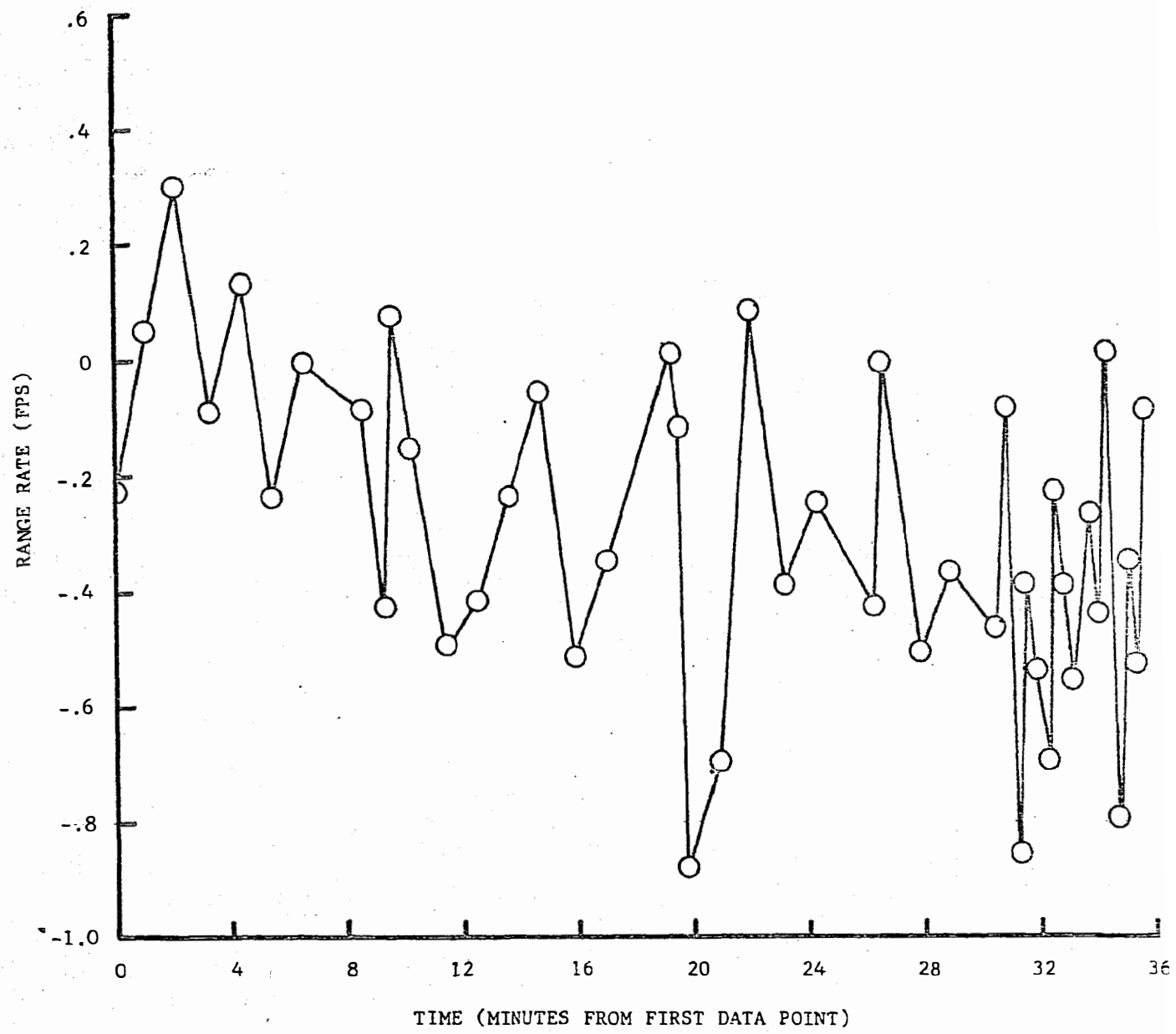


Figure 7-6 Concluded

Table 7.6 Rendezvous Radar Only Solution Residual Statistics

	INS-CSI	CSI-CDH	CDH-TPI	
Shaft	-.00007	.00028	.018	Mean
	.015	.014	.031	S. Dev.
Trunnion	-.00013	.00002	-.0005	Mean
	.0066	.0074	.0085	S. Dev.
Range	.55	.026	2.89	Mean
	39.	37.2	72.45	S. Dev.
Range Rate	-.343	-.105	-.196	Mean
	.187	.314	.304	S. Dev.

The range rate residuals were also of good quality. Mean values were all less than the downlink readout error (.6278 fps).

One sigma noise calculations for shaft, trunnion, and range rate from three missions are plotted as a function of average range in Figures 7-7 through 7-9. These figures show that the Apollo 11 noise estimates compare well with similar estimates from missions 9 and 10. Note that no definite trend is apparent in the angular noise as relative range varies. Figure 7-9 does seem to indicate, however, that the noise estimate for the range measurement does increase as average range increases. The Apollo 11 noise estimates for all three observables appear to be generally smaller than those obtained from previous missions.

#### VHF Ranging Data

Table 7.7 contains a summary of VHF ranging data residual statistics obtained from onboard free flight fits made over the three segments where adequate amounts of data were available. Figures 7-10, 7-11, and 7-12 contain plots of these residuals. Since only two observations were obtained from the insertion to CSI segment, only the DOI to PDI (18 observations), CSI to CDH (17 observations), and CDH to TPI (12 observations) segments are considered.

The VHF ranging data were generally of good quality. As expected, the smallest mean value was obtained during the DOI to PDI period when VHF ranging was the only range data type measuring the distance between vehicles. The mean values become increasingly large as more rendezvous radar data are included in the data set or as the data arcs become coincident in time. This can be seen in the large mean value for the CDH to TPI period. This large mean, however, is still within the bias specification limit of  $\pm 270$  feet.

Figure 7-13 shows that the calculated noise values compare favorably with Apollo 10 results and are relatively constant when compared to those obtained from Apollo 10. The residual statistics listed in Table 7.7 are illustrated graphically in Figure 7-14.

#### Sextant

The residual statistics shown in Table 7.8 indicate that the CSM sextant is a very accurate instrument. Sextant observations were obtained

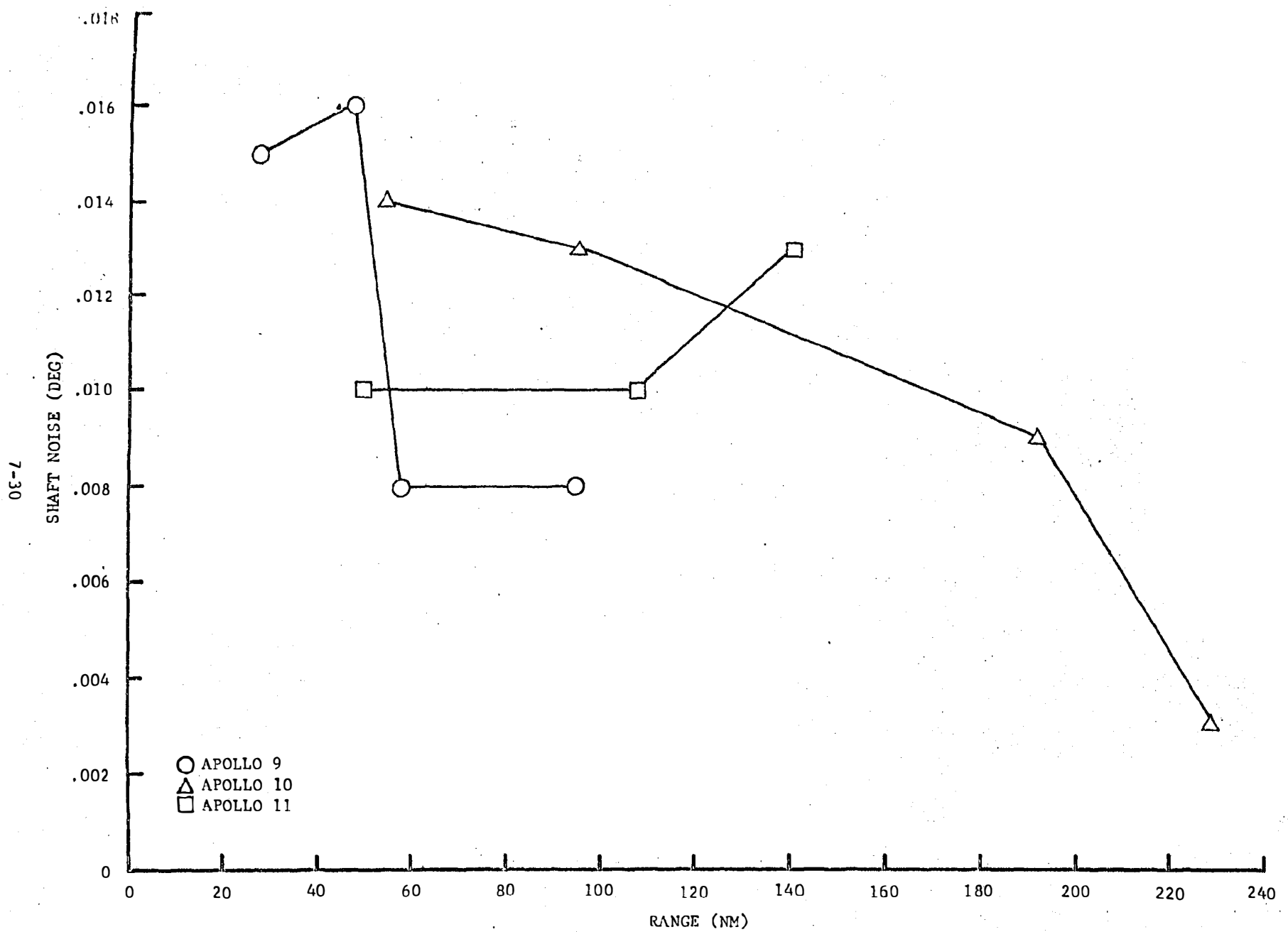


Figure 7-7 Rendezvous Radar Shaft Noise as a Function of Average Range

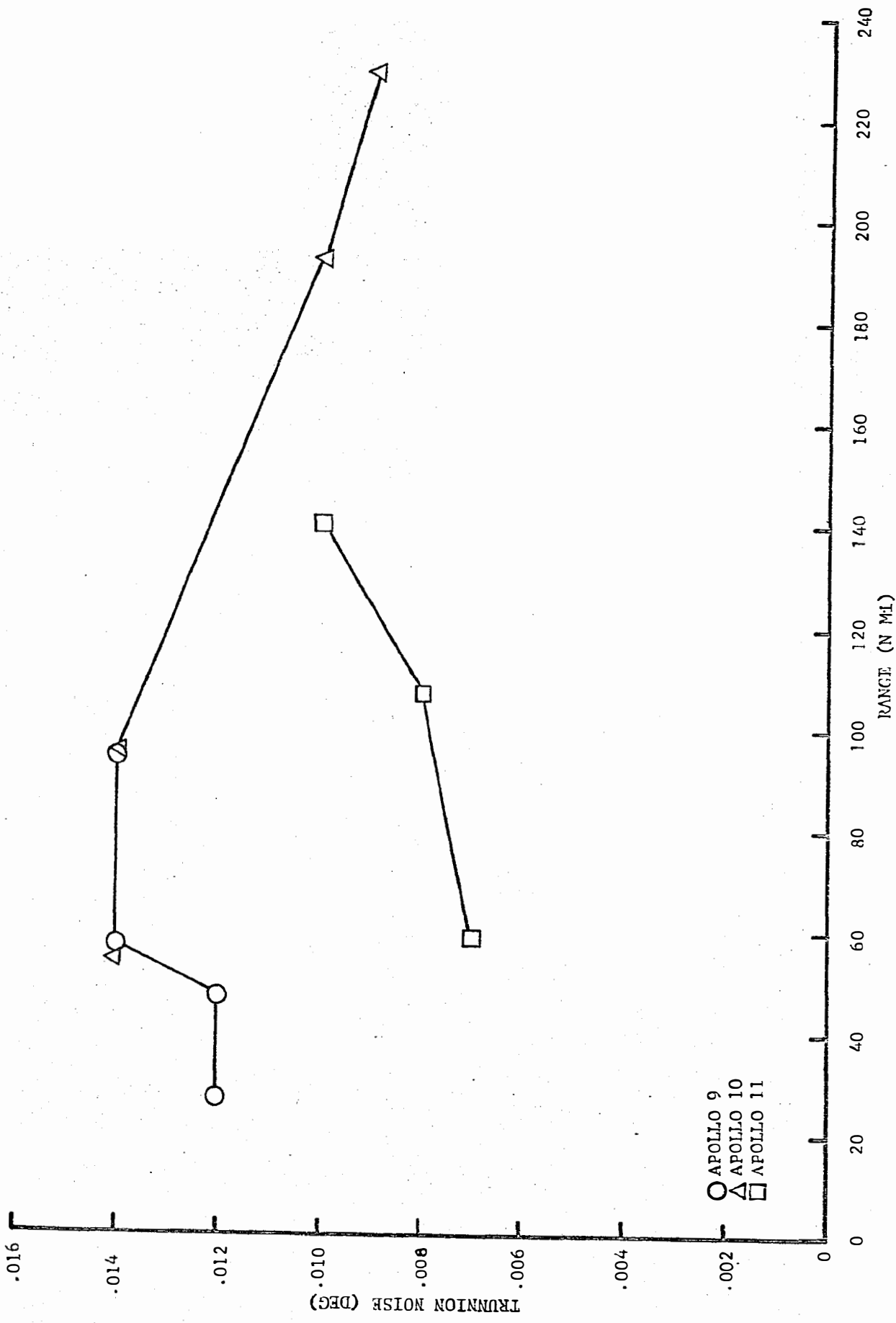


Figure 7-8 Rendezvous Radar Truncation Noise as a Function of Average Range

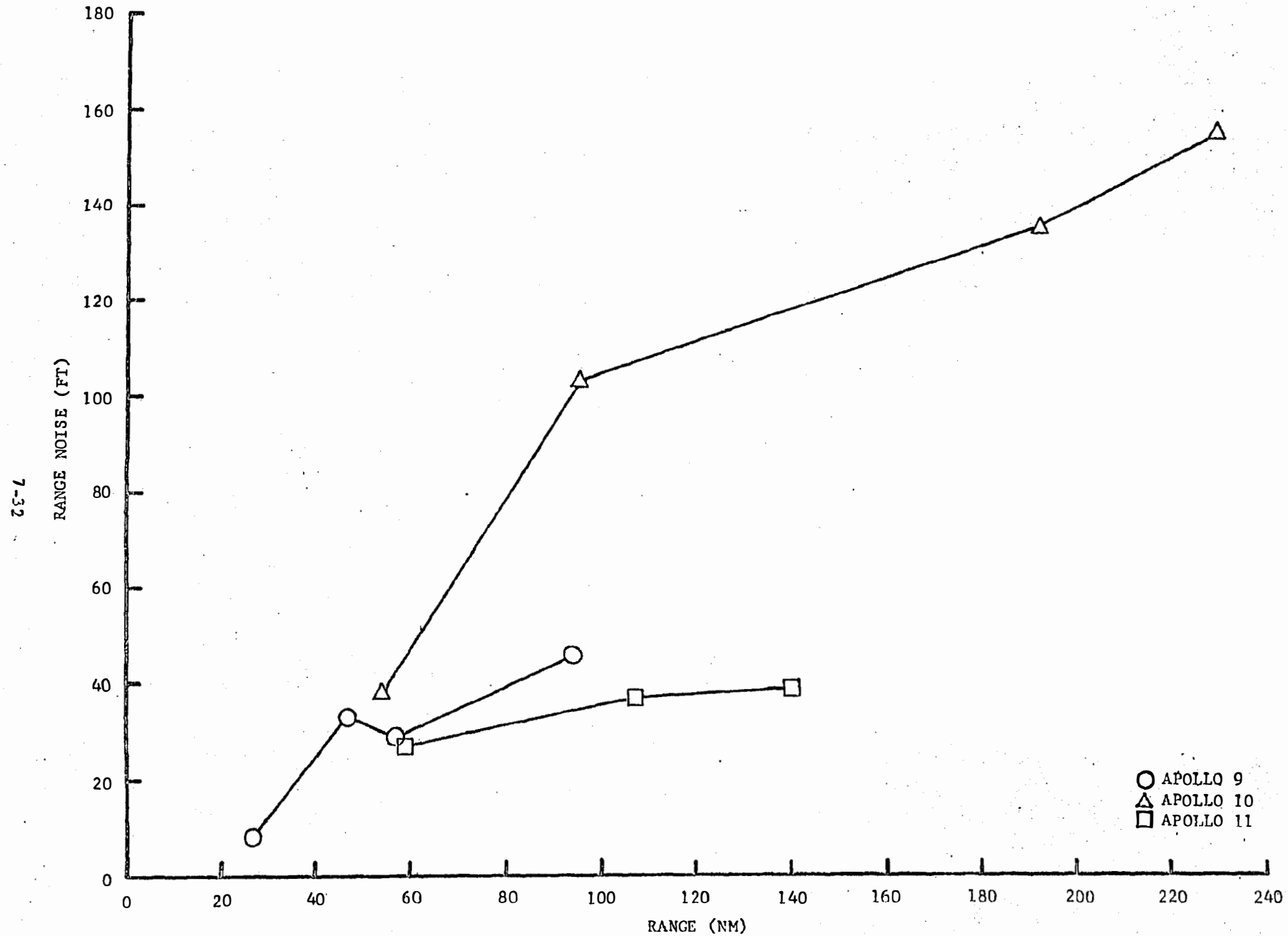


Figure 7-9 Rendezvous Radar Range Noise as a Function of Average Range

Table 7.7 Summary of VHF Ranging Residual Statistics

Range (feet)	DOI-PDI	CSI-CDH	CDH-TPI	
	-26.	-86.	-216.	Mean
	74.	104.	48.	S. Dev.
	23.	23.	19.	Noise

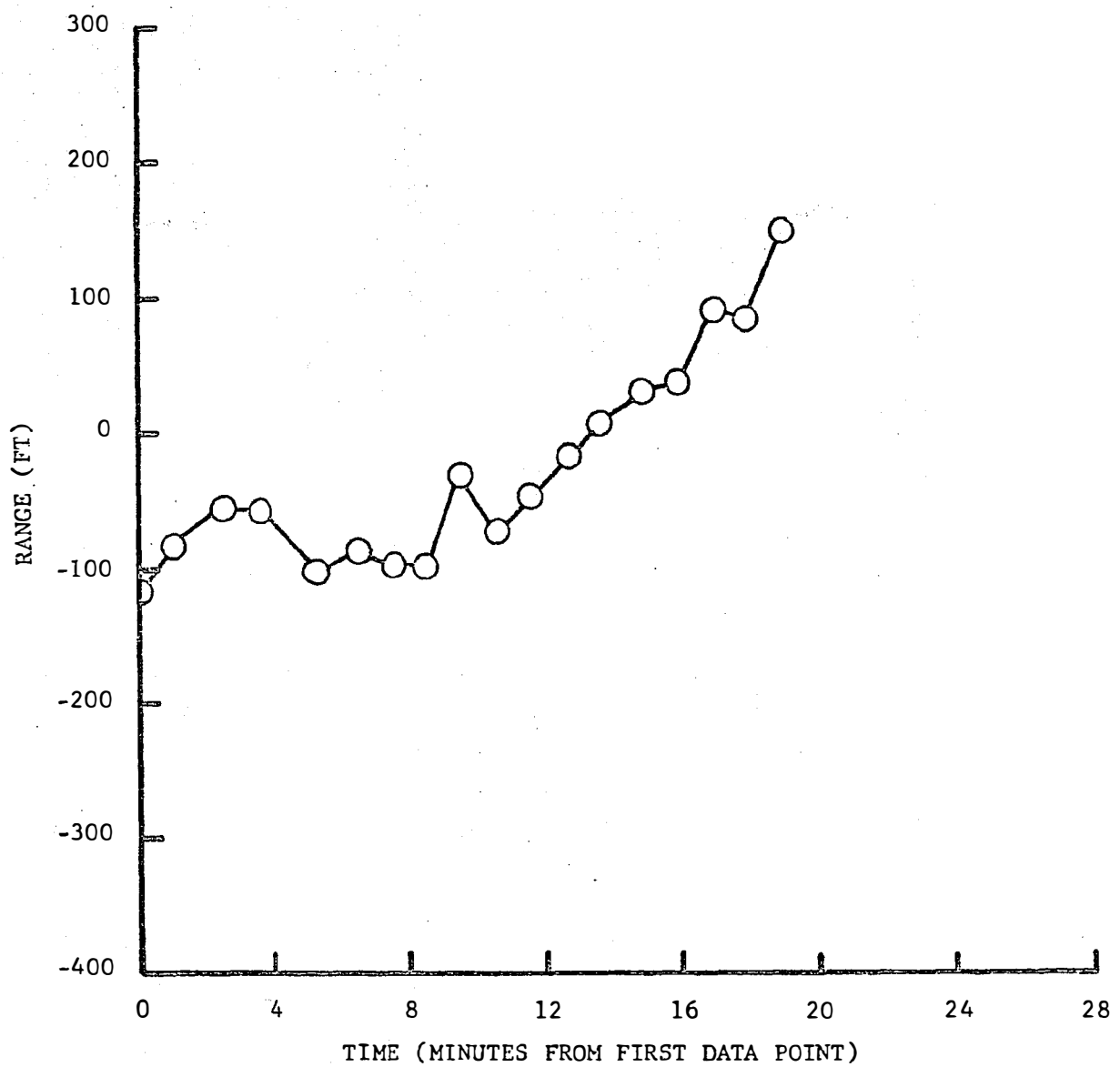


Figure 7-10 VHF Ranging Residuals (DOI to PDI)

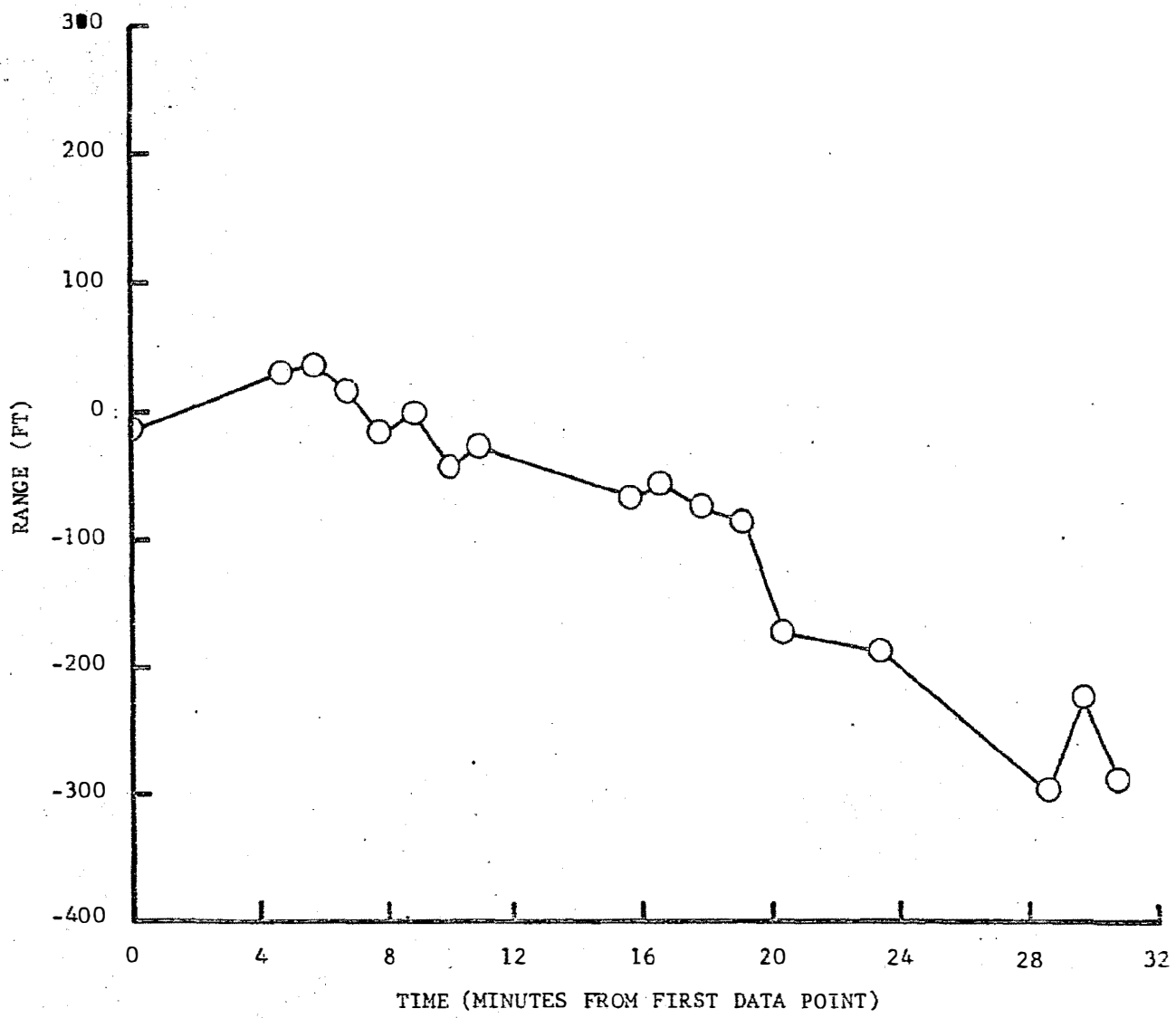


Figure 7-11 VHF Ranging Residuals (CSI to CDH)

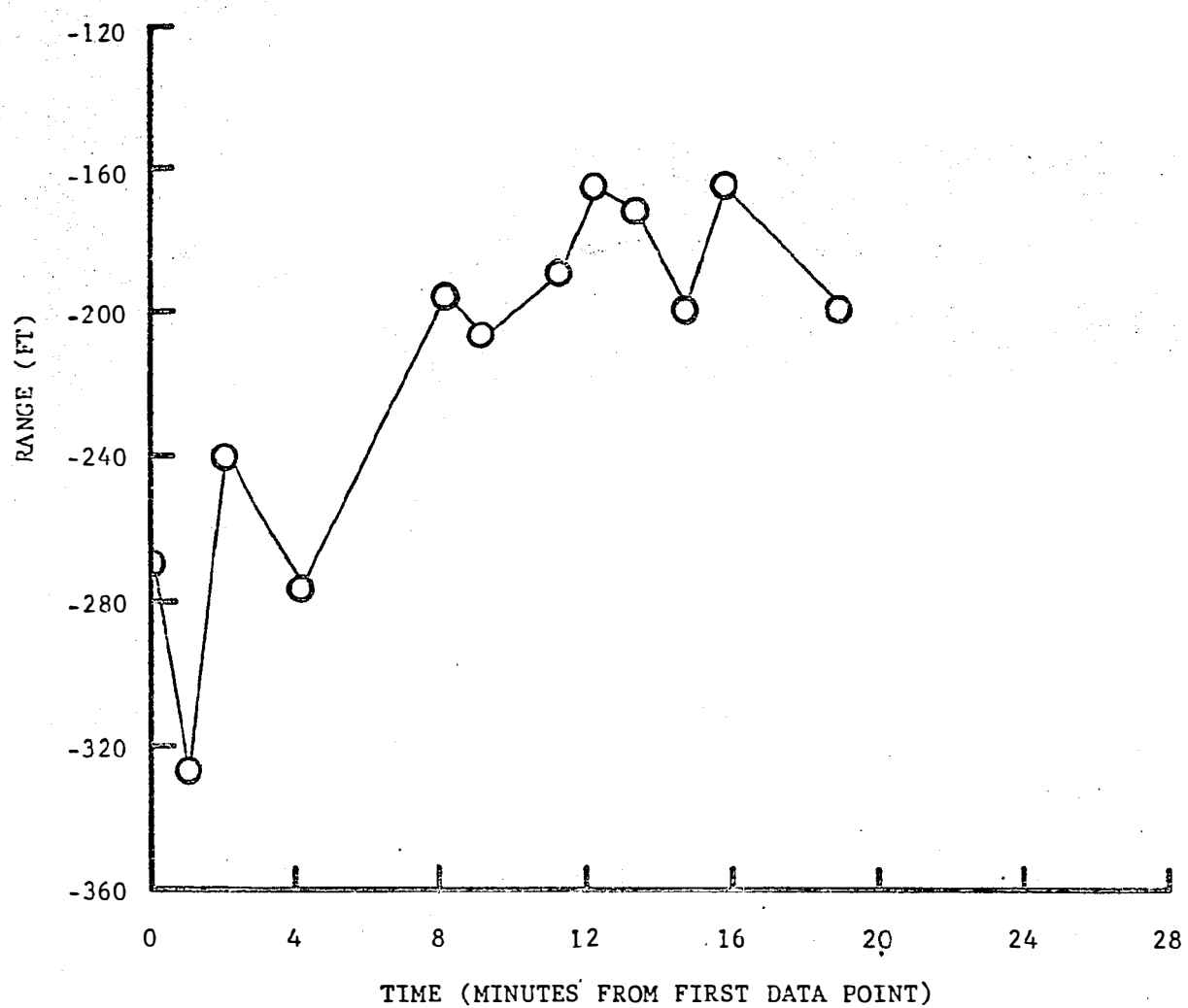


Figure 7-12 VHF Ranging Residuals (CDH to TPI)

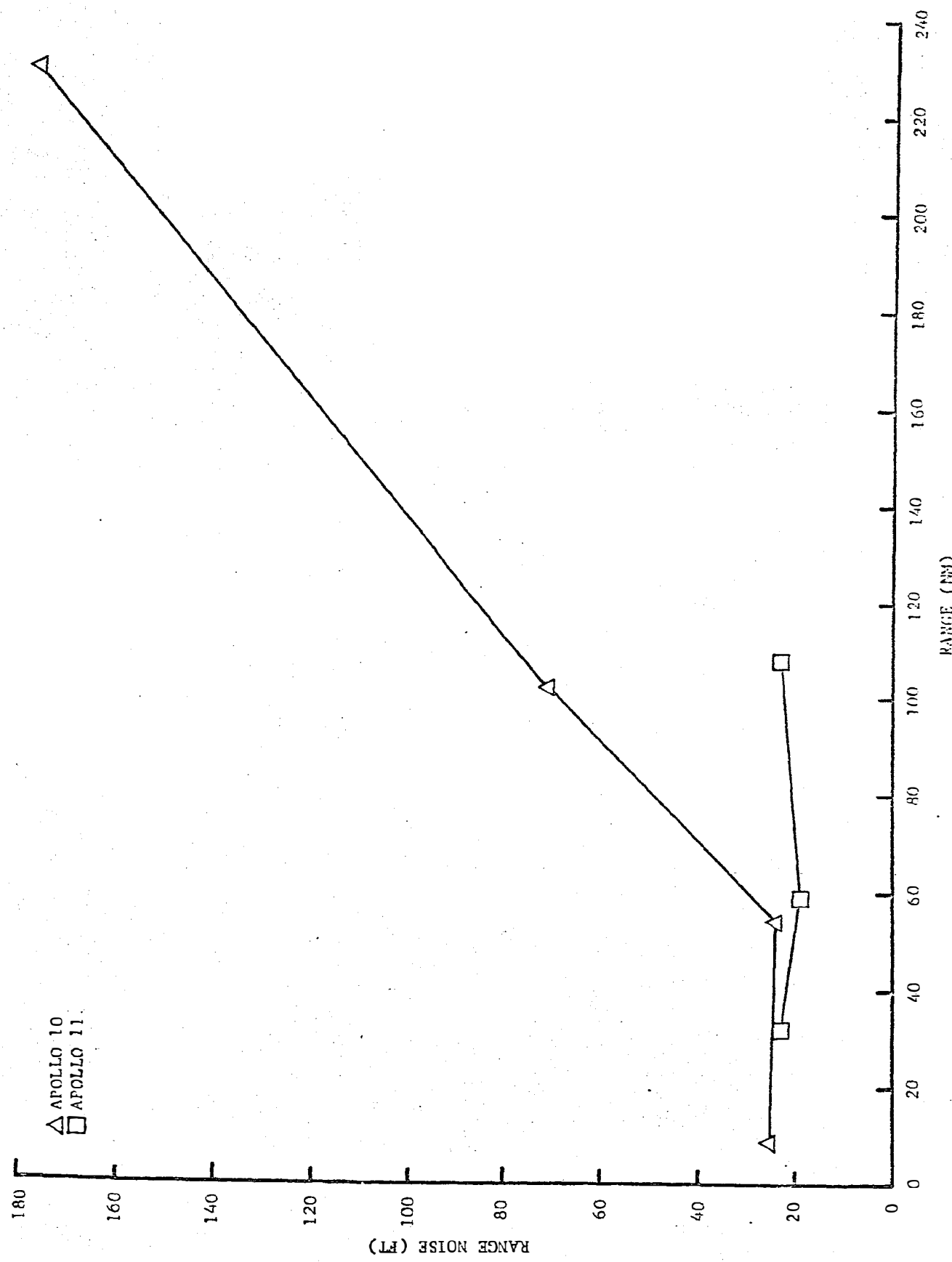


Figure 7-13 VHF Range Noise as a Function of Average Range

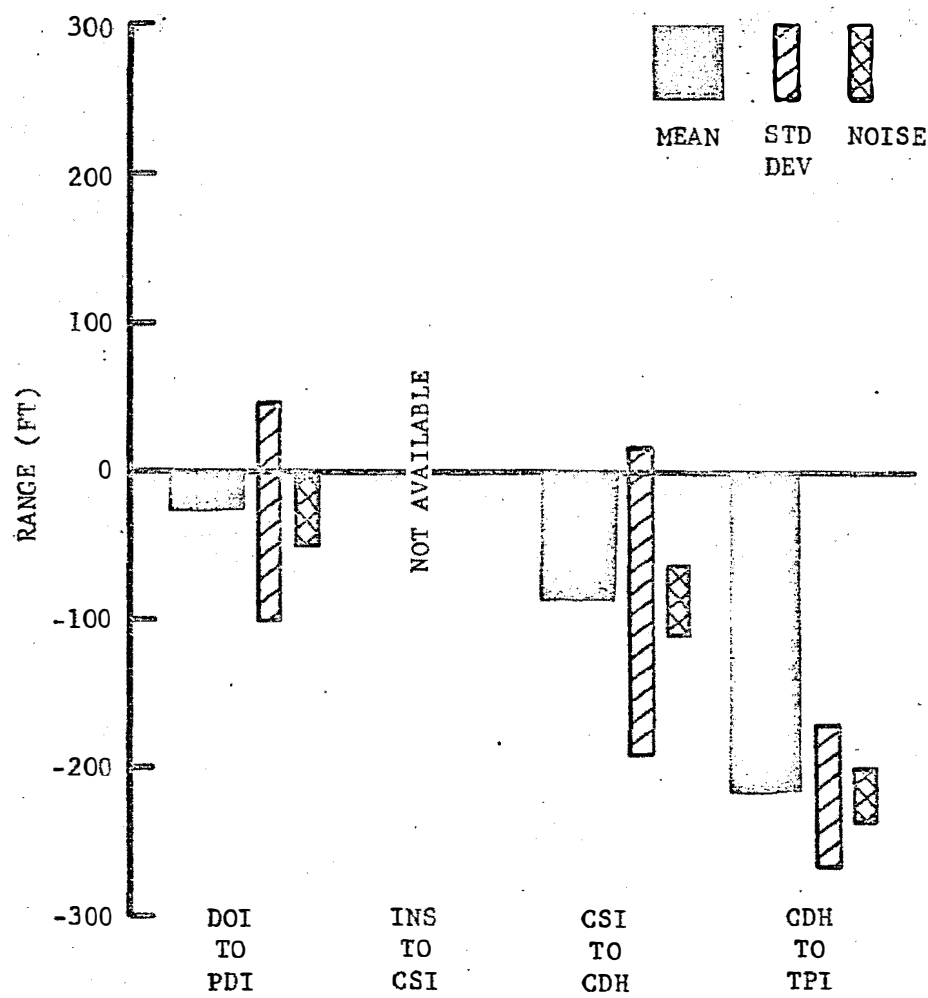


Figure 7-14 VHF Ranging Residual Statistics

Table 7.8 Summary of Sextant Residual Statistics

	DOI To PDI	Insertion To CSI	CSI To CDH	CDH To TPI	
Shaft (deg)	-.001	.0005	.0002	.0017	Mean
	.015	.005	.011	.013	S. Dev.
	.014	Insufficient Data	.010	.011	Noise
Trunnion (deg)	-.0004	-.00009	.0004	-.001	Mean
	.004	.003	.006	.008	S. Dev.
	.003	Insufficient Data	.006	.011	Noise

in four of the free flight segments; DOI to PDI (13 sightings), insertion to CSI (4 sightings), CSI to CDH (21 sightings), CDH to TPI (10 sightings).

The close agreement of the standard deviations with the noise estimates and the very small means listed indicate that there are essentially no biases in either angle.

The residual patterns (Figures 7-15 through 7-18) are very well behaved. The random noise estimates (Figure 7-19) compare well with rendezvous radar angular noise estimates and no trend can be identified with respect to average range. Note the good agreement with the Apollo 9 noise estimates plotted in Figure 7-19.

#### Onboard Tracking Data Consistency

In order to determine the consistency of trajectories reconstructed from onboard tracking data with those obtained from MSFN tracking data, state vector comparisons were made over the propagation intervals. These comparisons were made in a UVW-type coordinate system and the results are presented in graphic form. In the figures presented, RZ is the negative of the U or radial component, RX is the V or downrange component, and RY is the negative of the W or crossrange component of a system centered at the CSM. RXD, RYD and RZD are the respective velocities.

Three LM trajectories were obtained for the period from DOI to PDI. Figure 7-21 plots (as a function of time) the out-of-plane component of LM position relative to the CSM for a MSFN free flight trajectory, an onboard data free flight trajectory, and the final BET (combined high speed MSFN and onboard tracking data). It can be seen that the addition of onboard tracking data drastically improves this component of position. Figures 7-22 and 7-23 show the differences between relative trajectories obtained from the MSFN and from the onboard tracking free flight fits. There are large differences in the trajectories which are primarily due to the poor quality of the MSFN free flight fit, but the comparisons do show that the downrange and radial components compare fairly well inside the MSFN data arc.

Reproduced from  
best available copy

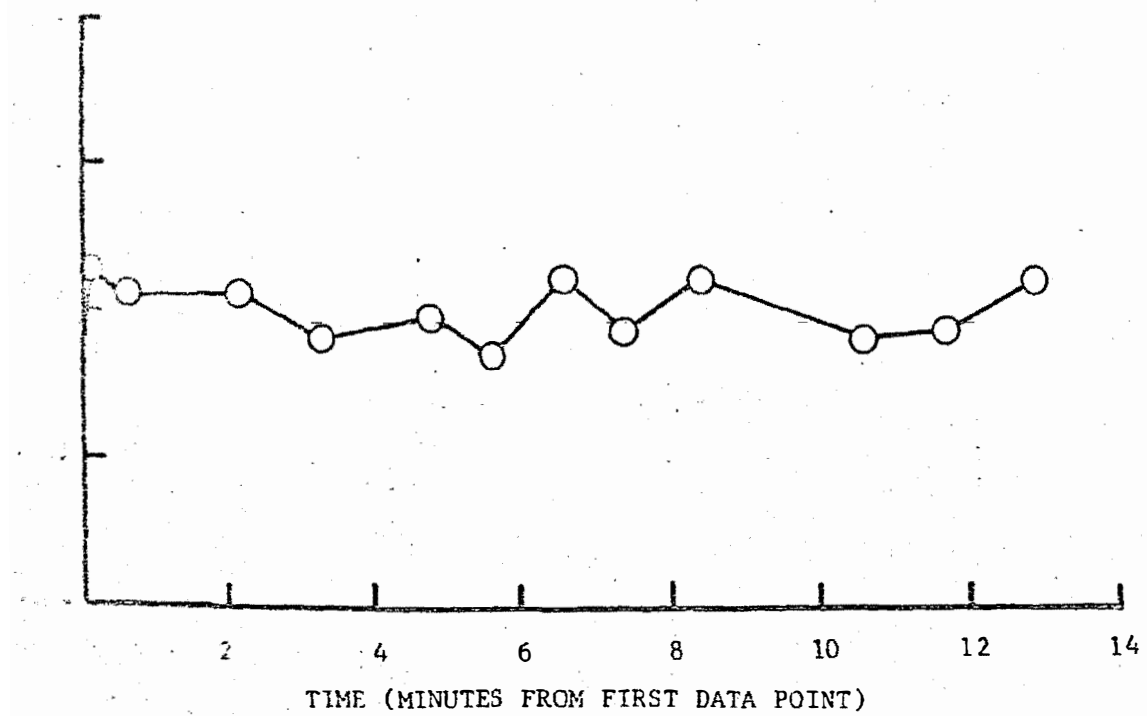
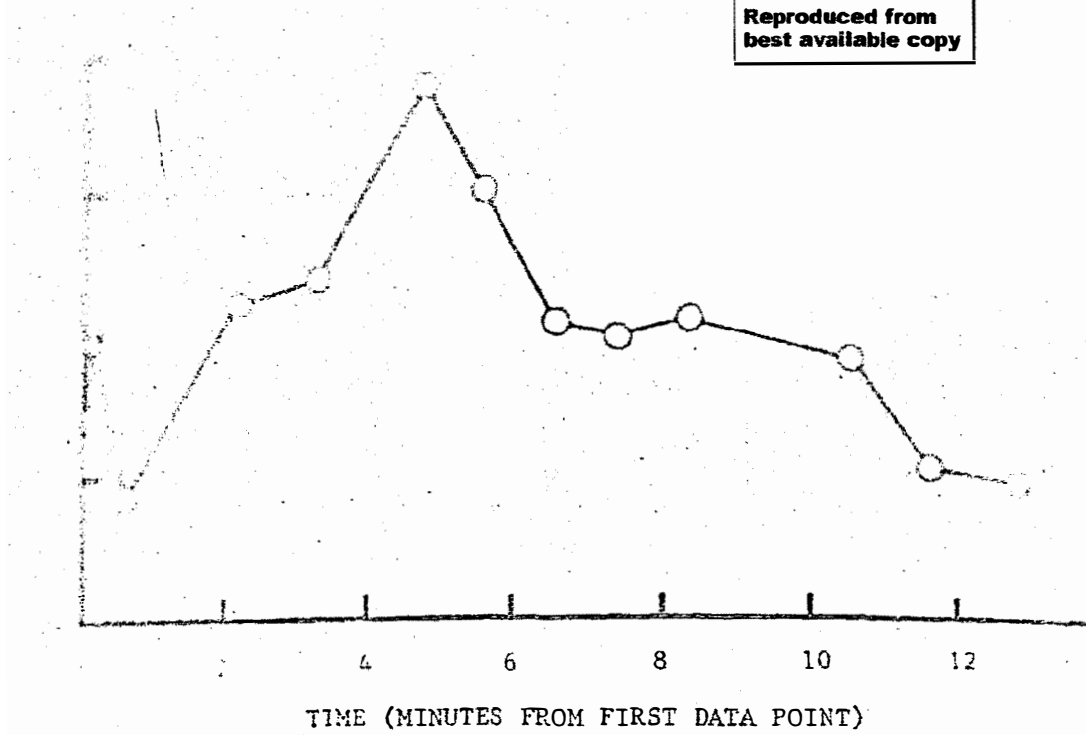


Figure 7-15 Sextant Residuals (DOI to PDI)

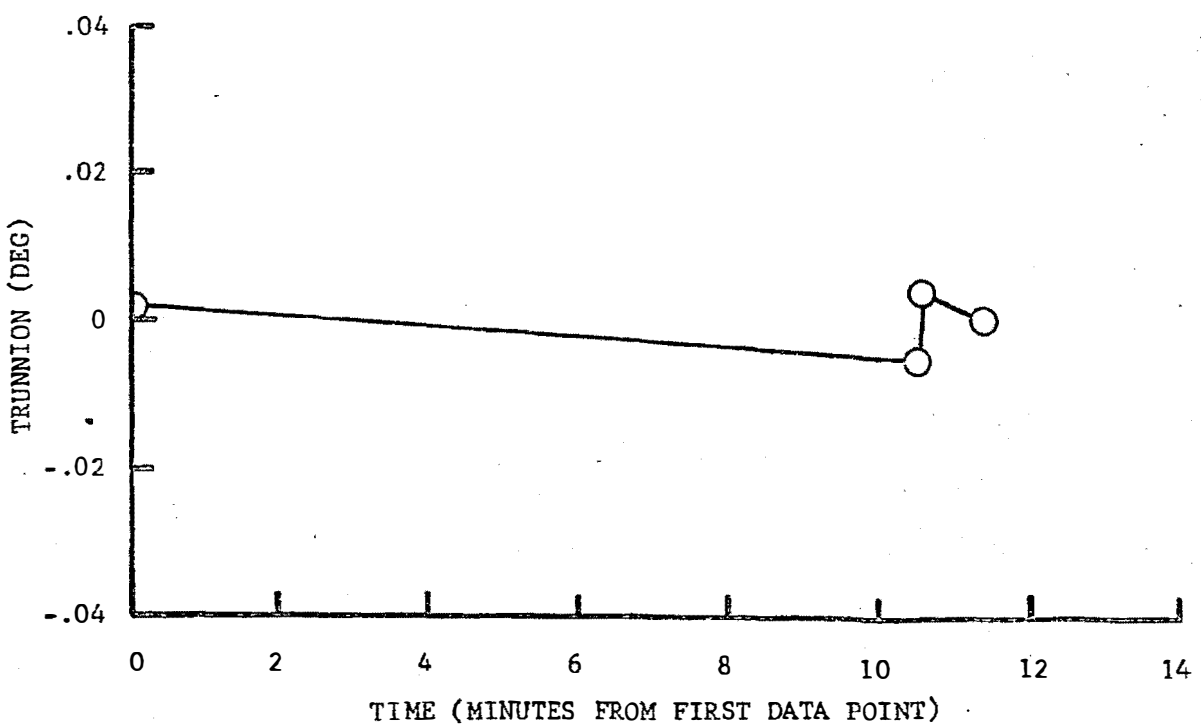
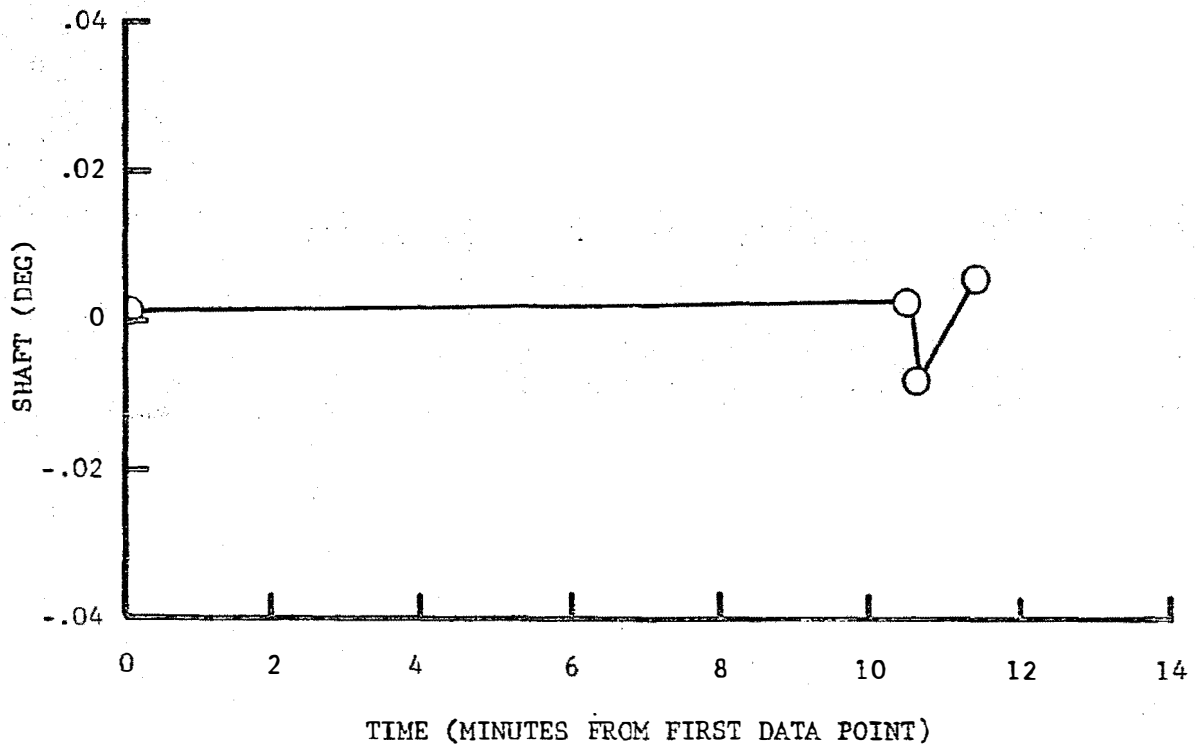


Figure 7-16 Sextant Residuals (Insertion to CSI)

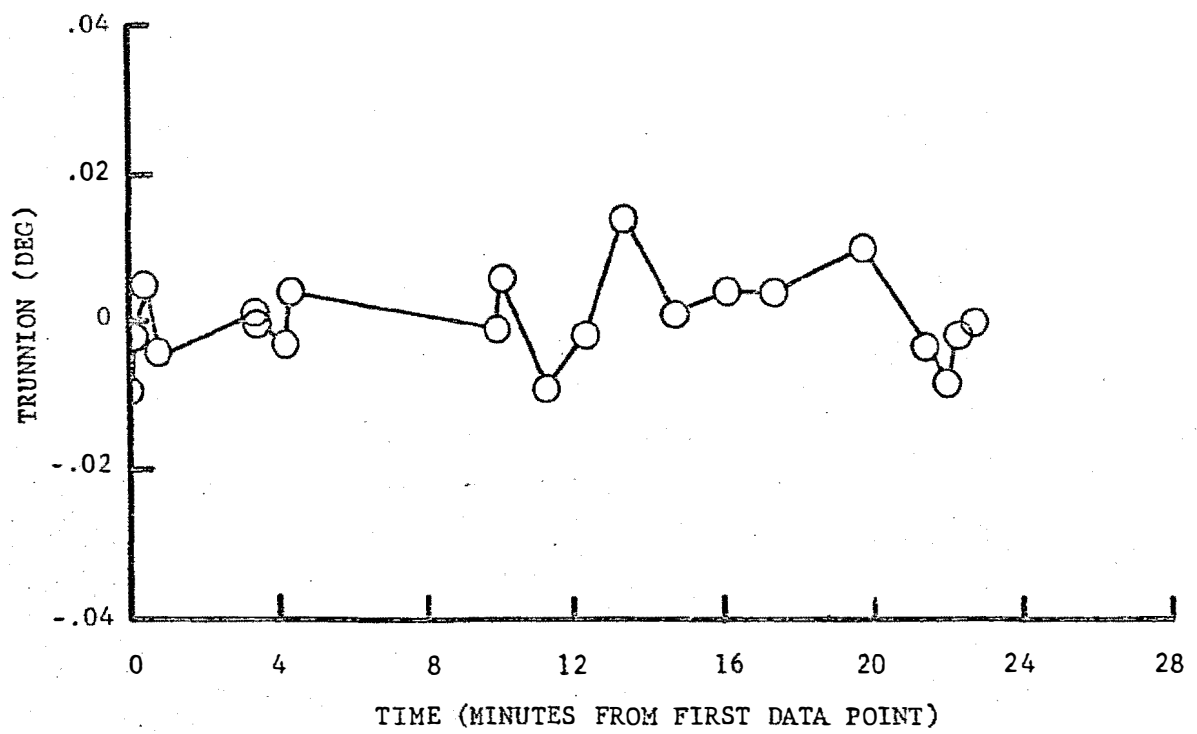
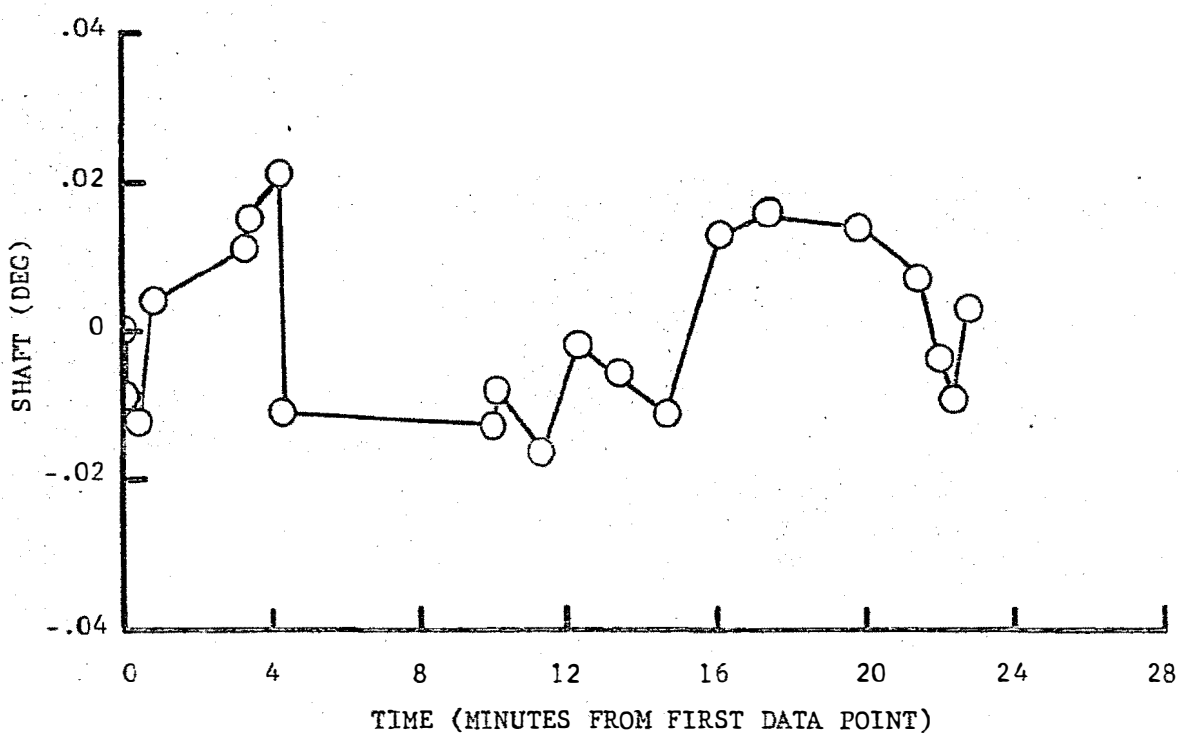


Figure 7-17 Sextant Residuals (CSI to CDH)

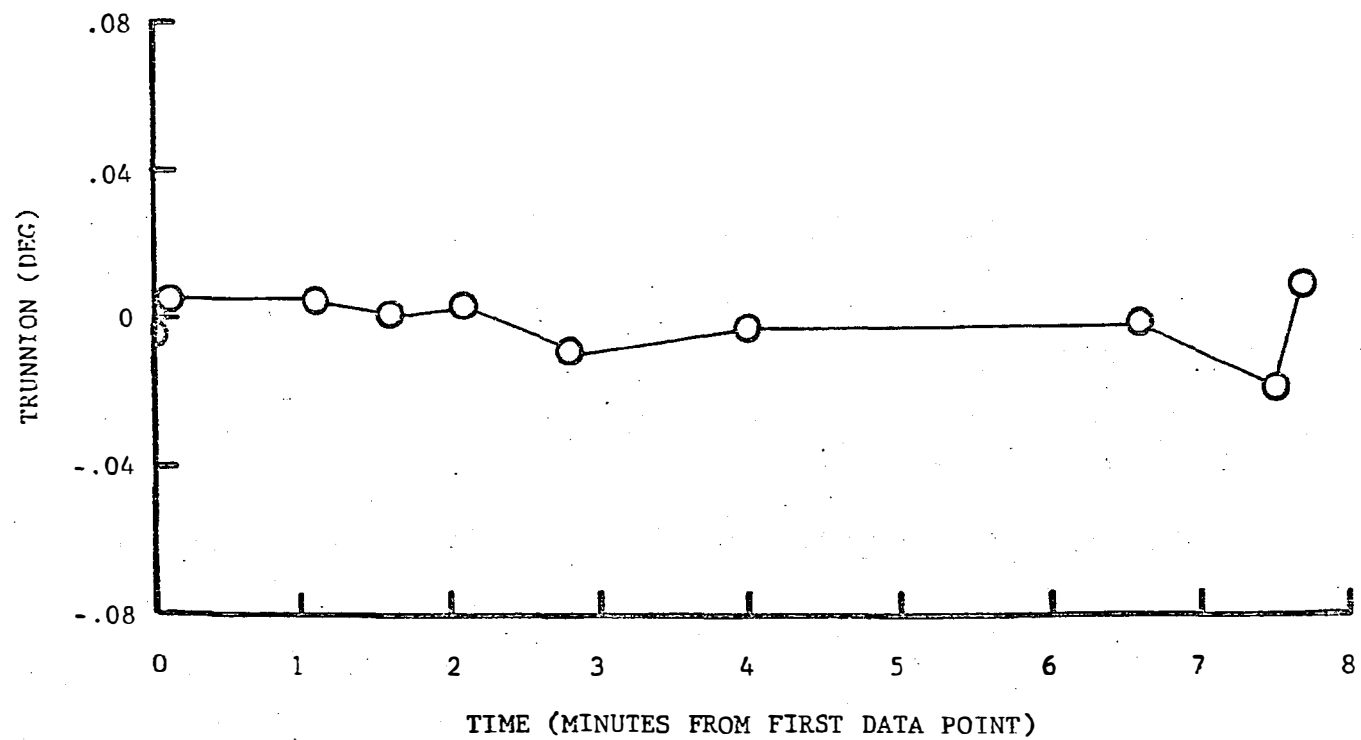
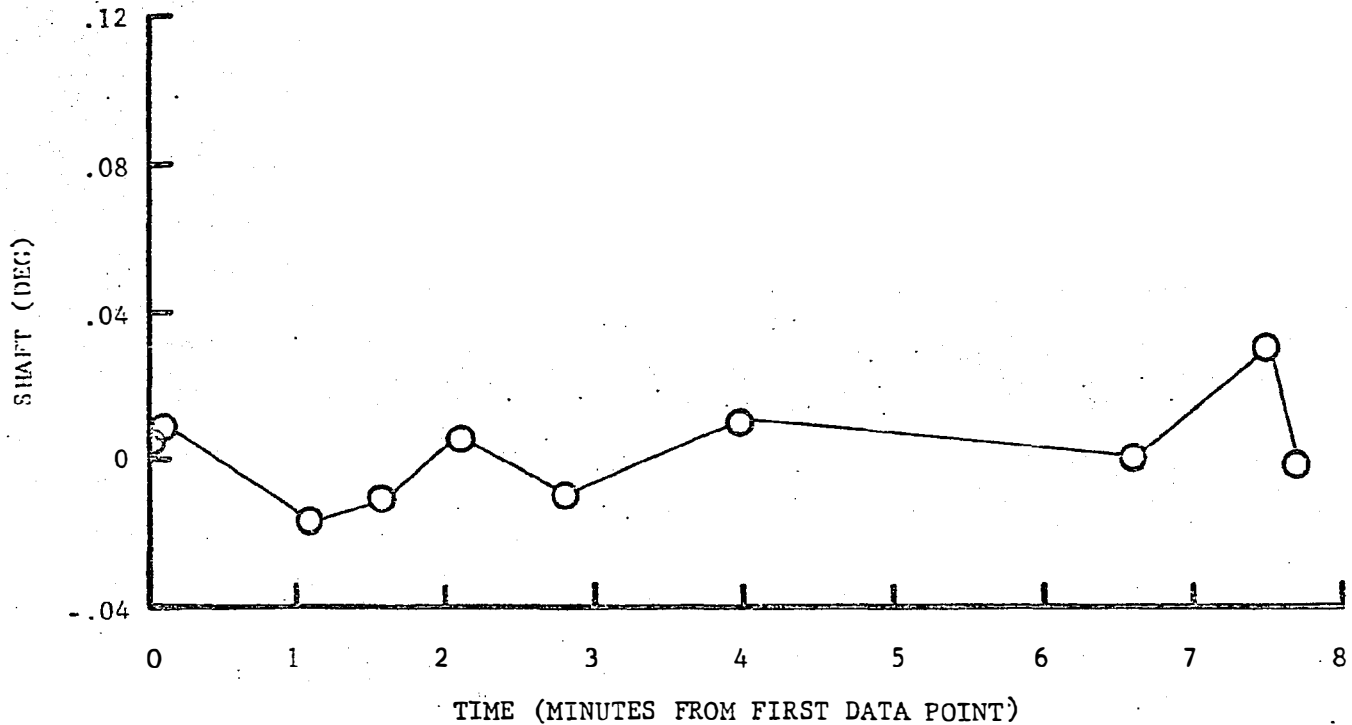
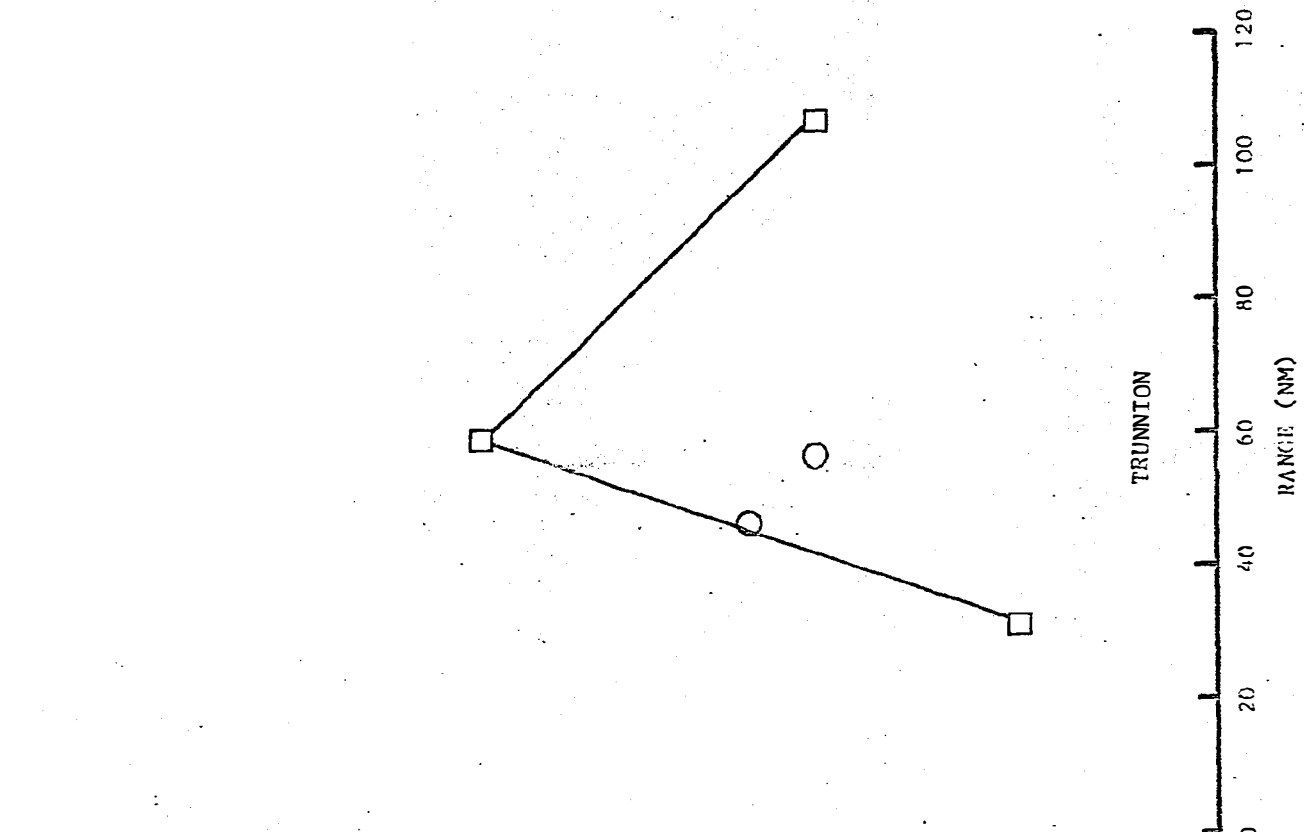
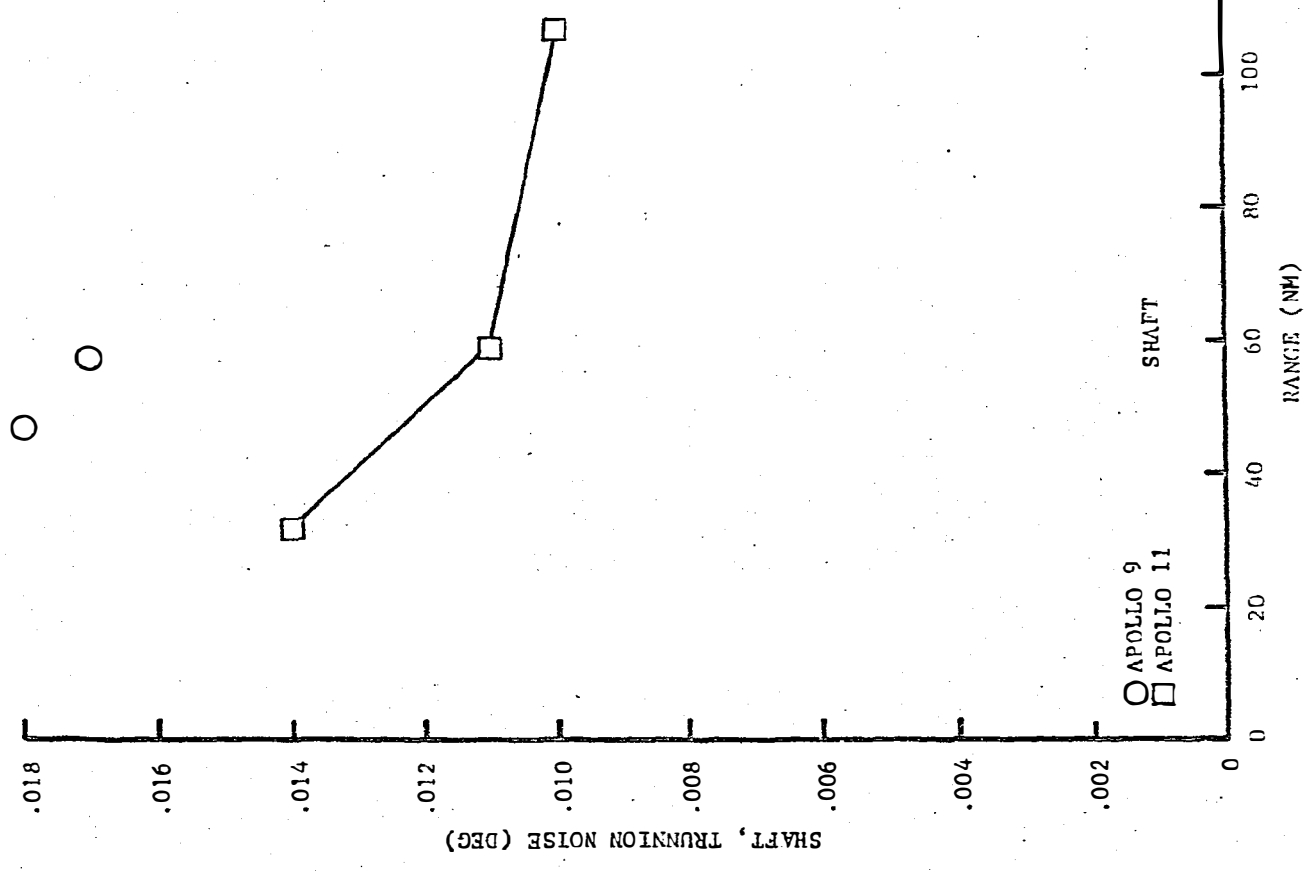


Figure 7-18 Sextant Residuals (CDH to TPI)



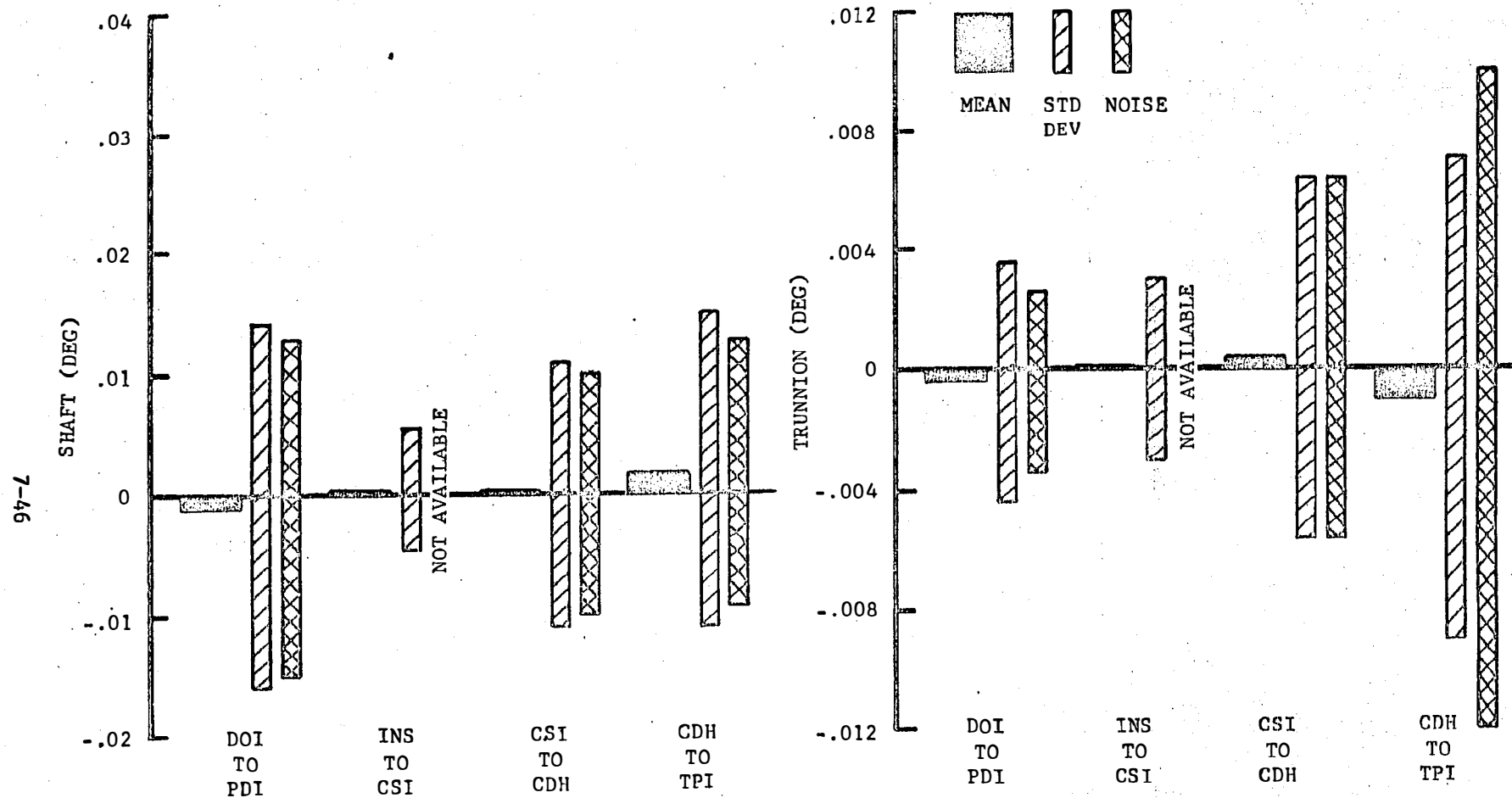


Figure 7-20 Sextant Residual Statistics

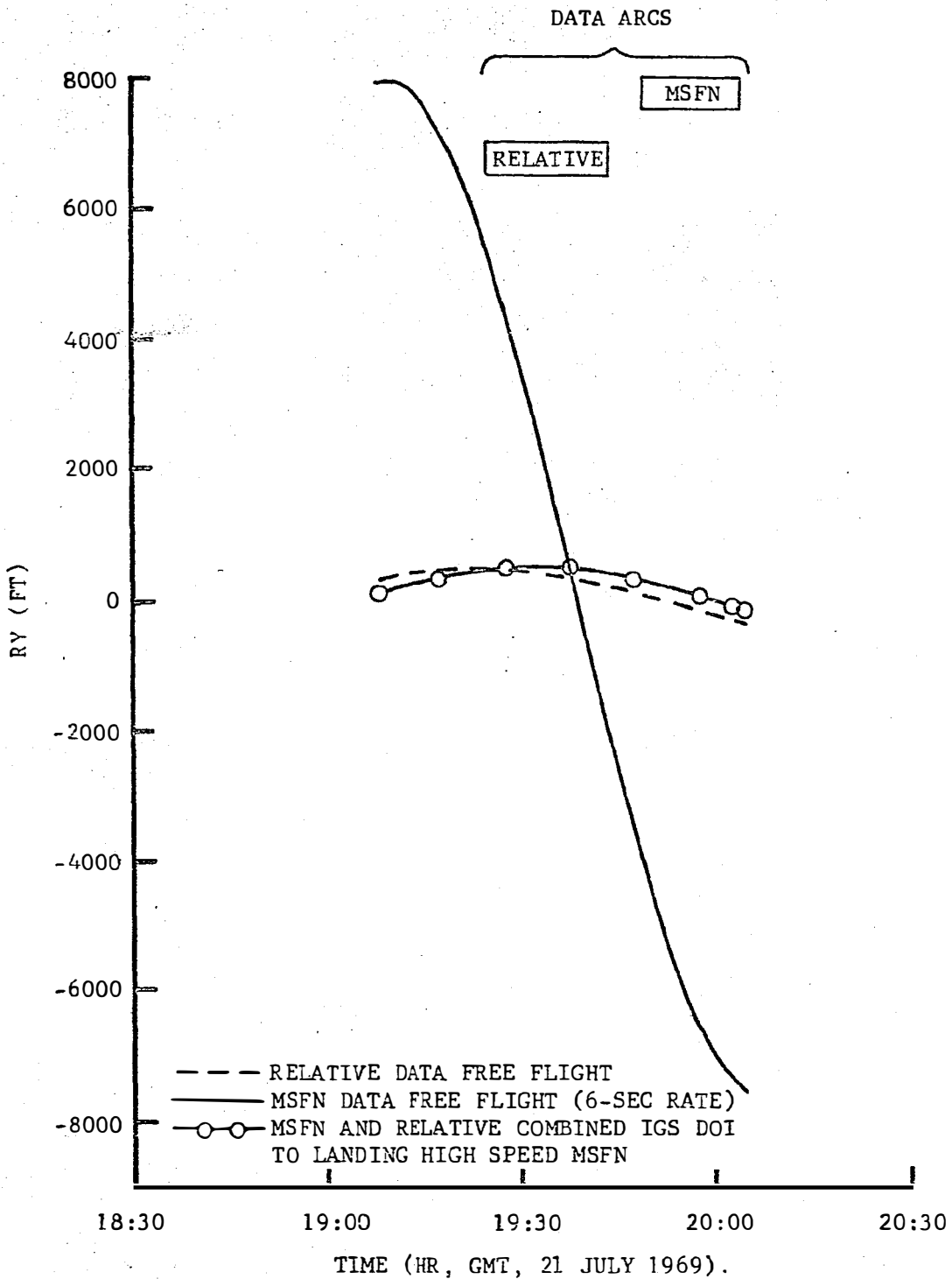


Figure 7-21 Out-of-Plane Component of LM Position Relative to CSM (DOI to PDI)

84-L

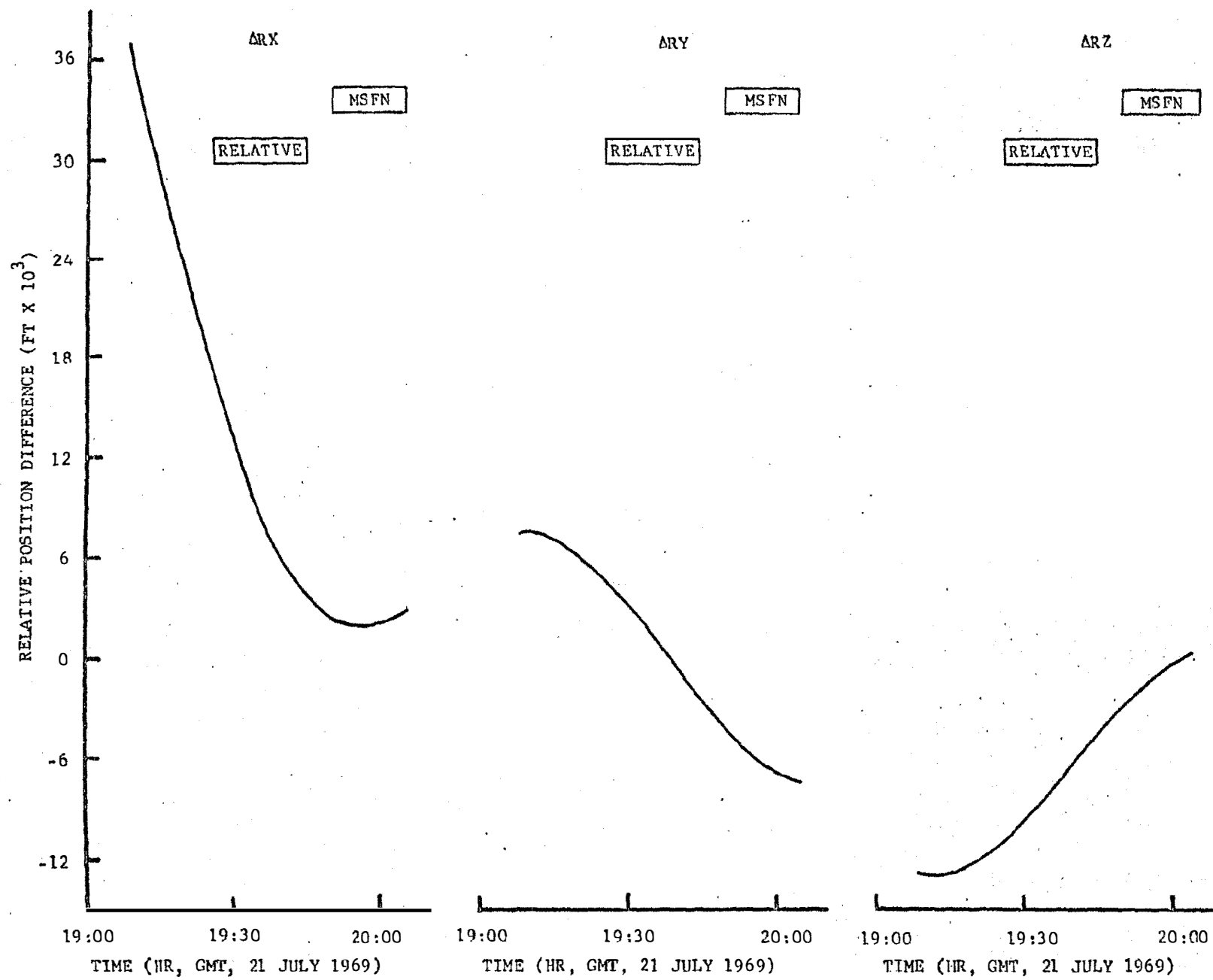


Figure 7-22 Differences Between Position Components of Relative Trajectories (DOI to PDI)

64-7

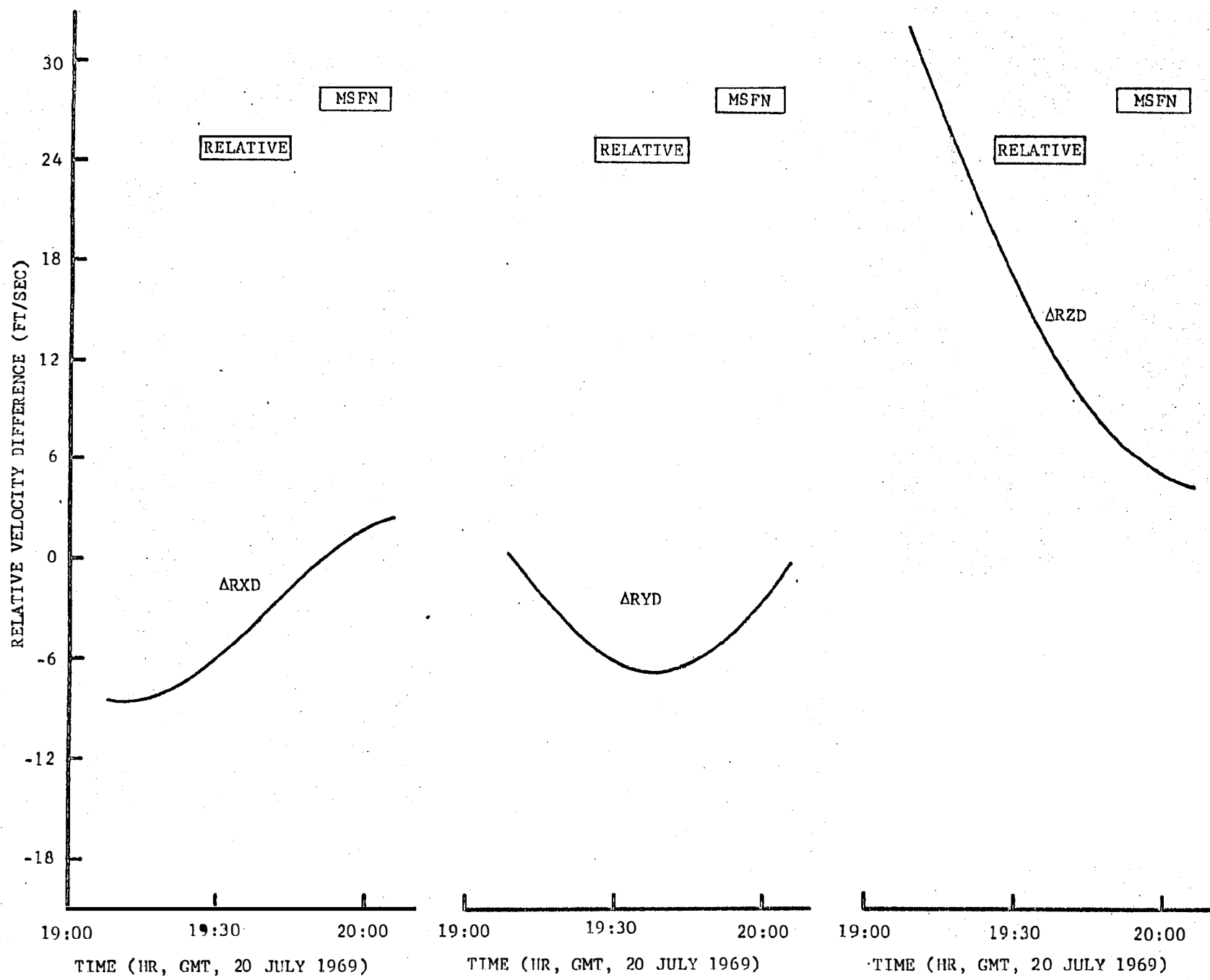


FIGURE 7-22. PLOTS OF THE THREE VELOCITY COMPONENTS OF RELATIVE MOTION FOR DAY 1969.

Figures 7-24 and 7-25 show the differences between position and velocity components of the two relative trajectories obtained for the Insertion to CSI period. These trajectories were obtained from a MSFN (low speed) data free flight fit and an onboard data free flight fit. Note that the differences between the RX and RZ components are nominal whereas the RY component (crossrange) is large. This characteristic is expected since onboard data fits produce a much better relative trajectory in the out-of-plane sense. Figure 7-26 illustrates the better crossrange position obtained from onboard data fits.

Figure 7-27 illustrates that the trajectory obtained from onboard tracking data eliminates three to four thousand feet of relative cross-range error which the MSFN data could not. The phase differences evident in Figures 7-26 and 7-27 result primarily from differences in the determination of the right ascension of the ascending node of the orbits. The results of this phase difference are very evident in the plot of the differences between out-of-plane position components of trajectories derived from MSFN and from onboard data (Figure 7-28 ( $\Delta$ RY)).

The important feature to note in these figures is that the trajectories based on onboard tracking data eliminate a large portion of the cross-range error present in independent MSFN fits for both vehicles. It is also interesting to note that in the out-of-plane position curves shown in Figures 7-26 and 7-27, that the trajectories produced from relative data match across the CSI burn much more closely than the fits produced from MSFN data. While this agreement does depend, to some extent, on a good match between the CSM trajectories, the relative data did produce a more continuous trajectory in the out-of-plane sense from one independent fit to another.

Despite the large out-of-plane differences, it can be seen that trajectories produced from onboard tracking data are generally consistent with MSFN based fits, especially in overlapping data arcs (Figures 7-24 and 7-28). Therefore, because of better characteristics in the relative sense, trajectories produced from relative tracking data are more suitable for detailed rendezvous analysis purposes.

15-2

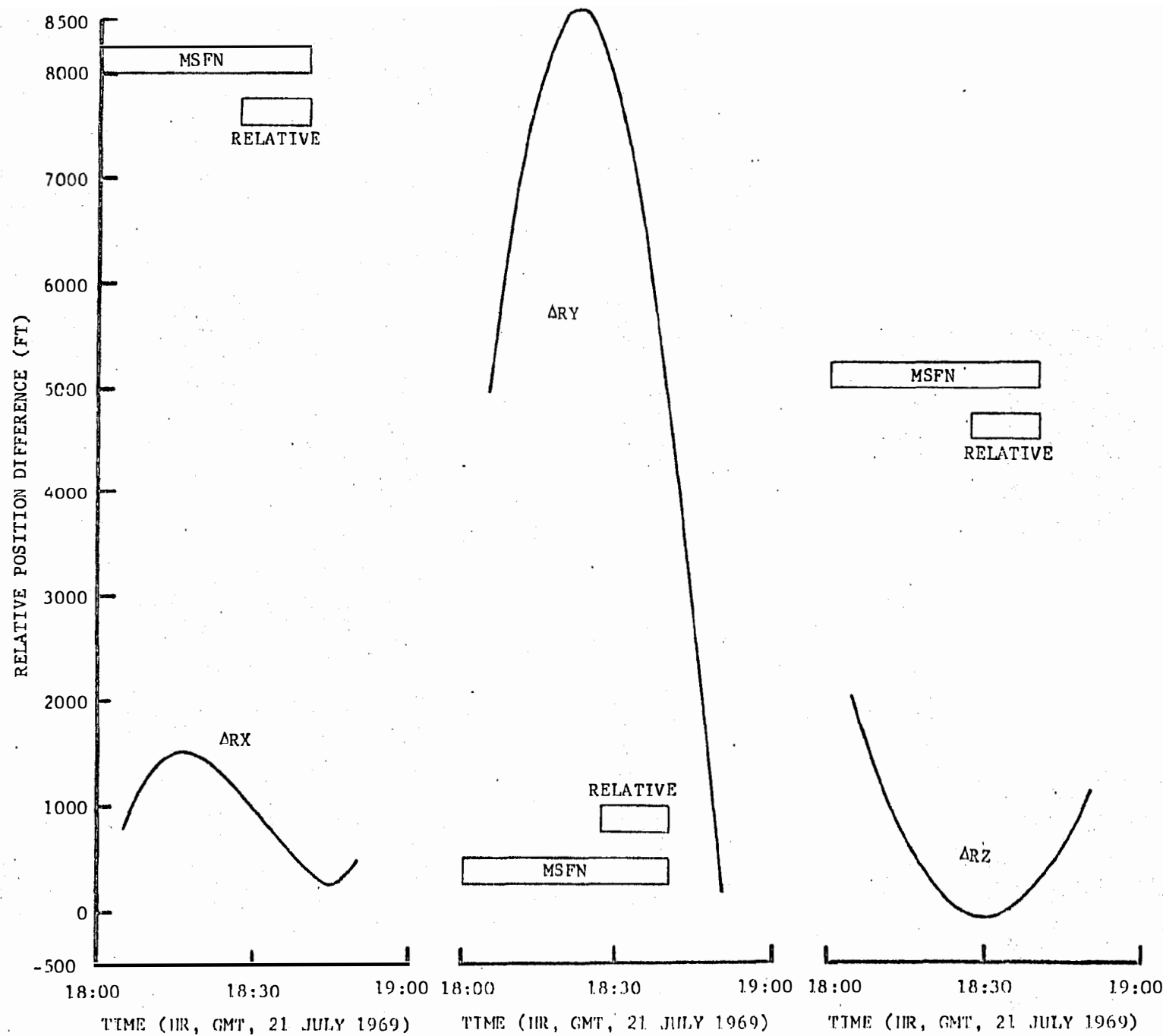


Figure 7-24 Differences Between Position Components of Relative Trajectories (Insertion to CST)

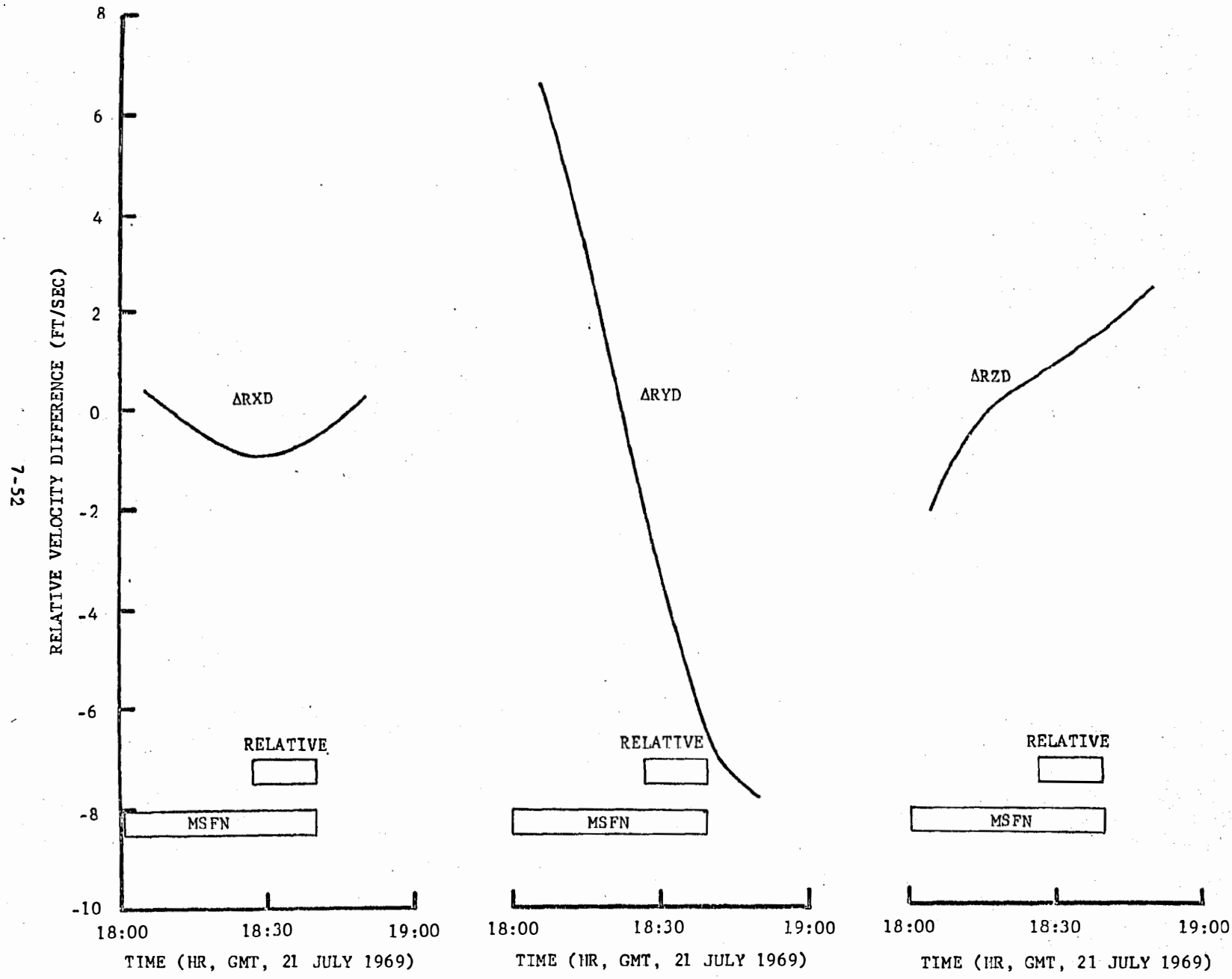


Figure 7-25 Differences Between Velocity Components of Relative Trajectories (Insertion to CSI)

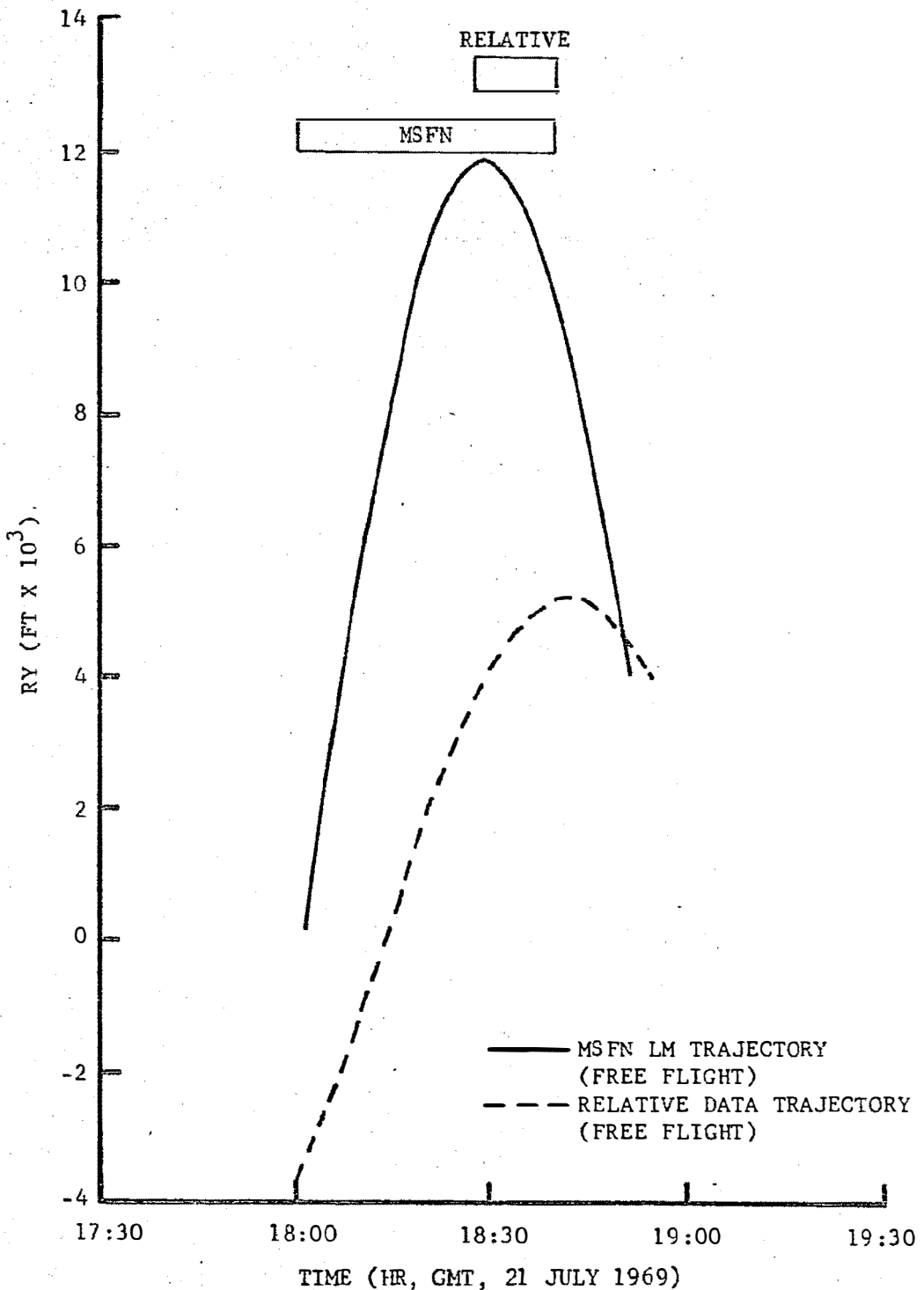


Figure 7-26 Out-of-Plane Component of LM Position Relative to CSM (Insertion to CSI)

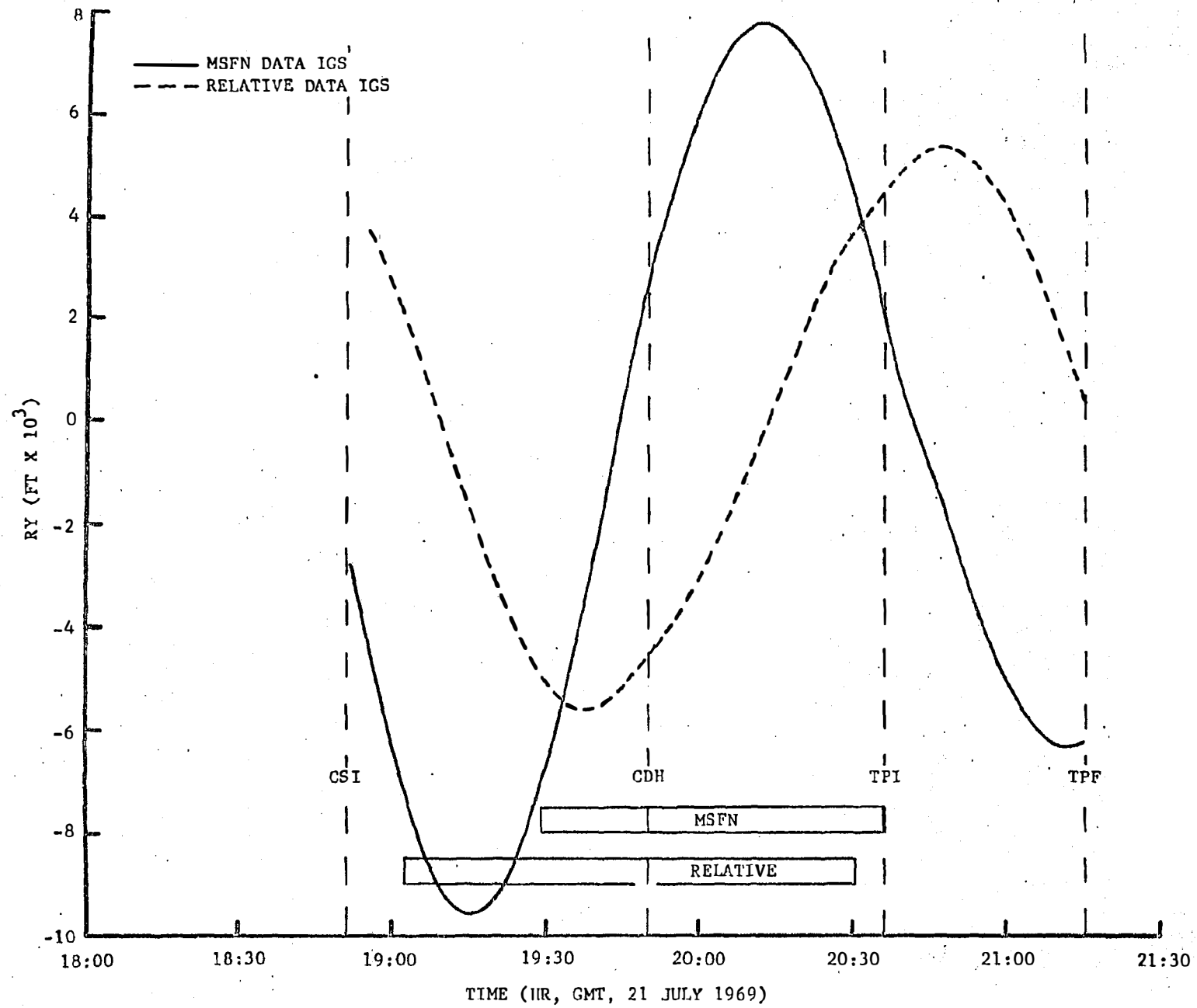


Figure 7-27 Out-of-Plane Component of LM Position Relative to CSM (CSI to TPF)

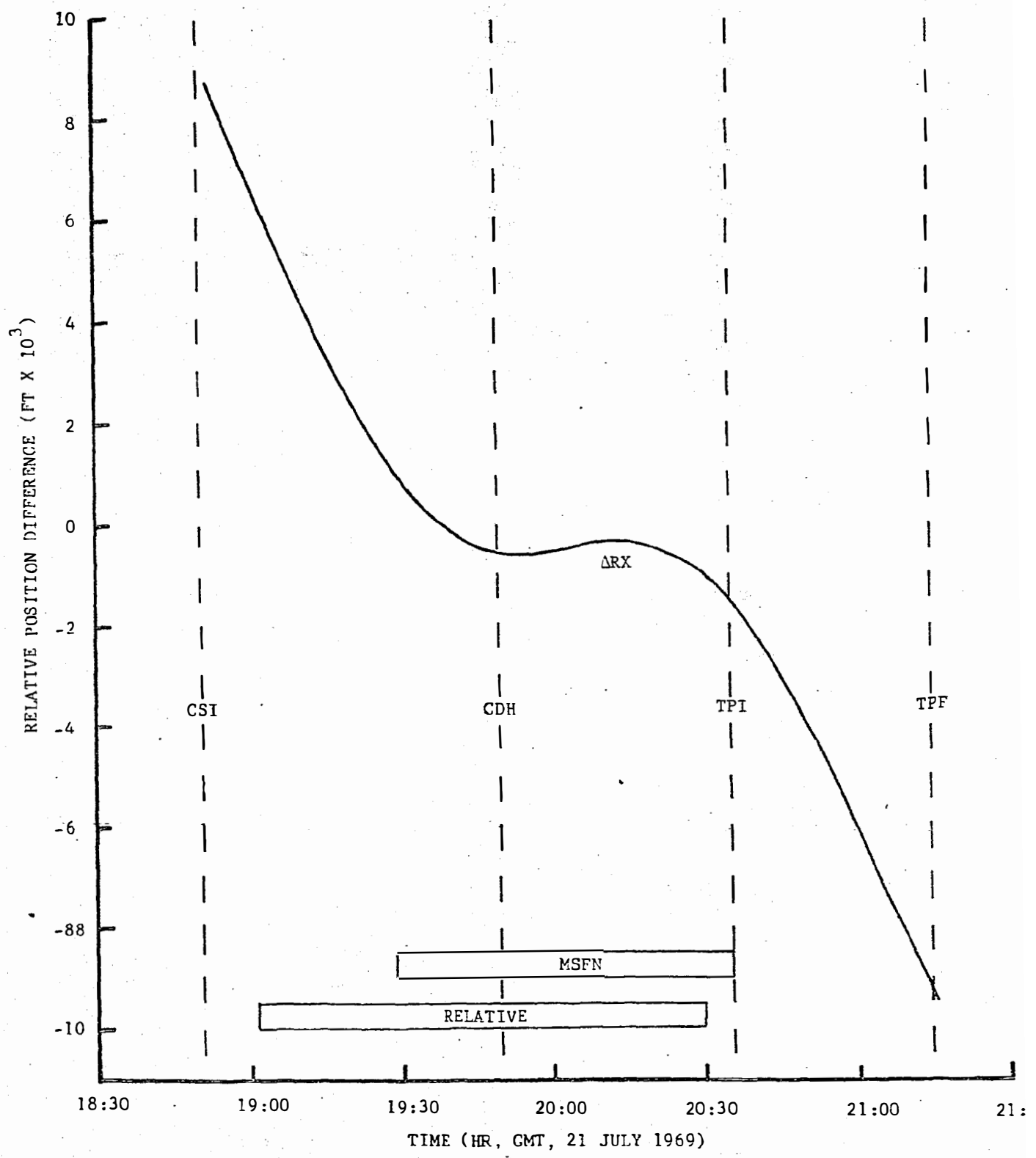


Figure 7-28 Differences Between Position Components of Relative Trajectories  
(CSI to TPF)

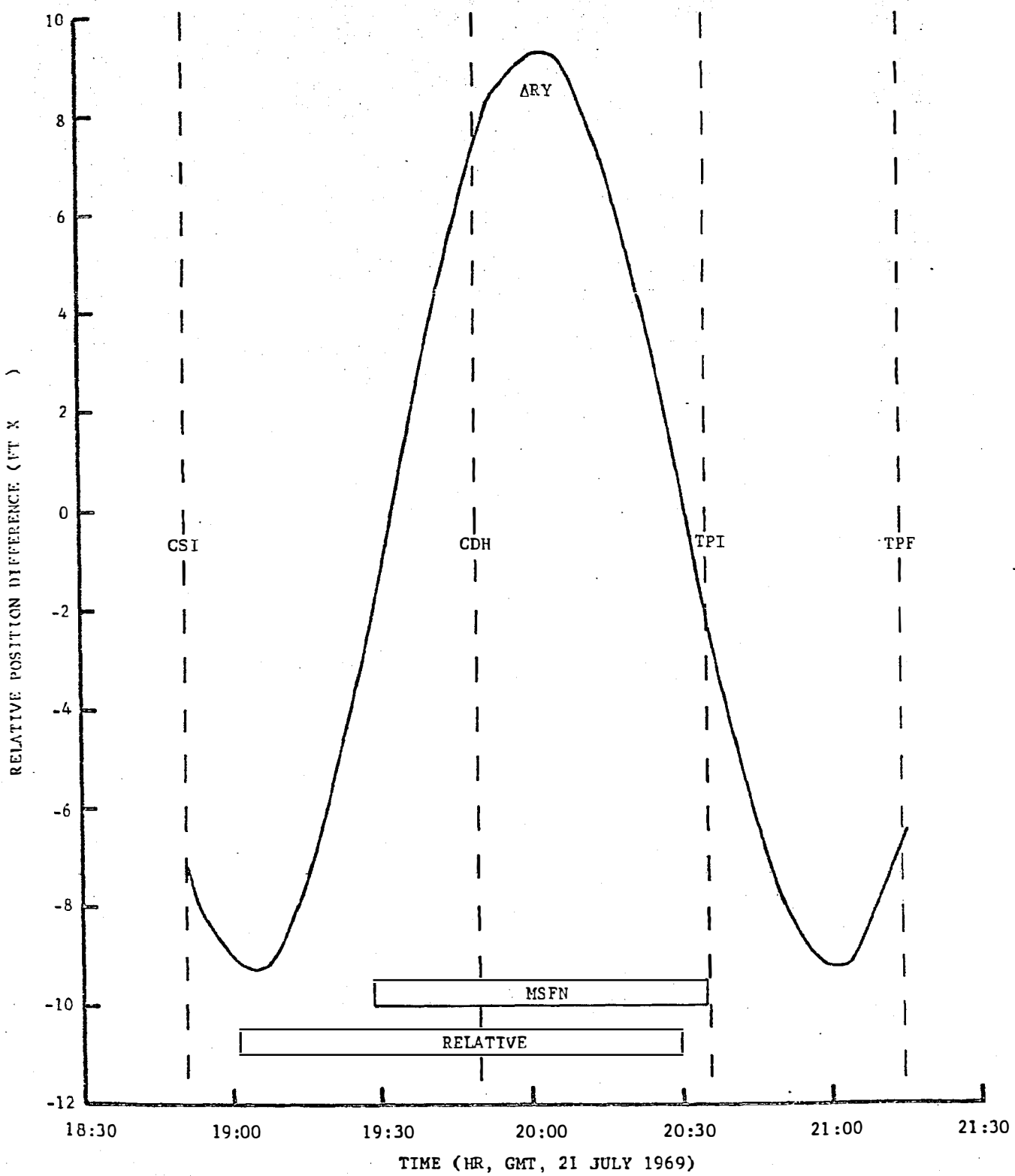


Figure 7-28 (Continued)

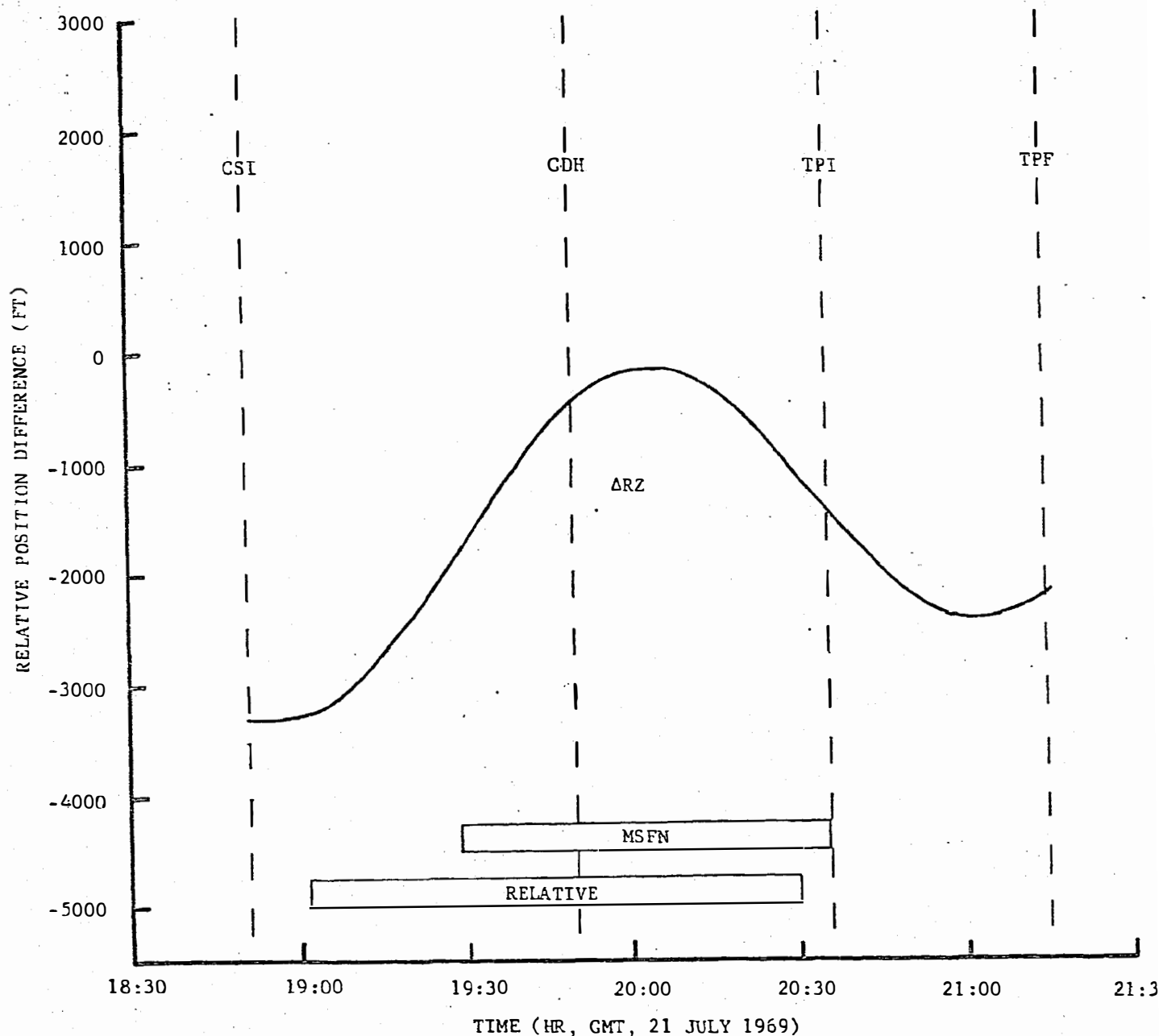


Figure 7-28 (Concluded)

85-L

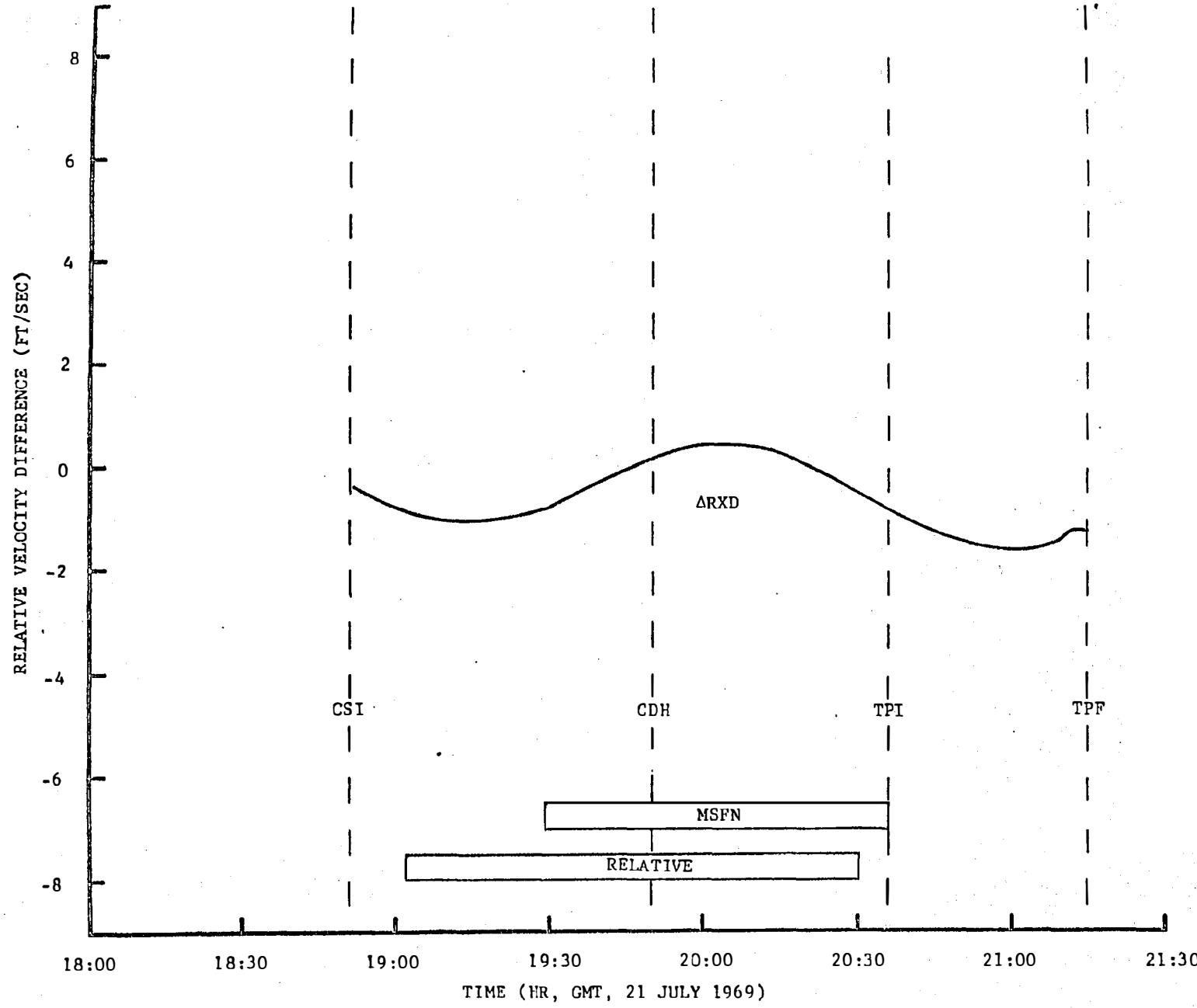
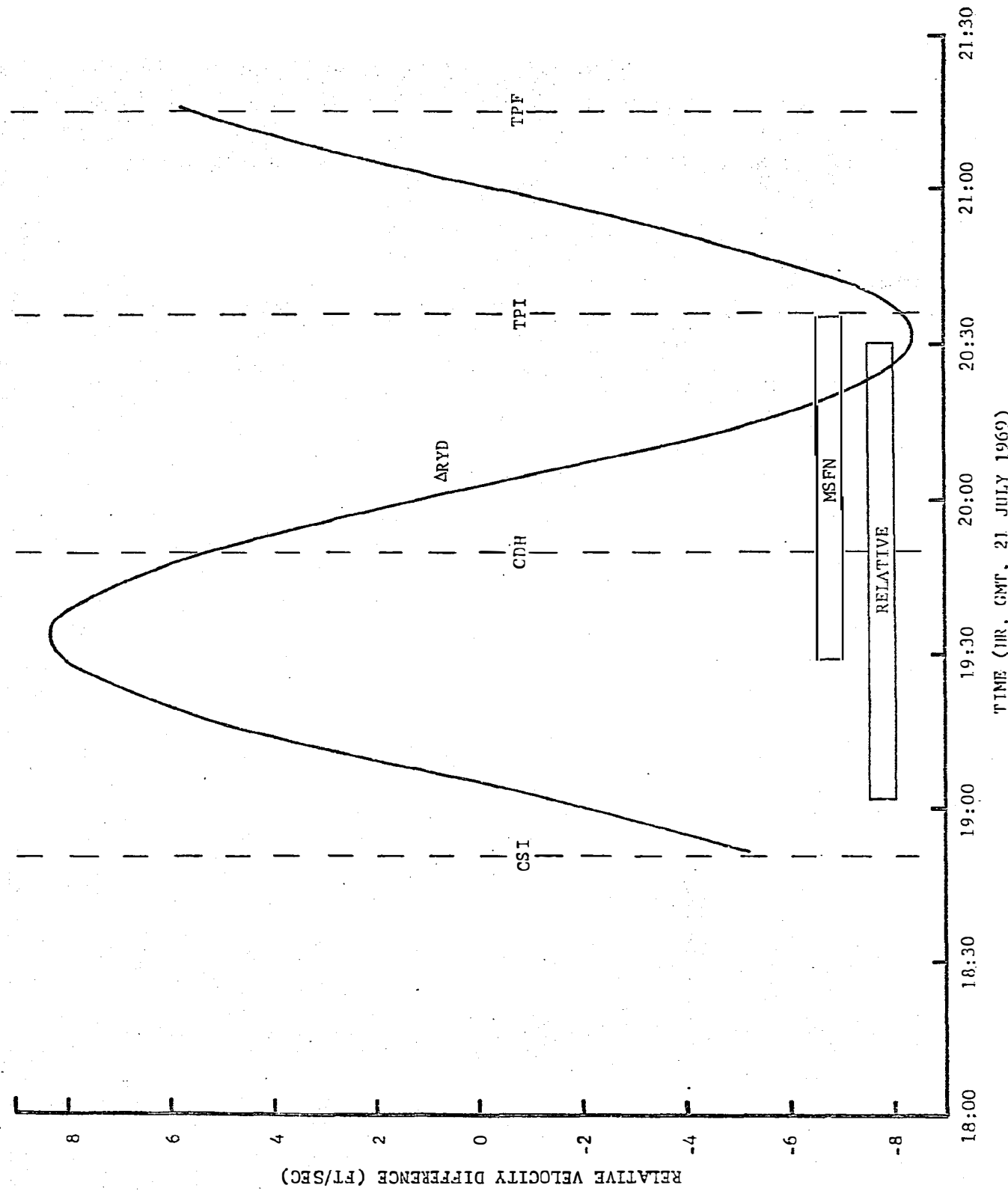


Figure 7-29 Differences Between Velocity Components of Relative Trajectories  
(CSI to TPF)



09-L

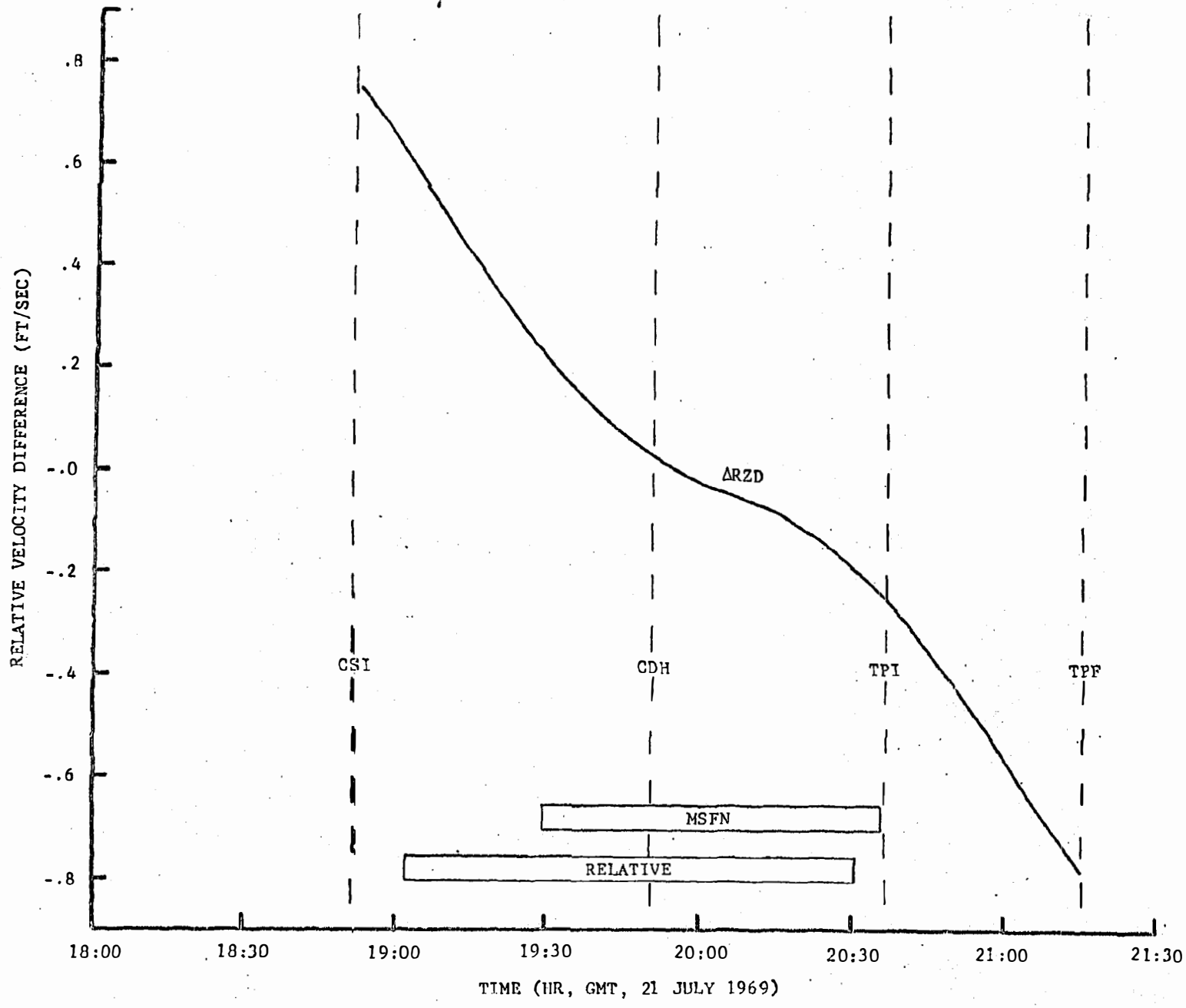


Figure 7-29 Concluded

**Table 7.9 Comparison of Rendezvous Radar Noise Estimates with Specification Requirements**

Free Flight Segment	Average Range (n. mi.)	Angular Noise		Range Noise	
		$3\sigma$ (deg) Est.	Spec.	$3\sigma$ (feet) Est.	Spec.
INS to CSI	140	.049	.1146	117.	2126.
CSI to CDH	107	.038	.1146	111.	1627.
CDH to TPI	59	.037	.1146	81.	890.

**Table 7.10 Comparison of VHF Ranging and Sextant Noise Estimates with Specification Requirements**

Free Flight Segment	Average Range (n. mi.)	Sextant Angular Noise		VHF Ranging Range Noise	
		$3\sigma$ (deg) Est.	Spec(1)	$3\sigma$ (feet) Est.	Spec.
DOI to PDI	32	.043	-	69.	180.
INS to CSI	140		NA		NA
CSI to CDH	107	.035	-	69.	180.
CDH to TPI	59	.047	-	57.	180.

(1) No specification value was available.

### Specification Comparisons

Table 7.9 compares the  $3\sigma$  values of noise estimated from the rendezvous radar residuals with specification requirements. It can be seen that the estimates were all well within specification limits. Noise estimates for the sextant and VHF ranging data are listed in Table 7.10. Although no specification value was found for the sextant, the values obtained (RSS of individual angle noise estimates) were all within acceptable limits. The VHF ranging noise estimates also compare well with specifications.

### Conclusions

The following conclusions were drawn from the analysis.

1. The onboard data was generally of good quality. The sextant data, examined for the first time, appeared to be as accurate as the rendezvous radar angular measurements.
2. Estimates of data random noise were all within specification and expected values.
3. Trajectories produced from onboard tracking data proved to be generally consistent with those produced from MSFN data. It was found that a method used in the past to demonstrate trajectory consistency was inadequate. On Apollo 10, trajectories were compared only at selected times. Because of the significantly large phase differences found to be present in relative trajectories, the values for out-of-plane position differences obtained at selected times may be misleading. The out-of-plane position components must be plotted as a function of time in order to see the total differences in the trajectories.

## 7.4 LANDING RADAR DATA ANALYSIS

The landing radar data analysis consisted of generating and evaluating landing radar residuals (difference between observed measurement and computed measurement) and mapping of the lunar surface profile and ground-track with the slant range measurement.

The landing radar data were obtained by processing the downlink telemetry data with a special purpose computer program which outputs onboard observations on punched cards in a HOPE-compatible format.

The HOPE Program was used to compute simulated landing radar observables from selected LM trajectories and from auxiliary information such as REFSMAT, gimbal angles, and radar operating mode. The LM trajectories were generated by the HOPE Program utilizing telemetered acceleration data in the IGS burn option to model the descent burn. Residuals were then formed by subtracting the computed from the actual observable value. Paragraph 7.4.2 presents statistics and selected plots of residuals obtained from various LM state vectors.

Terrain mapping data were obtained from a small, special purpose computer program designed to compute terrain altitude above a mean lunar radius as a function of latitude and longitude. The results of an attempt to correlate this terrain data with lunar contour maps are presented in Paragraph 7.4.3.

### 7.4.1 Descent Trajectories

Six different descent trajectories were examined in the landing radar data analysis. The origins of these trajectories are summarized as follows:

- (a) RTCC - This vector was obtained in the RTCC in real time.
- (b) MSFN (LS) - This vector was obtained from an IGS fit using low speed MSFN data obtained from acquisition of signal to LM touchdown (revolution 14). The doppler data were compacted to two observations per minute.
- (c) Onboard - This vector was obtained from a free flight fit using CSM sextant and VHF ranging observations. The technique required fixing the CSM trajectory as a reference and updating the LM state from onboard observations and the CSM reference trajectory.

- (d) BET #3 - The MSFN state vector described in item (b) above, was used as the basis for this trajectory. The BET #3 was obtained by correcting the MSFN low speed state with a linear error analysis program so that the resultant powered descent trajectory would impact a desired landing site with a relative velocity of zero. The landing coordinates used as reference were the MPB photographic estimate.
- (e) Lear - High speed MSFN data (ten samples per second) obtained over a 232 second data arc just prior to PDI were fit by the Lear Powered Flight Processor producing this state vector.
- (f) Onboard/MSFN (H-S) - This trajectory was obtained with the HOPE Program and used high speed MSFN doppler data which had been compacted to 30 observations/minute and from CSM sextant and VHF ranging data using the HOPE orbit determination program. The descent burn was modeled by the HOPE IGS burn option. The HOPE weighted least squares solution vector included position and velocity at epoch (which was prior to PDI), and Y platform misalignment. The tracking data interval was from DOI to LM touchdown. Figure 7-2 shows the tracking data timeline.

In order to gauge the quality of the landing radar data, it was necessary to determine that the above trajectories did accurately represent the actual descent trajectory. This quality judgement was based largely on the landing point conditions obtained from each trajectory. These landing sites obtained from each trajectory are summarized graphically in Figure 7-30. Note that both the BET #3 and the Onboard/MSFN H-S estimates are very close to the 16mm photographic estimate (accepted as the best estimate).

Since the data type being examined is a velocity measurement, it is most important that the reference trajectory be virtually free of velocity errors in the data arc. The onboard/MSFN H-S trajectory contains a large velocity error at landing where the BET #3 was constructed in such a manner that the velocities are zero at landing. Therefore, the BET #3 was chosen as the basic reference upon which to base the analysis of landing radar velocity residuals.

#### 7.4.2 Landing Radar Velocity Residuals

Table 7.12 lists the velocity residual statistics obtained from all the trajectories considered in the analysis. Note the small mean values obtained from the reference trajectory (BET #3). In the absence of a

real standard of comparison, the mean values obtained from BET #3 were reasonably small. Standard deviations indicate that  $V_{YA}$  and  $V_{ZA}$  are somewhat more erratic than  $V_{XA}$ . However, these values are still of reasonably good quality as shown by Figures 7-31 through 7-33. These figures show the BET #3 velocity residuals plotted versus time. In addition, specification limits have been plotted. Note that a few points fall outside specification.

It is difficult to isolate measurement errors from trajectory errors in this particular case. The descent trajectory is a particularly difficult one to reconstruct, and the landing radar velocity data are particularly sensitive to trajectory errors. Notice that the velocity residuals in Figures 7-31 through 7-33 tend toward zero at landing where the BET #3 velocities were constrained to zero. In contrast, the trajectory obtained from the Onboard/MSFN H-S fit is known to contain velocity errors at landing. The resultant total velocity at landing was 8.02 fps, with the primary contribution in the Z direction (North). The residual statistics show a mean value for  $V_{YA}$  of 6.966 fps. Since  $V_{YA}$  was directed roughly North, the large mean value reflects the -7.96 fps in the Z component of velocity at landing. The residuals obtained from the Onboard/MSFN H-S fit are plotted in Figures 7-34 through 7-36.

The residual statistics listed in Table 7.12 also indicate that the best trajectories do produce the best landing radar velocity residual statistics, that is, the BET #3 and the Onboard/MSFN H-S trajectories produce the smallest residual mean values. This fact, together with the sensitivity which the data has exhibited to trajectory velocities indicate that descent trajectory reconstruction activities will be aided considerably by the landing radar velocity data.\*

---

\* Subsequent reconstructions using landing radar data have produced a trajectory landing at acceptable coordinates (Lat. = .649 deg, Long. = 23.490 deg) with a total relative velocity of .96 fps. A report of this reconstruction will be forthcoming under a separate cover.

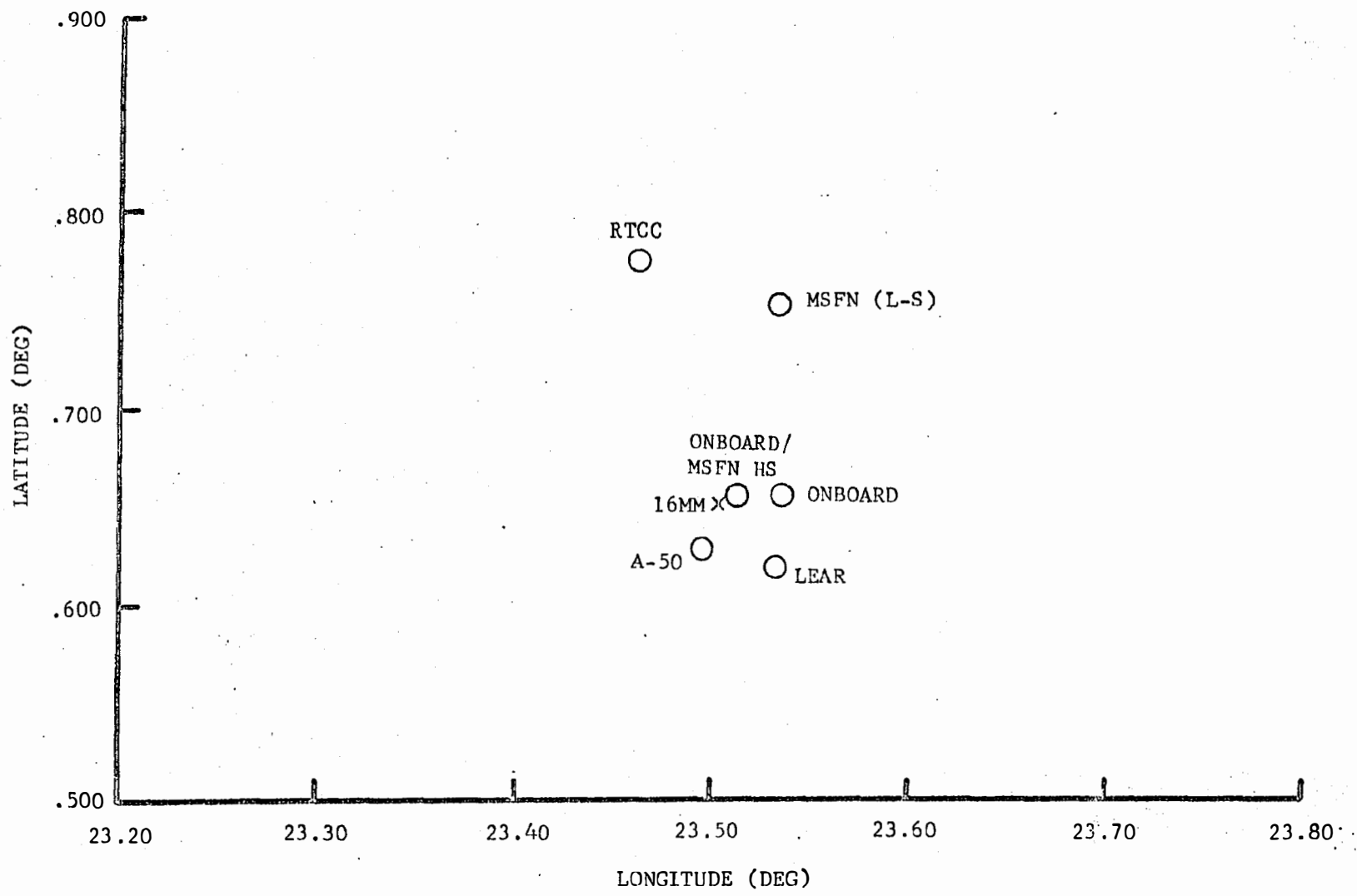


Figure 7-30 LM Landing Site Coordinates

Table 7.11 LM Landing Site Coordinates

VECTOR SOURCE	LATITUDE (deg)	LONGITUDE (deg)	RADIUS (n.mi.)
RTCC	0.777	23.461	936.59
MSFN (L-S)	0.756	23.537	937.93
ONBOARD (VHF, SXT)	0.656	23.538	936.90
BET #3	0.630	23.497	937.15
LEAR	0.620	23.532	936.66
16MM	0.647	23.505	N/A
ONBOARD/MSFN H-S	0.655	23.515	937.04

Table 7.12 Landing Radar Velocity Residual Statistics

Vector Source	V <sub>XA</sub>	V <sub>YA</sub>	V <sub>ZA</sub>
<u>RTCC</u>			
Mean	9.543	3.909	3.022
S.Dev.	1.532	5.455	3.918
Noise	1.172	3.891	3.446
<u>MSFN (LS)</u>			
Mean	-1.997	6.501	4.533
S.Dev.	1.758	4.081	3.486
Noise	1.120	3.281	3.661
<u>ONBOARD</u>			
Mean	2.681	6.724	4.640
S.Dev.	1.475	4.209	3.430
Noise	1.316	3.948	2.203
<u>BET #3</u>			
Mean	.857	.893	-.173
S.Dev.	1.829	4.306	3.689
Noise	1.142	4.565	2.361
<u>LEAR</u>			
Mean	4.733	5.625	4.287
S.Dev.	1.018	4.189	3.723
Noise	.718	3.932	2.340
<u>ONBOARD/MSFN (H-S)</u>			
Mean	.234	6.966	1.729
S.Dev.	1.183	3.866	2.978
Noise	.575	3.336	2.349

69-7

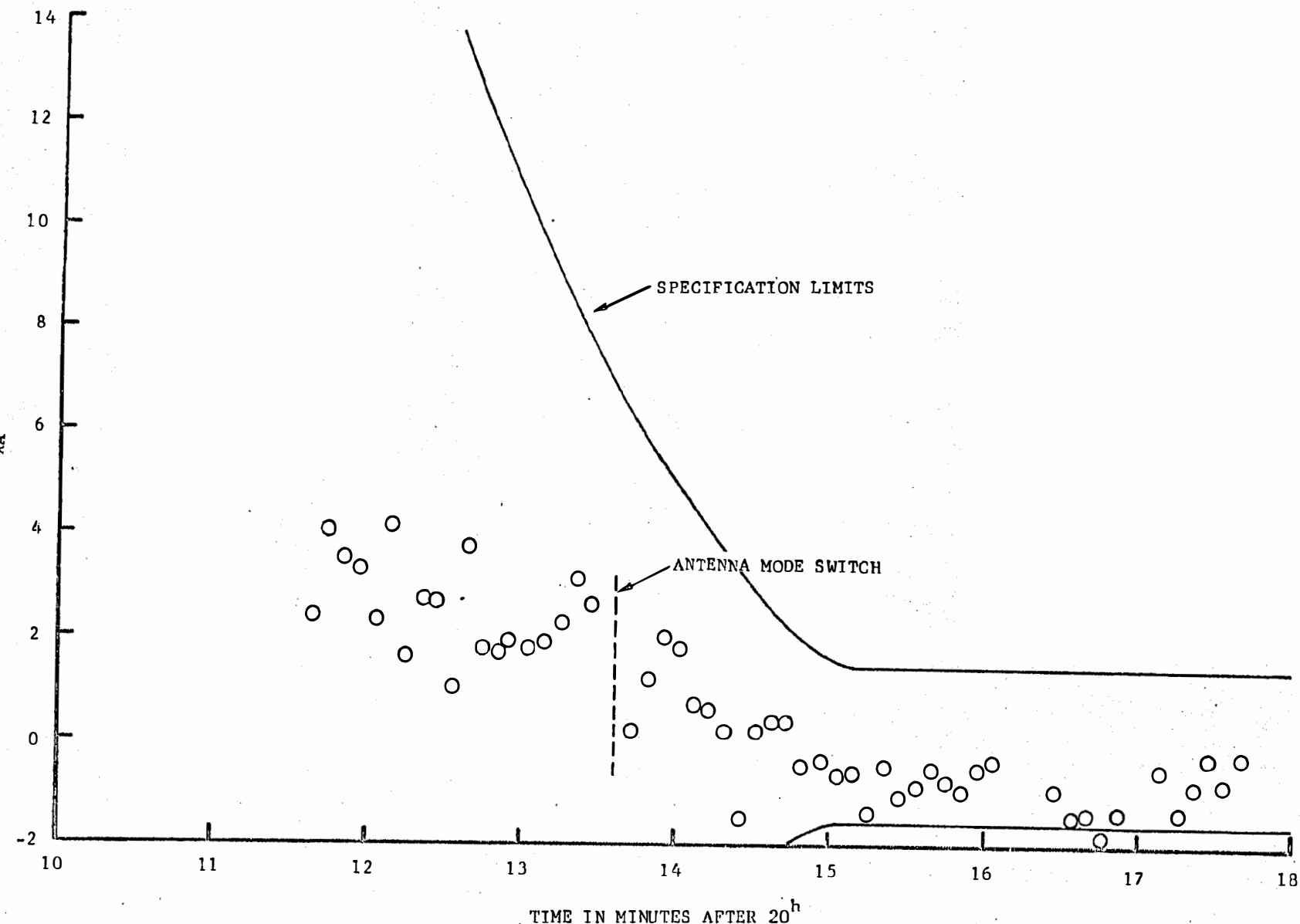


Figure 7-31. Landing Radar X-Antenna Velocity Residuals (RET#3)

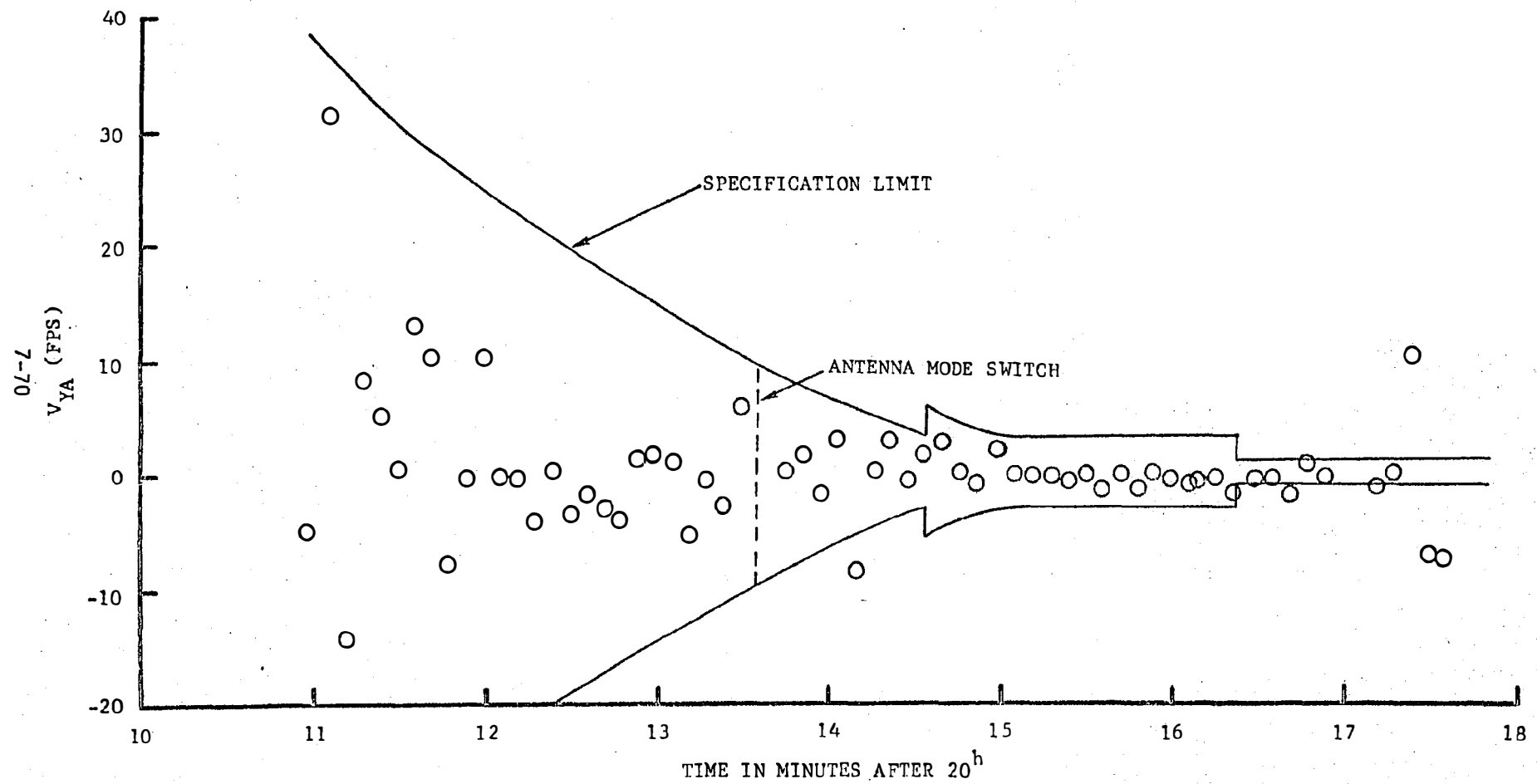


Figure 7-32 . Landing Radar Y-Antenna Velocity Residuals (BET#3)

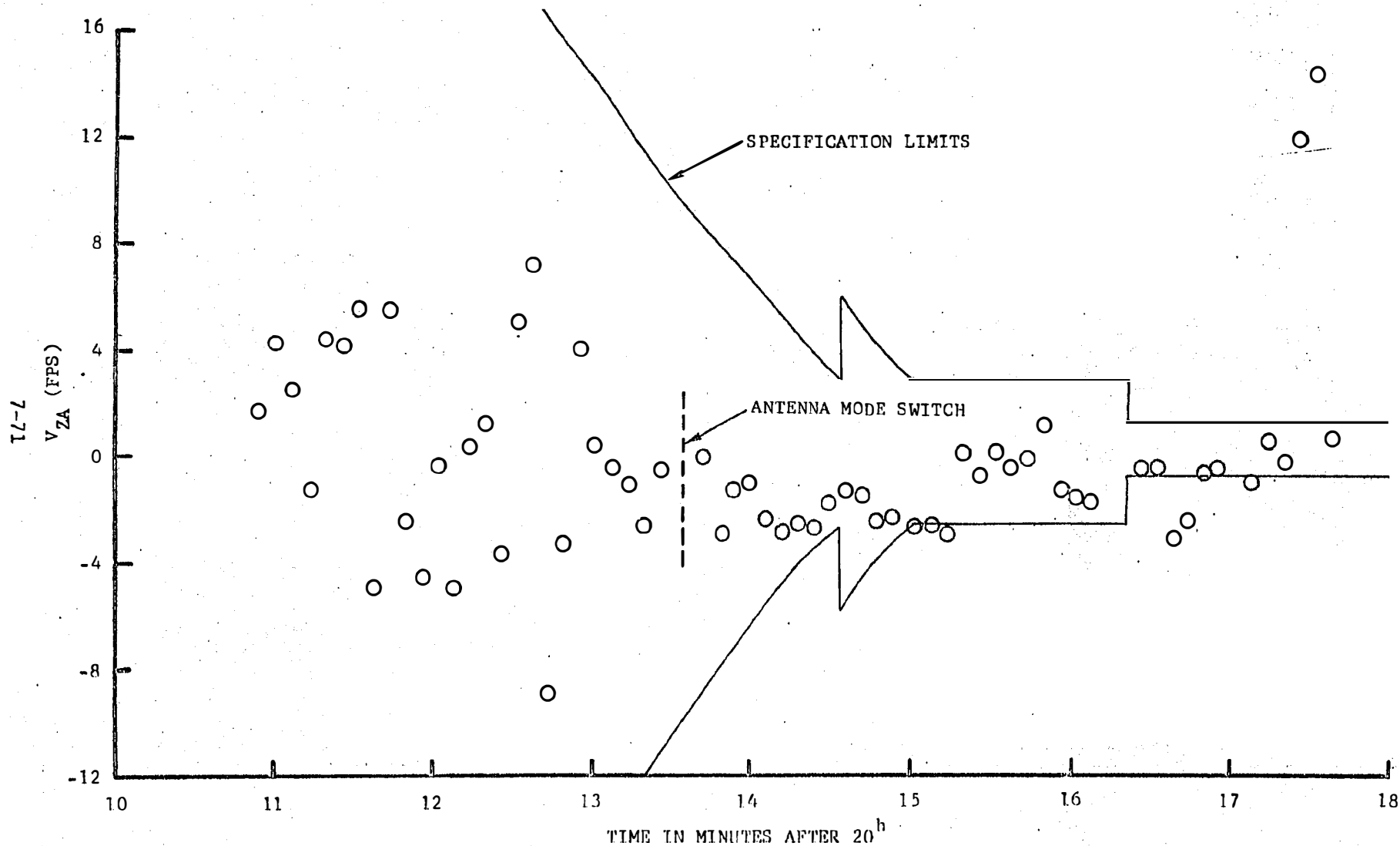


Figure 7-22 Landing Radar Z-Antenna Velocity Readings Appendix

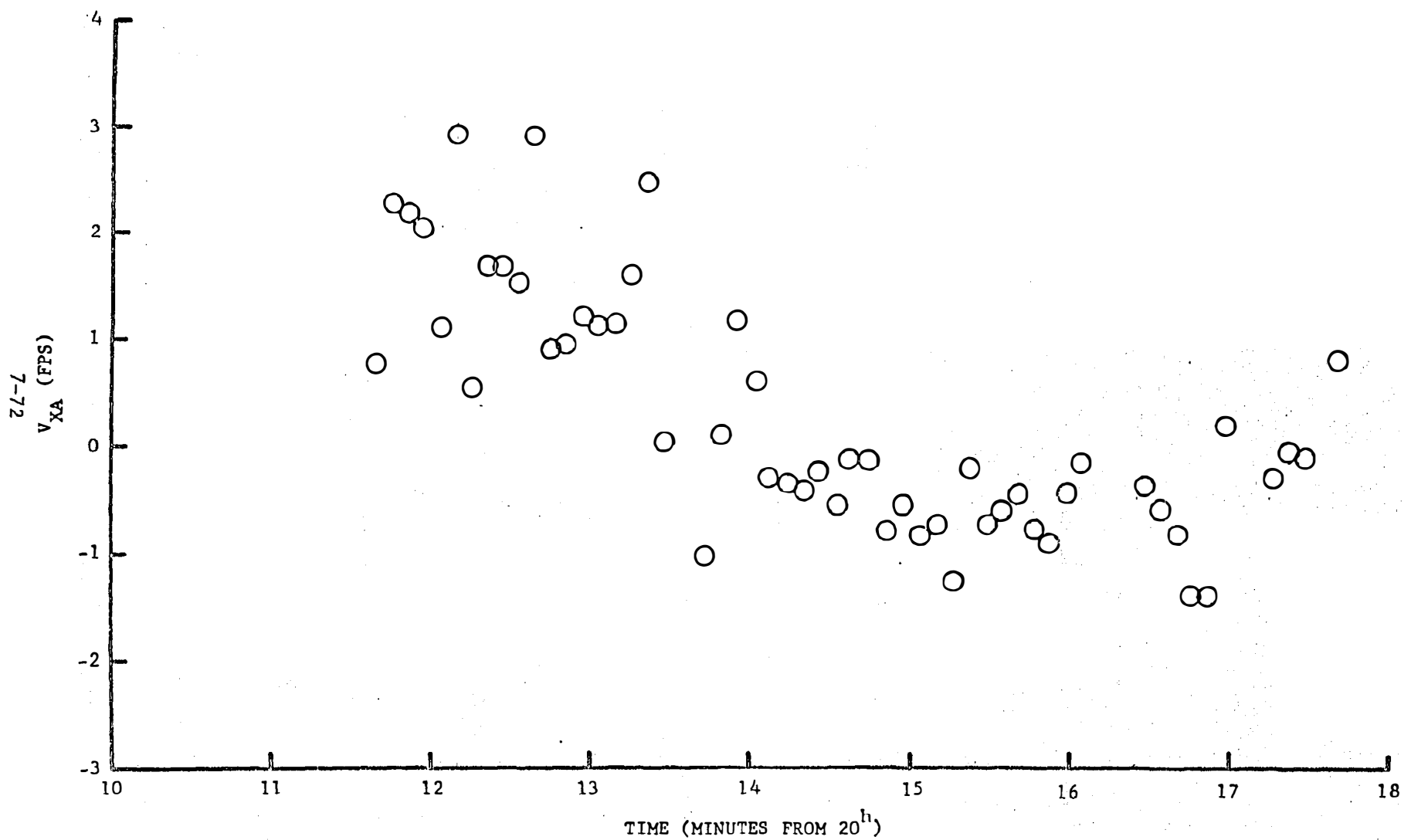


Figure 7-34 . Landing Radar X-Antenna Velocity Residuals (Onboard/MSFN H-S)

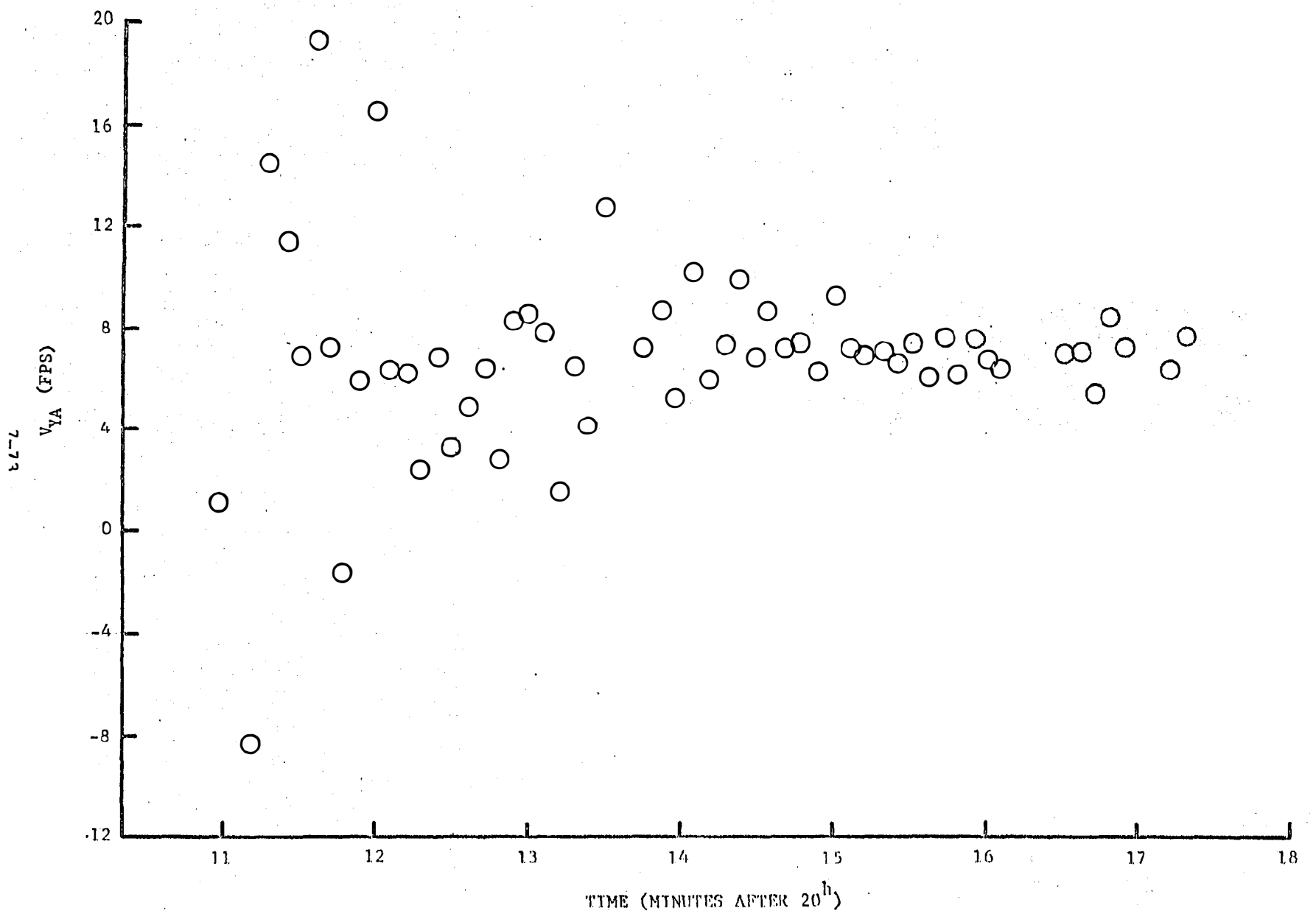


Figure 7-35. Landing Radar Y-Antenna Velocity Residuals (Onboard/MSFN H-S)

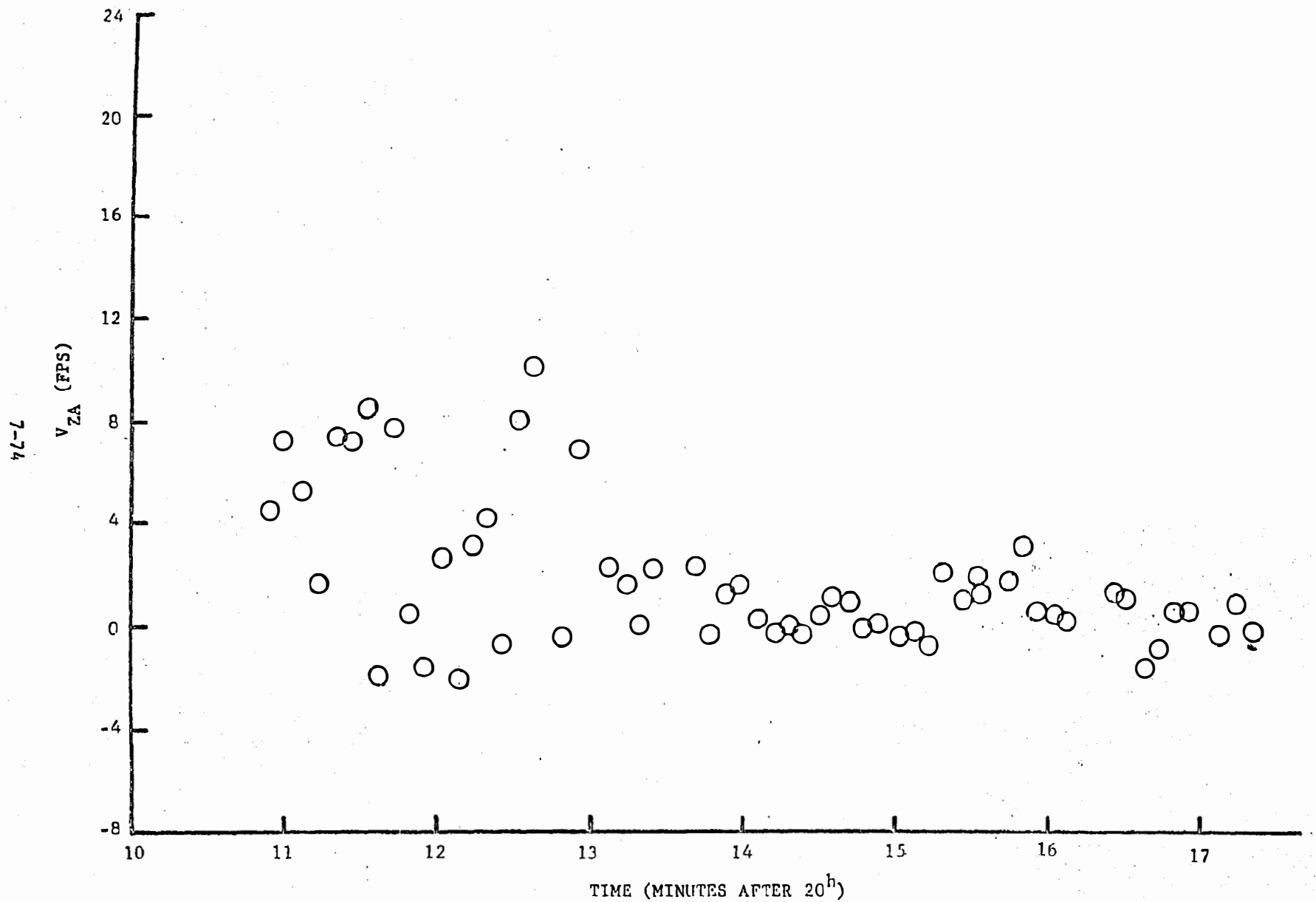


Figure 7-36. Landing Radar 2-Antenna Velocity Residuals (Onboard/MSTN H-S)

#### 7.4.3 Lunar Surface Altitude Along Groundtrack

Landing Radar range residuals are used to compute an estimate of the relative altitude of the surface along the groundtrack of the piercepoint.

Surface altitude relative to the landing site is plotted versus angular range in Figure 7-37. Time ticks are indicated at the LR range read times (2-second intervals).

The ground track of the range beam piercepoint is shown in Figure 7-38. The plot is made on Lunar Maps ORB-II-6 and ORB-I-3 (scale 1: 100,000)\*. The latitude does not agree with postflight estimates of Tranquility Base coordinates. Time ticks are at LR range read times and correspond to those on the surface altitude plot. The size of the range beam on the surface is indicated by the small ellipses drawn periodically along the groundtrack.

Little quantitative information can be obtained from Figure 7-38.1 except to note that the gentle upward slope of the terrain on the approach to the landing site is in general agreement with the surface altitude plot.

On Figure 7-38.2, surface altitude variations can be correlated to several prominent features:

The 170 ft drop in altitude between the readings at 102:39:37.19 and 102:39:39.19 correspond to range beam centers at the top and bottom of a cliff.

The point at 102:39:51.19 is centered in a fairly large crater. A depression of approximately 300 ft is clearly outlined in the surface altitude plot.

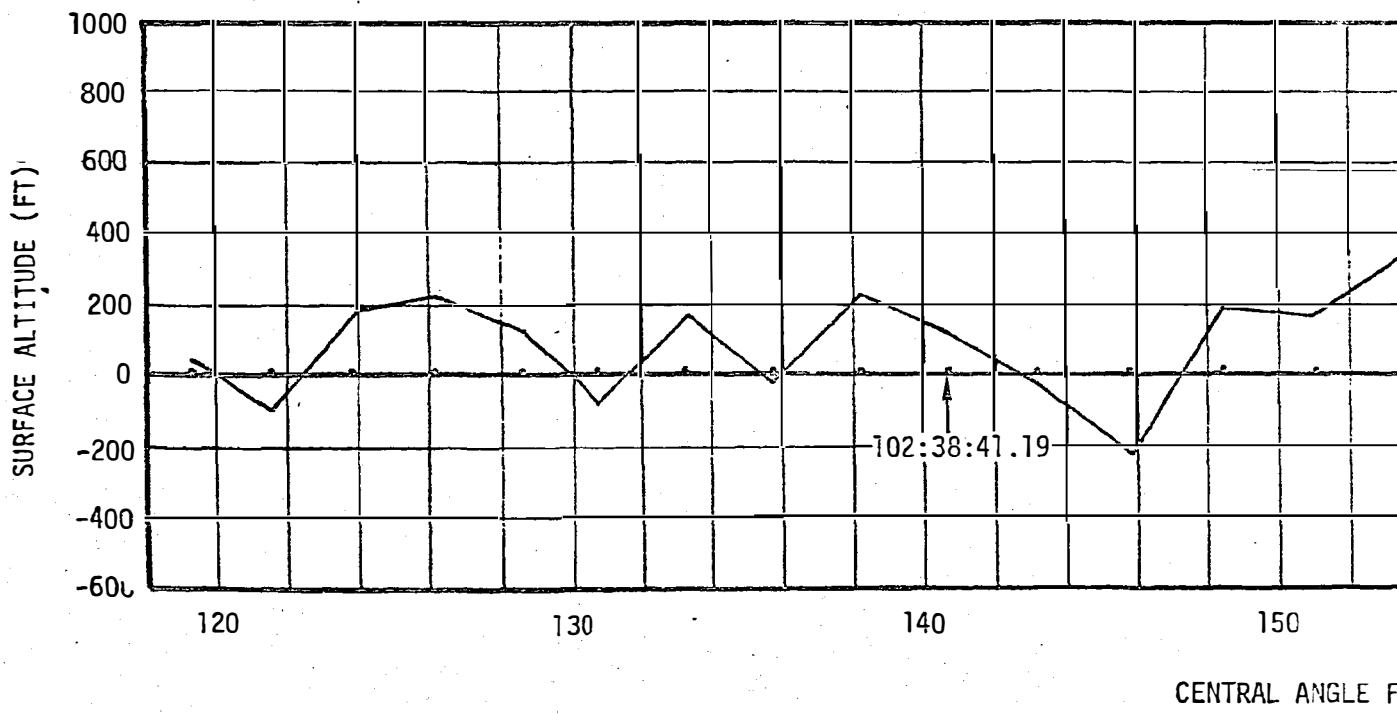
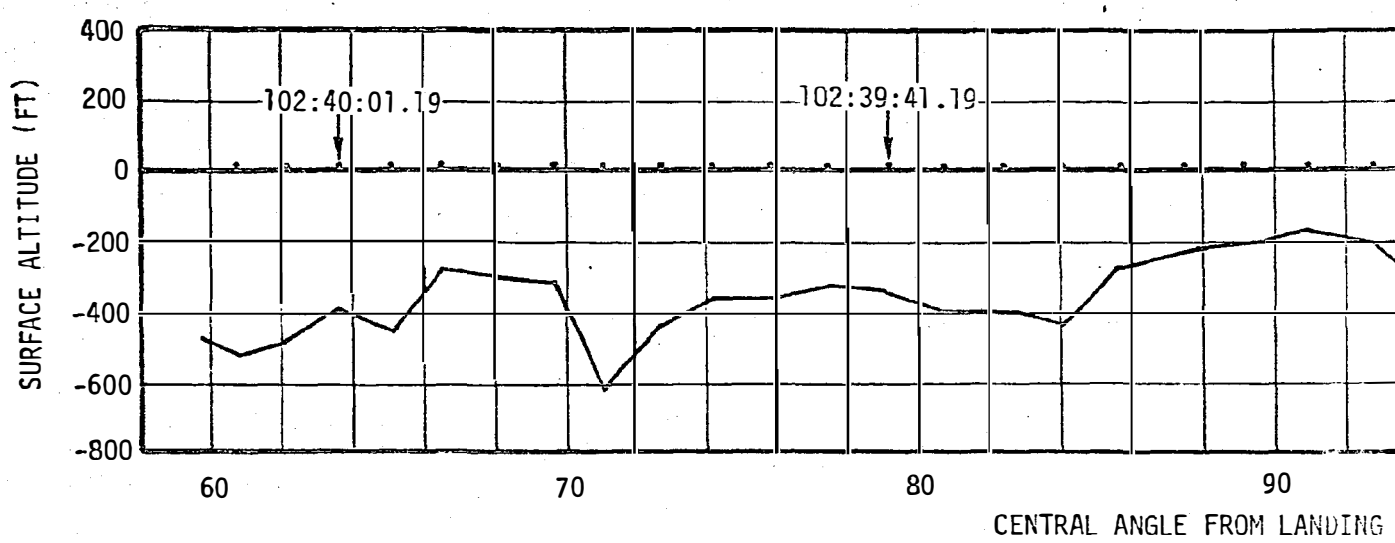
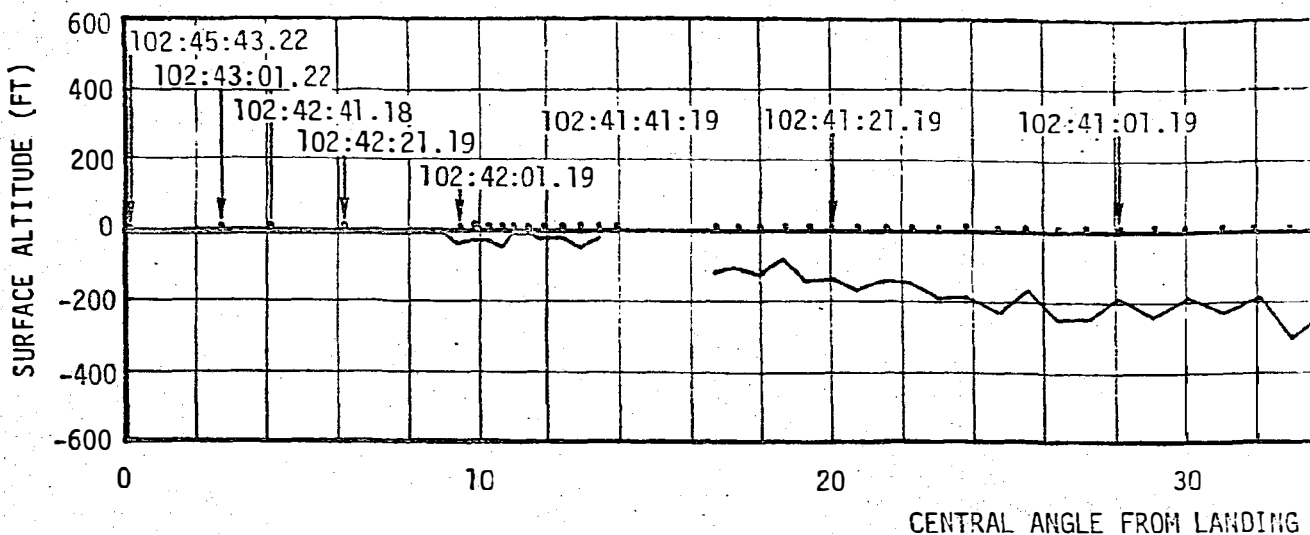
\* Map legend: Contour lines (at 50 meter intervals) are indexed by an estimate of the radius in meters with the first three digits omitted. Crater markings such as 45R (110) indicate - Height of rim above terrain = 45 meters, Crater depth (floor to rim) = 110 meters.

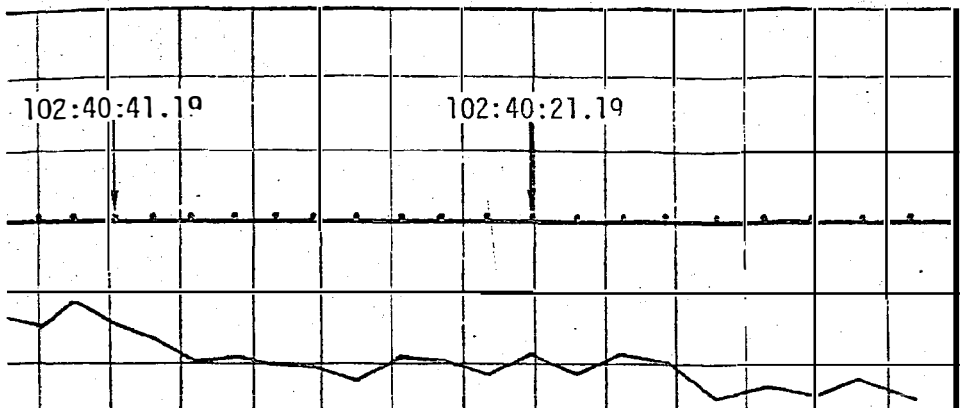
The point at 102:39:23.19 falls inside a crater, and a depression of approximately 200 ft is indicated.

As the range beam intersection grows in size with increasing LM altitude, surface details become increasingly difficult to resolve. The overall downward terrain slope along the ground-track in Figure 7-38.3 is in general agreement with the surface altitude plot.

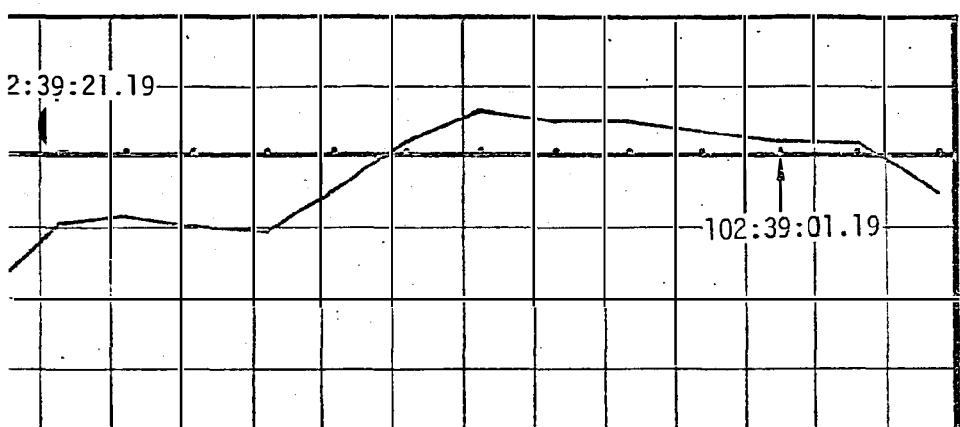
The altitude of the LM above the LLS radius during LR range data coverage is shown in Figure 7-39.

The data presented in this section results from a HOPE program orbit determination which includes LR velocity in the DC fit. This option has only recently become available and the results presented here are among the first obtained using Apollo 11 data. The principal effect of including LR velocity in the fit is to produce a more accurate relative velocity profile. Surface altitude plots, derived from earlier versions of the descent trajectory, show unrealistic terrain slopes due to small inplane velocity errors.

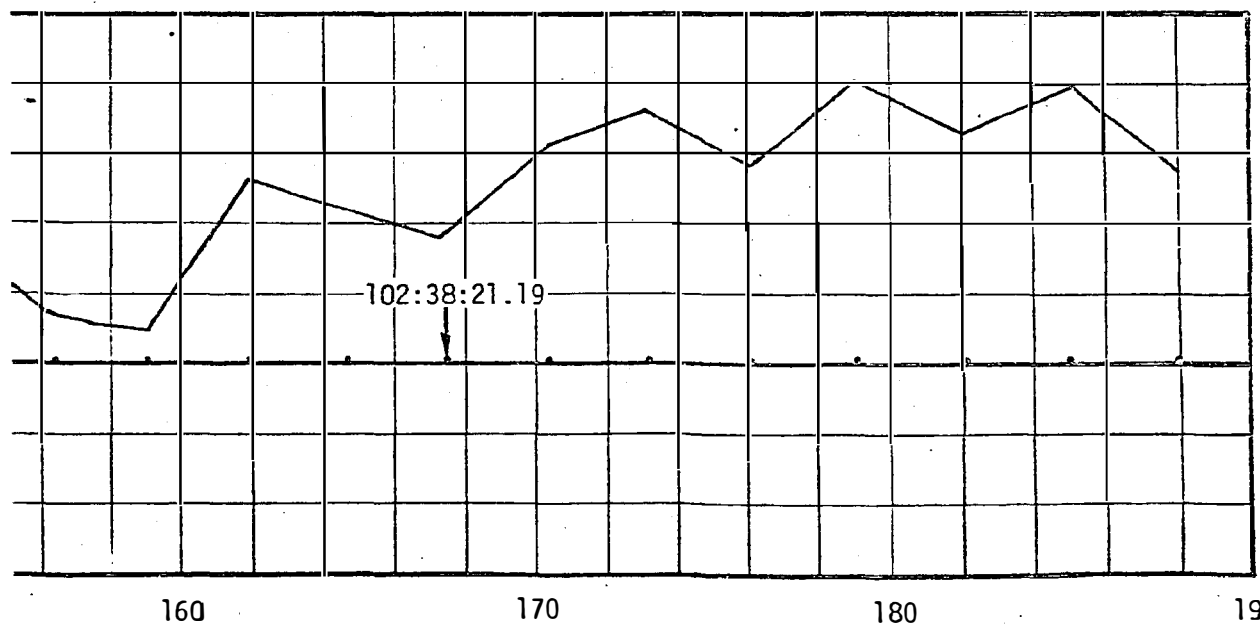




(MIN)



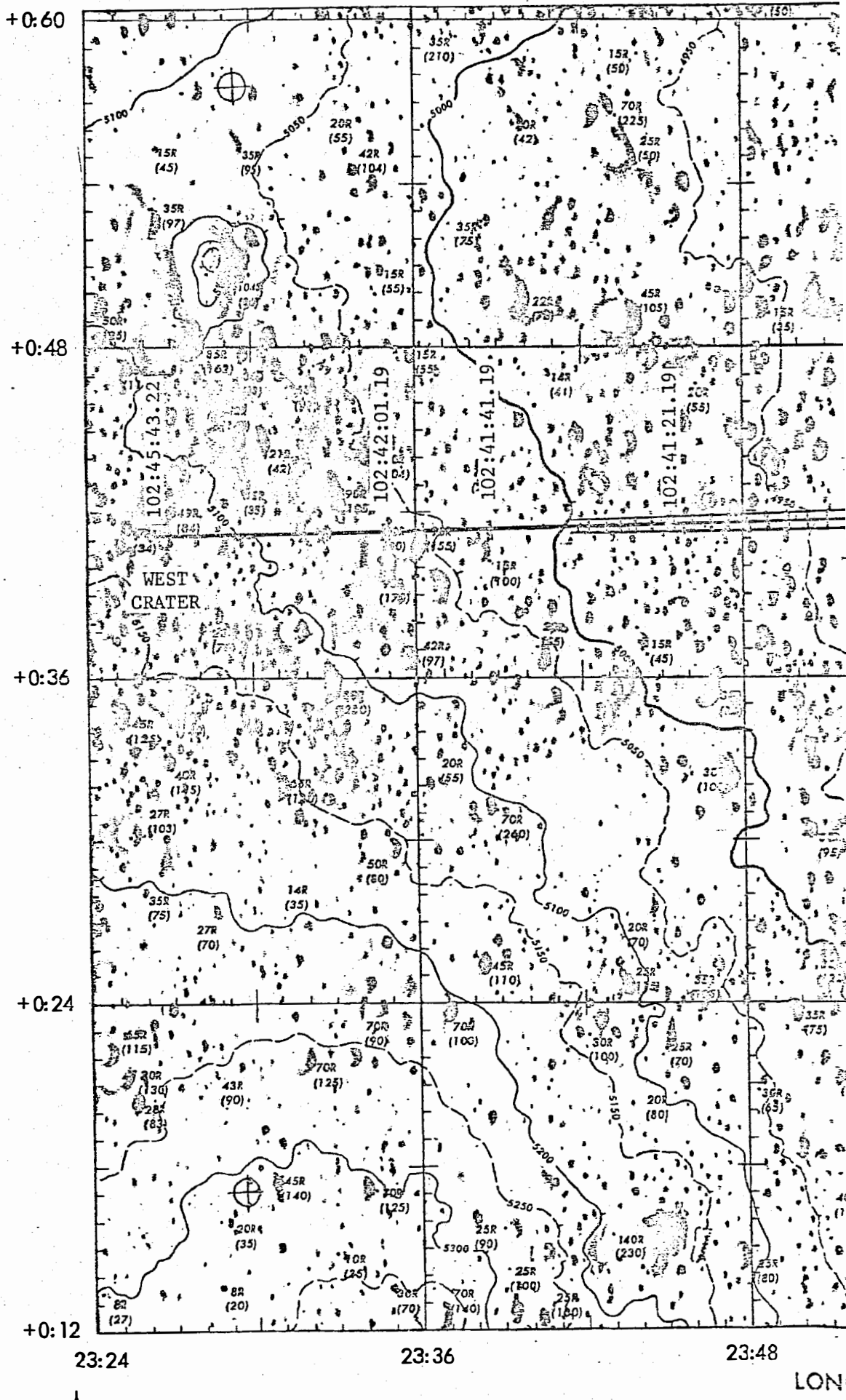
(MIN)



LANDING SITE (MIN)

Figure 7-37 Surface Altitude Along Groundtrack.

FOLDOUT FRAME



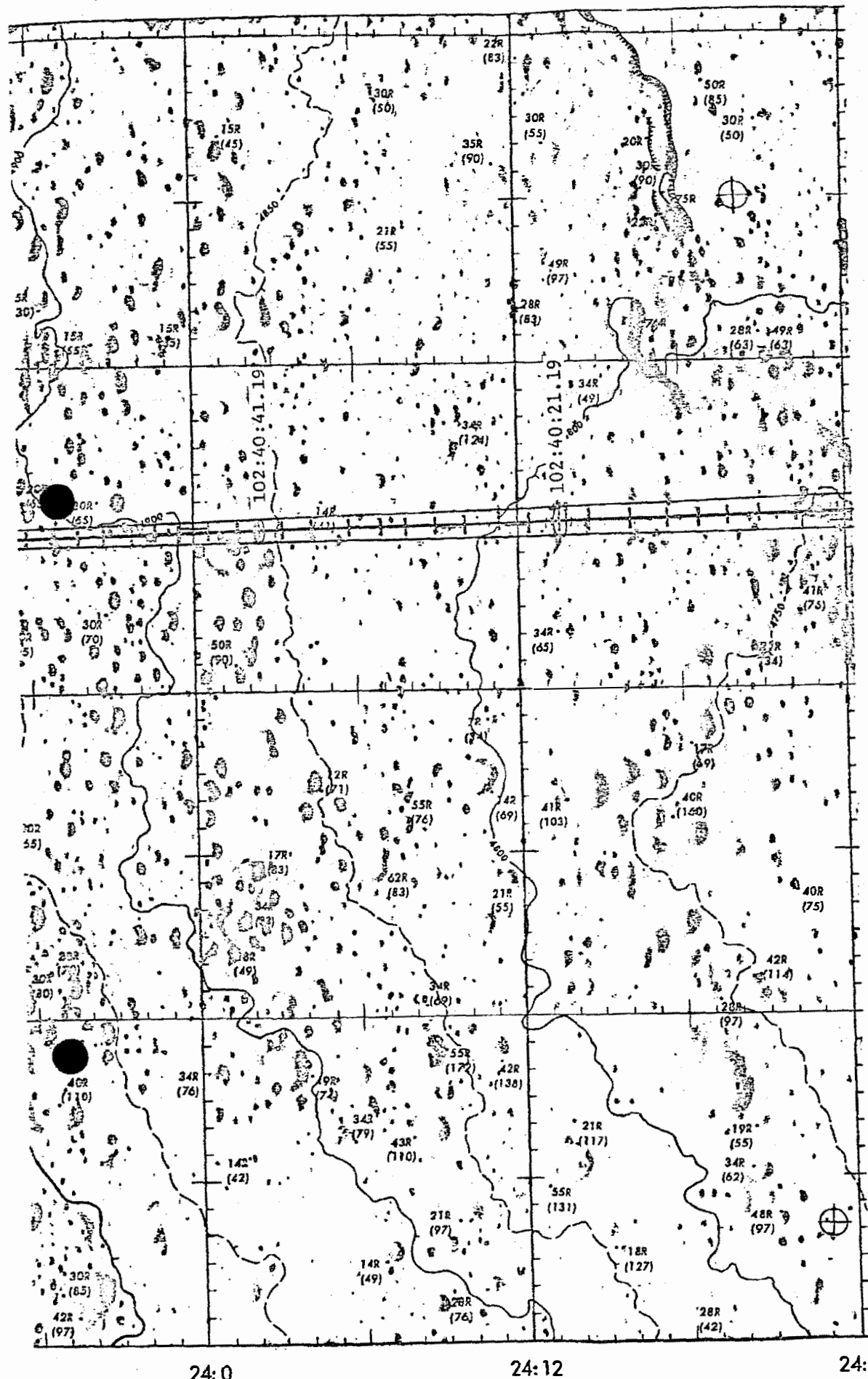
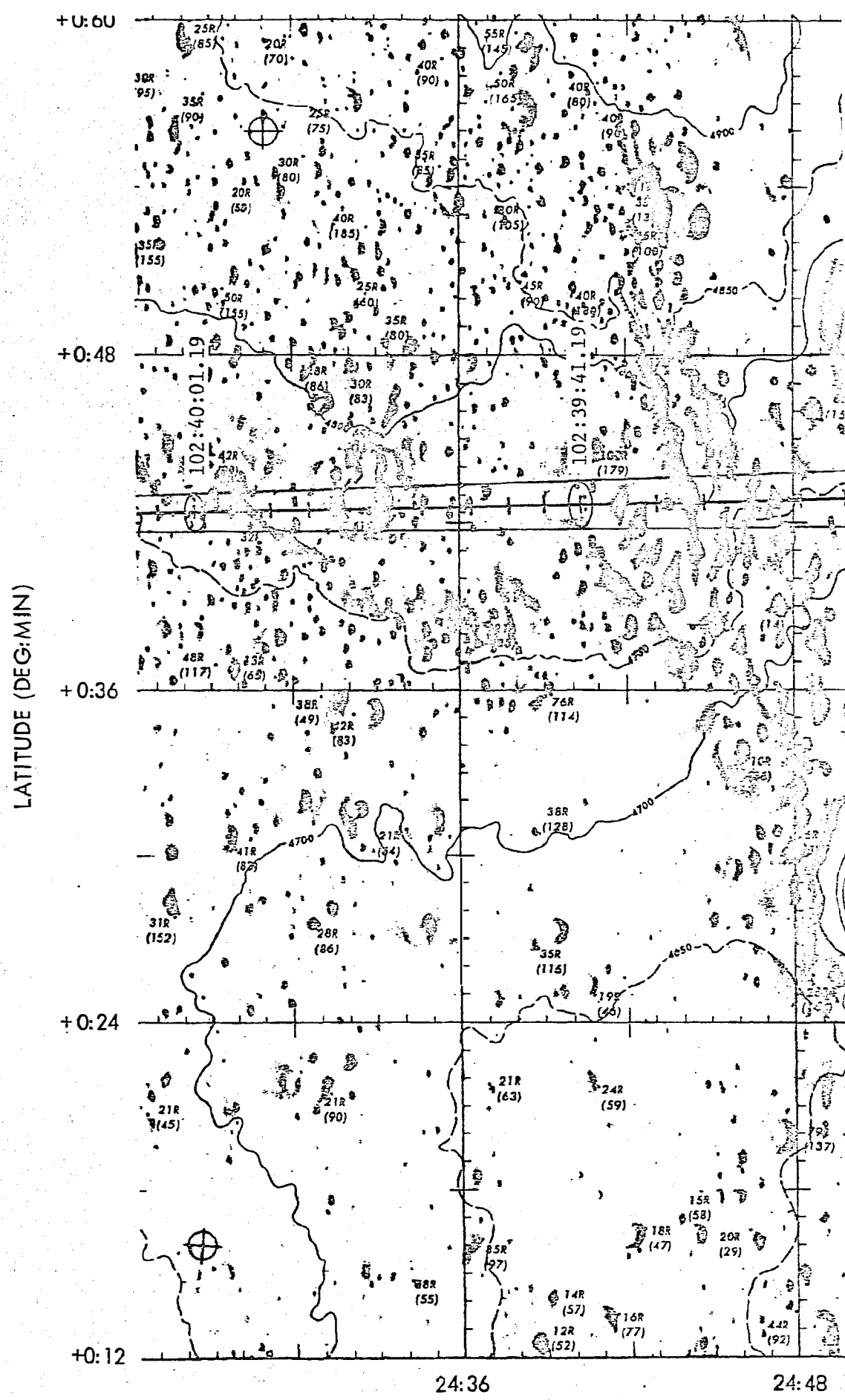


Figure 7-38.1 Groundtrack of LR Range Beam Piercepoint

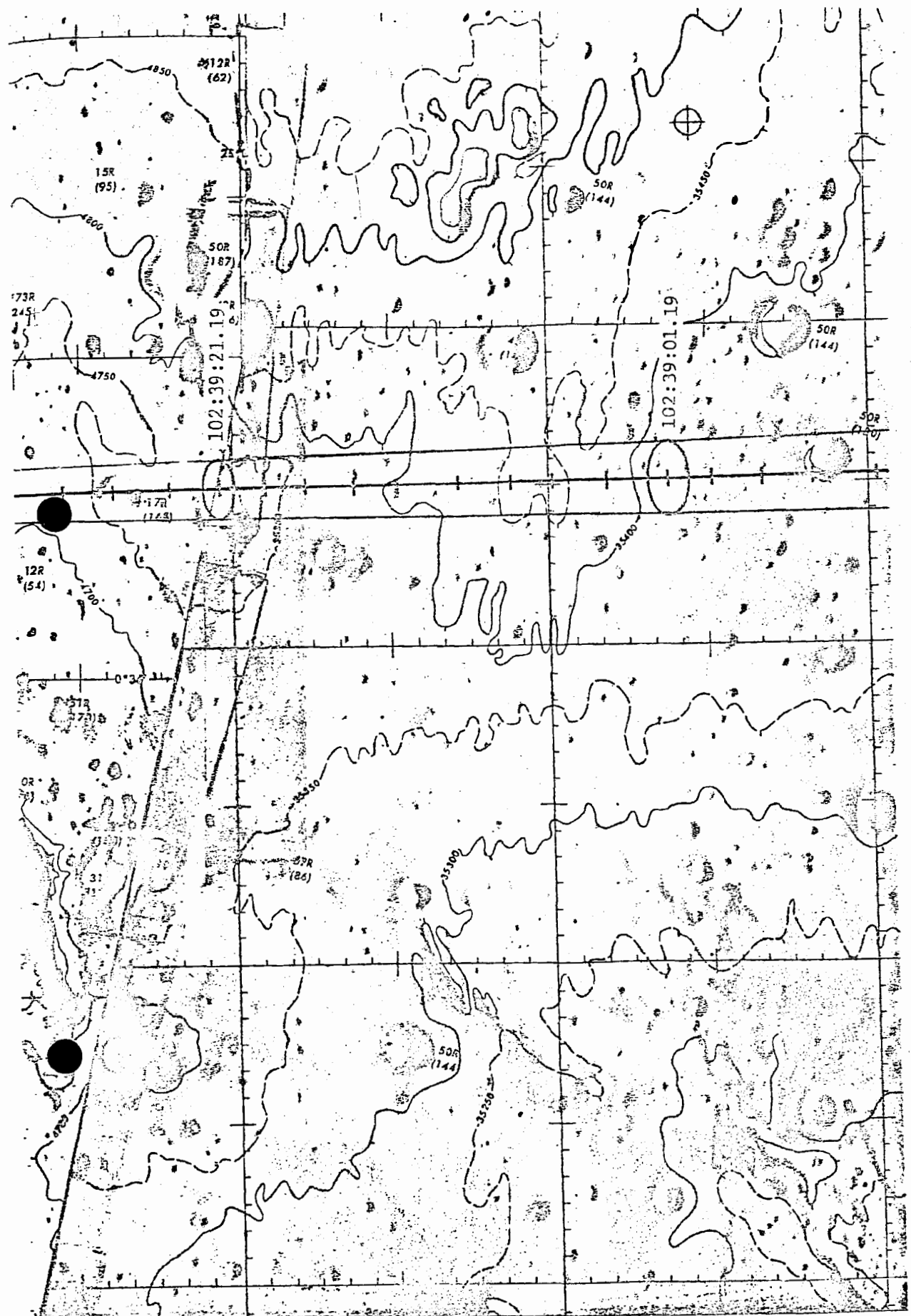
DE (DEG:MIN)

## **FOLDOUT FRAME**

24:24



FOLDOUT FRAME



25:0

25:12

25:24

### LONGITUDE (DEG:MIN)

Figure 7-38.2

LATITUDE (DEG:MIN)

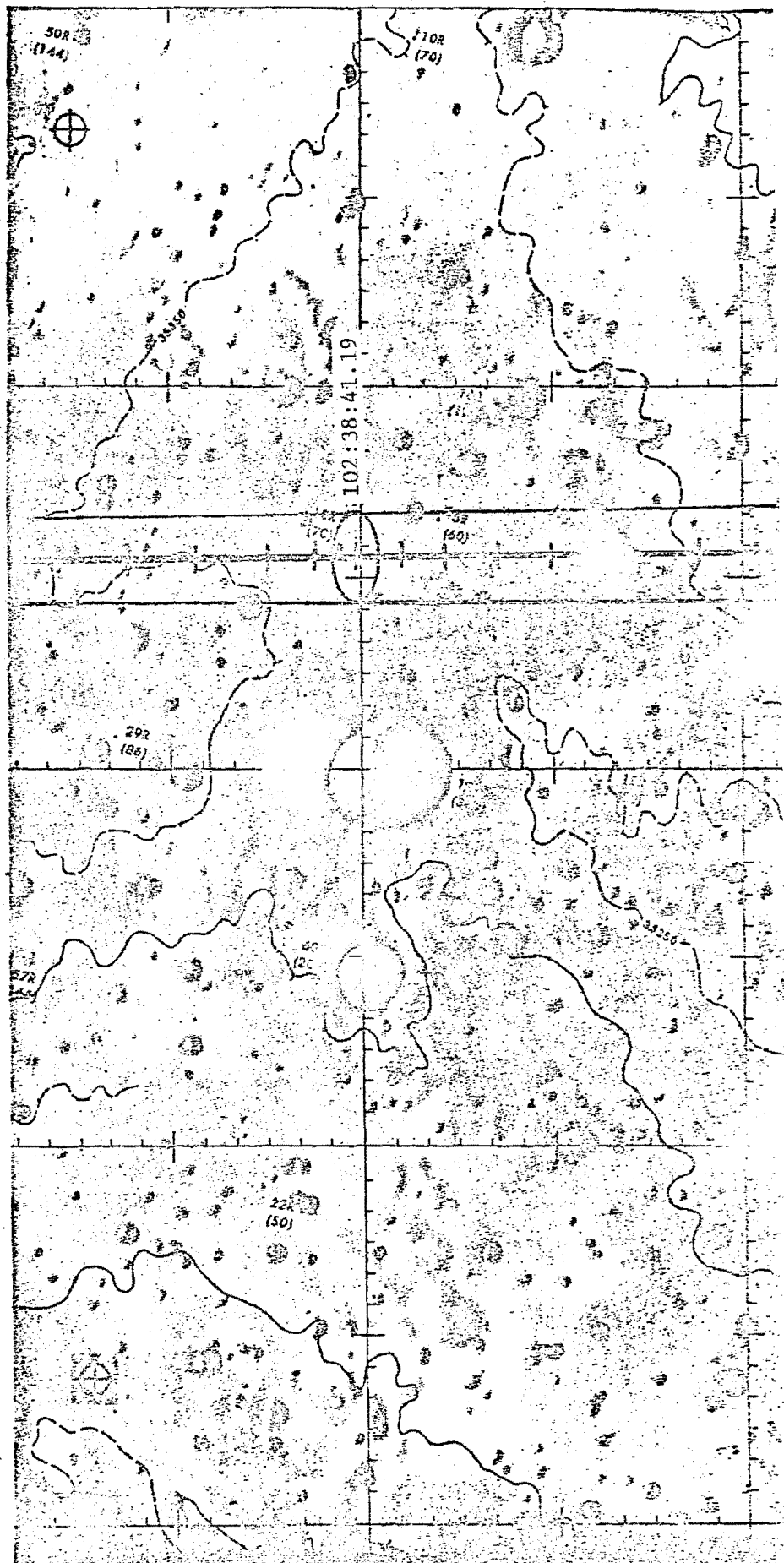
+0:60

+0:48

+0:36

+0:24

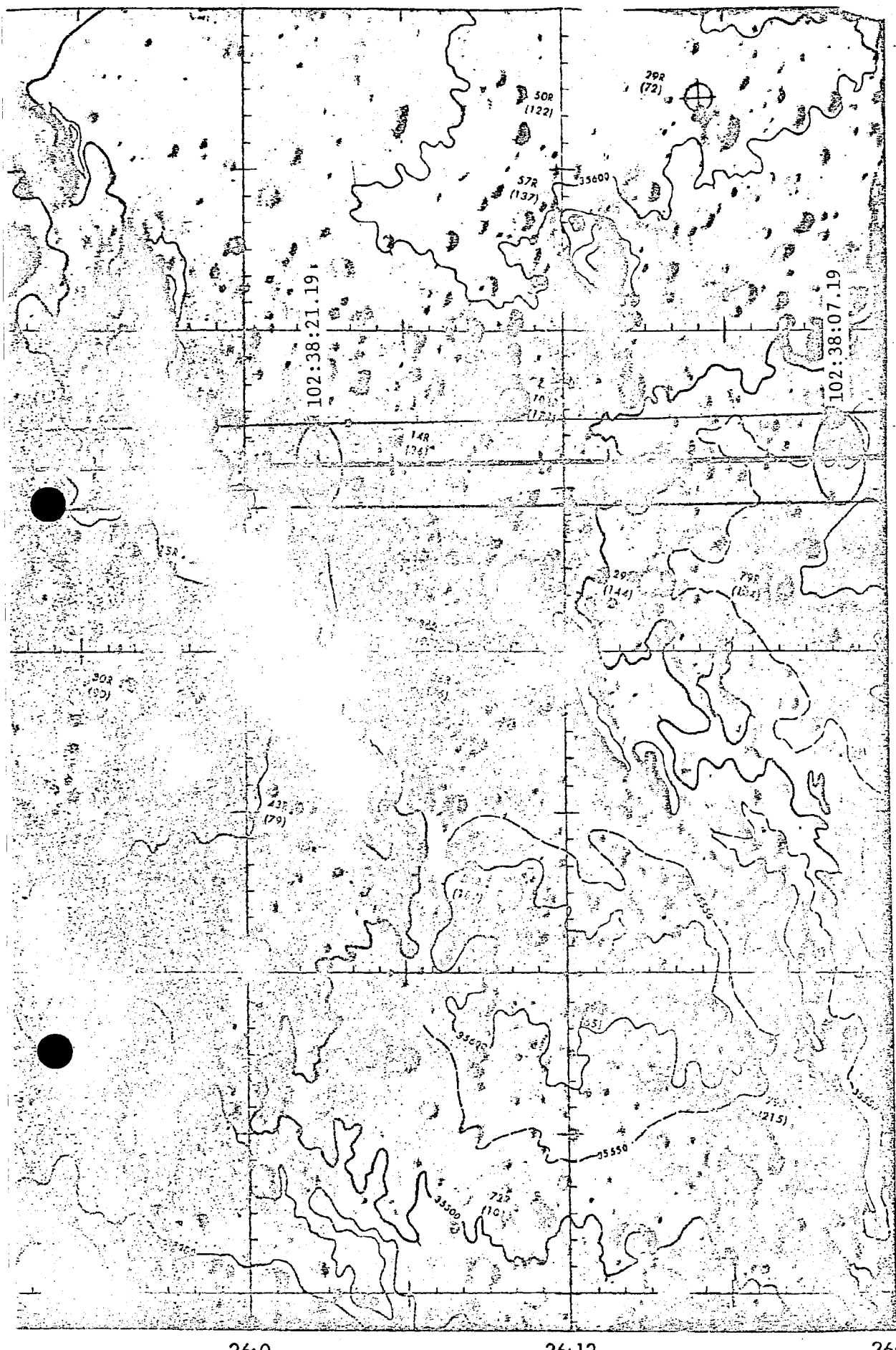
+0:12



25:36

25:48

FOLDOUT FRAME



LONGITUDE (DEG:MIN)

26:0

26:12

26:24

Figure 7-38.3

7-83

FOLDOUT FRAME

2

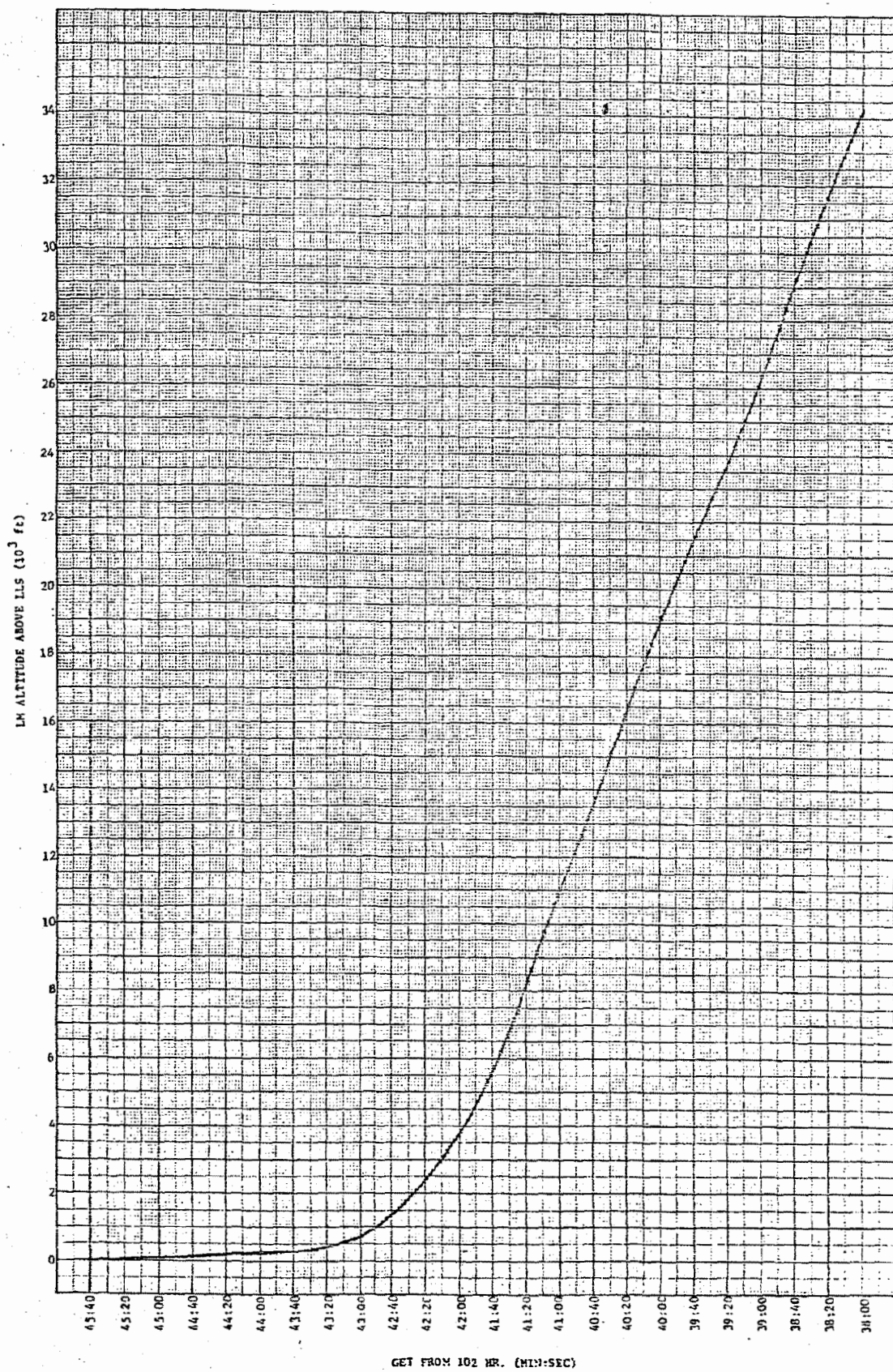


Figure 7-39 Altitude of IM During LR Range Sampling

**Page Intentionally Left Blank**

## REFERENCES

1. Barnett, E. L. and Moore, W. L., "Analysis of Apollo 10 LM Rendezvous Radar Data and CSM VHF Ranging Data", TRW IOC 5522.8-67, 25 July 1969.
2. Barnett, E. L., "Method to Estimate Radar Data Noise", TRW IOC 3422.6-110, 17 May 1967.
3. Barnett, E. L., "Postflight Reconstruction of the Apollo 11 Descent Trajectory Using the HOPE Program", TRW IOC 5522.8-106, 5 November 1969.
4. "CSM/LM Spacecraft Operational Data Book - Part I", North American Rockwell Corporation, SNA S-D-027, 1 November 1968.
5. Friedlander, M. M., "Analysis of LM Rendezvous Radar Data for Apollo 9", TRW IOC 5522.8-2, 9 May 1969.
6. Friedlander, M. M., "Preliminary Analysis of Apollo 11 Landing Radar Data", TRW IOC 5522.8-76, 15 August 1969.
7. Hinely, A. O. and Norris, P., "Lunar Model Analysis For Apollo 12", TRW IOC 5522.8-84, 31 August 1969.
8. Jankowski, S. C., "Summary of the CSM, LM Vectors Used to Generate the Preliminary NAT for Apollo 11", TRW IOC 5522.8-77, 19 August 1969.
9. "Master End Item Spec for Lunar Module", Grumman AED, LSP-470-2D.
10. Schiesser, E. L., "Apollo 11 Landing Site and LM Landing Position Determination", NASA/MSC Memorandum 69-FM41-349, 30 October 1969.

**Page Intentionally Left Blank**

## APPENDIX A

### Summary of CSM, LM Vectors Used to Generate the Preliminary NAT for Apollo 11

Appendix A documents the vectors used to generate the NAT trajectory in order that the user may know the quality of the trajectory. Since most of the vectors were not based on postflight fits but rather on RTCC vectors which were then propagated, propagation errors arise which can degrade the trajectory.

In order to reduce the error, the lunar orbit propagation times were kept to a minimum. Also, the total difference in position and velocity (which is a measure of the quality of the trajectory) were calculated at a common time point for adjacent trajectory intervals and tabulated in Table A.1 (CSM) and Table A.2 (LM) for user convenience. Whenever two intervals were separated by a maneuver, the  $\Delta V$  as exhibited in Tables A.1 and A.2 represents the difference between the total velocity difference and the measured velocity of the maneuver.

Each table lists the vector ID and RTCC batch number, the source of the vector, the initial time of the vector, the propagation interval, the total differences in position and velocity of adjacent intervals, and comments relevant to a particular propagation interval. Maneuvers are listed between the appropriate free flight intervals for easy reference.

Most lunar trajectories were generated using RTCC SS2 (inclination constrained) solution vectors as opposed to SS1 (no a priori) solution vectors. Unlike the Apollo 10 SS2 vectors which were constrained to the pre-LOI1, rev 18, and rev 29 planes, the Apollo 11 SS2 vectors were constrained on a rev-to-rev basis. Each SS2 vector contained two revs of data and was constrained to the SS1 solution plane of one of these two revs (exceptions existed at maneuvers).

By using the new SS2 scheme, the Apollo 11 out-of-plane error was not allowed to accumulate as it did during the Apollo 10 mission.

It should be noted that the vectors used to generate the trajectory from insertion to TPI were based on free flight solutions utilizing MSFN data and not RTCC vectors. The quality of the vector from DOI to PDI was

questionable, but was included because no better vector was available at that time.

In general, the quality of the CSM trajectory was better than the quality of the LM trajectory during the rendezvous period.

Table A.1 Apollo 11 CSM NAT Trajectories

Vector ID	Source	Vector Time (d:h:m:s) GHT	Trajectory Interval (GHT) (d:h:m:s)	ΔR (ft)	ΔV (fps)	Comment
GDS5061	RTCC <sup>**</sup>	16:17:33:48	16:16:22:03	16:17:49:13	346	0.6
MILX103	RTCC	16:17:49:24	16:17:49:13	16:18:12:01	6066	0.8
HSKS153	RTCC	17:03:33:18	16:18:12:04.39	17:16:16:57.92	---	0.2
PIRX034	RTCC	17:16:21:06	17:16:17:01.47	19:04:00:00	15438	0.6
ANGX389	RTCC	19:07:45:24	19:04:00:00	19:17:27:52.38	---	19 <sup>d</sup> 04 <sup>h</sup> 00 <sup>m</sup> to LOI1
PIIX407	RTCC	19:17:47:36	19:17:27:52.18	19:19:28:00	2338	8.91
RIDX420	RTCC	19:17:47:36	19:19:28:00	19:21:43:36	6201	3.8
GWIX455	RTCC	19:22:07:24	19:21:43:53	20:01:37:00	16789	5.76
GWIX472	RTCC	20:02:02:12	20:01:37:00	20:03:37:00	5438	3.50
HAWX479	RTCC	20:04:02:48	20:03:37:00	20:05:37:00	5092	3.56
HAWX485	RTCC	20:05:58:48	20:05:37:00	20:07:37:00	3963	3.17
CROX490	RTCC	20:07:57:18	20:07:37:00	20:09:32:00	4629	6.03
CROX496	RTCC	20:10:01:42	20:09:32:00	20:11:37:00	4093	2.10
CROX501	RTCC	20:11:53:36	20:11:32:00	20:13:27:00	10114	8.10
MILX507	RTCC	20:13:52:00	20:13:27:00	20:17:22:00	7597	6.39
ANGX507	RTCC	20:15:50:18	20:17:22:00	20:18:11:58.24	5166	6.36
ACNX527	RTCC	20:18:12:36	20:18:11:58.24	20:21:17:00	3666	2.36
HAWX535	RTCC	20:19:46:54	20:21:17:00	20:23:17:00	5126	3.48
GDSX522	RTCC	20:21:47:06	20:23:17:00	21:01:17:00	8472	5.12
GNIX550	RTCC	20:23:43:12	21:01:17:00	21:03:17:00	3921	3.15
GNIX555	RTCC	21:01:41:42	21:03:17:00	21:05:12:00	4023	3.07
CROX564	RTCC	21:03:40:48	21:05:12:00	21:07:12:00	3915	3.47
HAWX569	RTCC	21:05:38:06	21:17:12:00	21:09:12:00	3754	3.44
NBEX573	RTCC	21:07:36:18	21:09:12:00	21:11:07:00	4342	4.21
MADX579	RTCC	21:09:34:36	21:11:07:00	21:13:07:00	3814	3.05
CROX584	RTCC	21:11:33:06	21:13:07:00	21:15:02:00	6678	5.84
ACNX595	RTCC	21:15:29:12	21:15:02:00	21:18:57:00	5070	3.38
GDSX600	RTCC	21:17:27:10	21:18:57:00	21:20:57:00	5813	2.99
HAWX625	RTCC	21:21:30:00	21:20:57:00	22:00:02:07.1	4052	4.46
HSKX651	RTCC	22:00:03:06	22:00:02:07.1	22:02:57:00	3065	2.85
CDSX657	RTCC	22:01:20:12	22:02:57:00	22:04:58:12	7604	5.00
ANGX695	RTCC	22:07:37:36	22:04:58:12	22:14:00:00	---	TBI
PAO <sup>**</sup>	RTACF <sup>**</sup>	22:20:01:54.53	22:14:00:00	22:20:02:05.29	---	0.1
PAO	RTACF	23:05:31:59.00	22:20:02:05.29	23:15:30:00	19159	0.3
PAO	RTACF	23:15:31:59.99	23:15:30:00	24:01:30:00	20419	0.4
PAO	RTACF	24:01:32:00	24:01:30:00	24:16:21:18	21098	4.7
PAO	RTACF	24:16:39:06	25:16:21:18	24:16:35:06	---	Entry interface

<sup>\*</sup>Real Time computer center (RTCC) on-line listing.<sup>\*\*</sup>Real Time auxiliary computer facility (RTACF) checkout monitor for the Postflight Analysis Office (PAO).

Table A.2 Apollo 11 LM NAT Trajectories

Vector	Source	Vector Time (d:h:m:s) GMT	Trajectory (d:h:m:s)	Interval (d:h:m:s) GMT	ΔR (ft)	ΔV (fps)	Comment
MSFN FIT	TRW	20:19:08:06.6	20:17:45:38.	20:19:08:14.1	---	---	Undock to DOI
REAL TIME	MPAD	20:20:04:35.17	20:19:08:43.9	20:20:05:04.4	---	---	DOI to PDI
MSFN FIT	TRW	21:18:01:14.88	21:18:01:14.88	21:18:51:34.7	8400	0.7	INS to CSI
MSFN FIT	TRW	21:19:49:46	21:18:52:21.7	21:19:49:46	8558	1.4	CSI to CDH
MSFN FIT	TRW	21:19:50:04.08	21:19:50:04.08	21:20:36:30.8	---	---	CDH to TPI

## APPENDIX B

### Supplementary Data

Appendix B contains supplementary information which is too detailed for the main body of the report. This information includes a summary of the radar data used in each BET fit segment, a summary of ground and on-board data weights used in HOPE, a summary of the USBS station locations, and a summary of the components used in the R2 and L1 lunar potential models.

Tables B.1 and B.2 list by vehicle statistics computed from the data used in each BET fit, the type and number of observables, and the mean and standard deviations obtained from the residuals calculated in the final iteration of the fit. The range statistics are in feet, doppler units are cycles per second, range rate units are in feet per second, and angular units are degrees.

Table B.3 lists the data weights used in the HOPE Program for ground based radar data and Table B.4 lists the data weights used in the HOPE Program for onboard data by type of observable.

Table B.5 lists the terms of the R2 lunar potential model.

Table B.6 lists the terms of the Langley 1 lunar potential mode, a modification of the R2 model.

Table B.7 lists the S-band tracking stations and their locations as used in the Apollo 11 postflight analysis. All locations are referenced to the Fischer Ellipsoid of 1960. The mean surface refractivity numbers for each station for the month of July are also listed.

Table B.1 CSM BET Ground Based Tracking Data Statistics

<u>Station</u>	<u>Data Type</u>	<u>Number of OBS</u>	<u>Méan</u>	<u><math>\sigma</math></u>
Rev 13 Segment				
MAD	2-way doppler	122	-.013	.236
MIL	3-way doppler	103	-.009	.246
ACN	3-way doppler	101	-.018	.235
Rev 14 Segment				
MAD	2-way doppler	142	.002	.186
GDS	3-way doppler	138	.009	.182
ACN	3-way doppler	63	-.004	.171
Rev 25 Segment				
MAD	2-way doppler	136	.002	.160
MIL	3-way doppler	52	.001	.165
ACN	3-way doppler	47	.007	.157
Rev 26 Segment				
MAD	2-way doppler	128	.001	.223
MIL	3-way doppler	114	.0005	.199
ACN	3-way doppler	114	.005	.188
GDS	3-way doppler	70	.006	.182

**Table B.2 LM BET Ground Based and Onboard Tracking Data Statistics**

<u>Station</u>	<u>Data Type</u>	<u>Number of OBS</u>	<u>Mean</u>	<u><math>\sigma</math></u>
Undock to DOI Segment				
RID	2-way doppler	141	-.023	.193
CYI	3-way doppler	140	-.049	.202
ACN	3-way doppler	112	-.014	.193
ANG	3-way doppler	137	.030	.219
MIL	3-way doppler	114	-.012	.189
DOI to PDI Segment				
Sextant shaft		13	-.0097	.015
Sextant trunnion		13	-.0004	.004
VHF ranging		18	-26.000	74.000
Insertion to CSI Segment				
RID	2-way doppler	74	-.022	.315
BDA	3-way doppler	69	-.019	.319
ANG	3-way doppler	72	.059	.315
ACN	3-way doppler	60	.011	.320
MIL	3-way doppler	63	.014	.316
CDH to Post-TPI Segment				
Sextant shaft		31	.030	.026
Sextant trunnion		31	..011	.023
VHF ranging		29	-394.000	222.000
Rend. radar shaft		65	-.012	.107
Rend. radar trunnion		65	-.084	.056
Rend. radar range		65	142.000	271.000
Rend. radar range rate		65	-.115	.543

Table B.3 Ground Based Radar Data Weighting

Data Type	Radar	Weighting
Range	USB: 30-ft. antenna 85-ft. antenna	600 ft.
Doppler (2-way)	USB: 30-ft. antenna 85-ft. antenna	0.1 cycle/sec.
Doppler (3-way)	USB: 30-ft. antenna 85-ft. antenna	0.1 cycle/sec.

Table B.4 Onboard Data Weighting

Data Type	Shaft	Trunnion	Range	Range Rate
Rendezvous radar	.01	.01	30.	1.
Sextant	.001	.001		
VEF ranging			30.	

Table B.5 R2 Lunar Potential Model

Term	Value
J2	$2.07108 \times 10^{-4}$
J3	$-2.1 \times 10^{-5}$
C22	$2.0716 \times 10^{-5}$
C31	$3.4 \times 10^{-5}$
All other harmonics are zero	

Table B.6 L1 Lunar Potential Model

Term	Value
J2	$2.07180 \times 10^{-4}$
J3	$-2.1 \times 10^{-5}$
C22	$2.0716 \times 10^{-5}$
C31	$3.4 \times 10^{-5}$
C33	$2.583 \times 10^{-6}$
All other harmonics are zero	

Table B.7 USBS Station Locations

Station	Antenna	Identification	Latitude* (deg.)	Longitude* (deg)	Altitude* (ft)	Surface Refractivity
Antigua	30'	ANG	17.01692	298.24715	141.08	378
Ascension	30'	ACN	-7.95510	345.67330	1843.83	353
Bermuda	30'	BDA	32.35195	295.34287	68.90	377
Canary Island	30'	CYI	27.76454	344.36519	567.69	343
Honeysuckle Creek	85'	HSK	-35.58361	148.97805	3757.55	296
Carnarvon	30'	CRO	-24.90705	133.72620	82.00	325
Goldstone	85'	GDS	35.34154	243.12655	2975.066	279
Grand Bahama	30'	GMB	26.63286	281.76234	16.40	386
Guam	30'	GWM	13.31062	144.73747	416.67	373
Guaymas	30'	GYM	27.96382	249.27943	62.34	368
Hawaii	30'	HAW	22.12666	200.33528	3772.97	308
Madrid	85'	MAD	40.45514	355.83183	2551.18	299
Merritt Island	30'	MIL	28.50866	279.30738	32.81	385
Texas	30'	TEX	27.65428	262.62220	32.81	395
Honeysuckle Creek Wing	85'	NBE	-35.40111	148.98153	2199.15	296
Goldstone Wing	85'	PIR	35.38952	243.14078	3186.02	279
Madrid Wing	85'	RID	40.42843	355.75128	2524.93	299

\*All quantities are referenced to the Fischer Ellipsoid of 1960.

## APPENDIX C

### LM Rendezvous Radar Data, CSM VHF Ranging Data and CSM Sextant (Apollo 11)

The LM rendezvous radar data that was used in the analysis are listed in the two card format of the HOPE orbit determination program. The first card specifies the vehicle taking the observation, the vehicle that is being observed, the time of the observation (year (mod 1900), month, day, hour, minute, and second (GMT)), three code numbers, shaft observable, trunnion observable, range observable, and range rate observable. The second card specifies the inner, middle, and outer gimbal angles. The units are feet, degrees, and seconds.

The CSM VHF ranging data are also listed in the same format. The card format differences are the following: 1) vehicle ID's are reversed, 2) code numbers are different, 3) range is the only observable, and 4) gimbal angles are not needed to process the ranging data.

The CSM sextant data are also listed. The card format is also similar to the rendezvous radar cards.

## DOI TO PDI

VEH1	VEH2	YYMMDDHHMMSS.SSS	XFSHAFT(DEG)	TRUN(DEG)	RANGE(FT)	RRATE(FPS)
			INNER(DEG)	MIDDLE(DEG)	OUTER(DEG)	

CSM	LEM	69 720184617.695	62 88.2641602 54.6350098	29.1824434 4.6472168	338.5437012 84093.437	1 2
CSM	LEM	69 7201925	3.547114			1 2
CSM	LEM	69 720192534.824	62 .5163574 327.7551270	23.3789155 1.8347168	2.5158691	1 2
CSM	LEM	69 720192540.676	62 .6372070 327.9528809	23.3349702 1.8457031	2.6037598 89136.613	1 2
CSM	LEM	69 7201926	3.816114			1 2
CSM	LEM	69 720192729.605114			97035.563	1 2
CSM	LEM	69 720192610.746	62 1.2524414 329.1064453	22.9257295 1.8676758	3.0322266 104205.380	1 2
CSM	LEM	69 720192839.305114				1 2
CSM	LEM	69 720192746.867	62 .4174805 332.3254395	22.0852754 2.0214844	2.5927734 115871.521	1 2
CSM	LEM	69 720193019.016114				1 2
CSM	LEM	69 720192856.437	62 359.9121094 333.7866211	22.3022554 2.1643066	2.5048828	1 2
CSM	LEM	69 720193026.348	62 359.7253418 336.0058594	22.1319673 2.2631836	2.5158691 125897.112	1 2
CSM	LEM	69 720193133.504114				1 2
CSM	LEM	69 720193112.766	62 359.5056152 336.9177246	22.1786592 2.3510742	2.5268555 134950.523	1 2
CSM	LEM	69 720193234.348114				1 2
CSM	LEM	69 720193212.098	62 .5493164 337.7526855	22.4670503 2.5158691	3.5156250	1 2

C2

CSM	LEM	69 720193335.516114		144915.354	1
CSM	LEM	69 7201933 1.707 62	359.3627930 338.0273437	23.0026338 2.6696777	1 1
CSM	LEM	69 720193436.426114		3.0212402 155791.600	2 1
CSM	LEM	69 720193538.477114		167700.785	2 1
CSM	LEM	69 7201934 1.316 62	.2197266 339.1369629	22.7362154 2.8125000	1 2
CSM	LEM	69 720193638.824114		3.8012695 180278.346	2 1
CSM	LEM	69 720193612.625 62	1.1206055 340.9167480	22.1814058 3.1311035	2 1
CSM	LEM	69 720193741.965114		4.8120117 194435.693	2 1
CSM	LEM	69 720193718.957 62	.2307129 341.3562012	22.0221040 3.2958984	1 2
CSM	LEM	69 720193850.777114		4.4714355 211023.488	1 2
CSM	LEM	69 720193829.965 62	.1098633 340.7299805	22.7060030 3.5156250	1 2
CSM	LEM	69 720193953.195114		4.8559570 227125.195	1 2
CSM	LEM	69 720194053.867114		243712.990	1
CSM	LEM	69 720194154.324114		261212.203	2 1
CSM	LEM	69 720194254.785114		279562.070	2 1
CSM	LEM	69 720194356.004114		299127.164	2 1

## INS TO CSI

VEH1	VEH2	YYMMDDHHMMSS.SSS	XFSHAFT(DEG)	TRUN(DEG)	RANGE(FT)	RRATE(FPS)
			INNER(DEG)	MIDDLE(DEG)	OUTER(DEG)	
CSM	LEM	69 721182722.246	62 359.3078613 36.1230469	22.7444551 1.6699219	1.5380859	1
LEM	CSM	69 721183052.766	11 359.9890137 259.4860840	.1208496 1.0437012	888923.836 .1098633	2 2
LEM	CSM	69 721183158.105	11 359.5605469 256.1901855	.0769043 1.0437012	876692.312 .1428223	-193.9901 -179.5511
LEM	CSM	69 7211833	7.746 11 359.9670410 251.7846680	.0439453 1.1096191	864835.992 .2087402	-164.4841 2
LEM	CSM	69 721183415.707	11 357.8906250 249.9938965	359.3188477 .9448242	854105.273 .8789063	-150.6721 2
LEM	CSM	69 721183523.215	11 354.1003418 249.8620605	355.5175781 4.0539551	844350.078 4.3395996	-136.8601 2
LEM	CSM	69 721183641.754	11 354.1113281 245.4125977	2.9113770 1.8786621	834294.719 357.1325684	-121.7931 2
LEM	CSM	69 7211837	.504 11 356.2646484 242.1936035	4.5483398 3.3398438	832043.516 355.4736328	-118.0261 2
LEM	CSM	69 721183719.246	11 358.7145996 238.6779785	2.5708008 3.8562012	829942.398 357.5939941	-114.2601 2
CSM	LEM	69 721183749.316	62 .8459473 .8569336	21.9534395 5.7238770	8.0639648	1 2
LEM	CSM	69 721183753.215	11 .9667969 234.4592285	358.7475586 5.5480957	826115.359 1.6040039	-107.9821 2
CSM	LEM	69 721183753.574	62 .8789063 .6262207	21.9479463 5.7458496	8.1188965	1
CSM	LEM	69 721183842.324	62 358.9782715 357.9016113	21.8518159 6.0974121	7.3608398 818270.469	2
CSM	LEM	69 7211839	4.004114			1
CSM	LEM	69 721184012.098114			812133.586	2

C-4

## CSI TO CDH

VEH1	VEH2	YYMMDDHHMMSS.SS	XFSHAFT(DEG)	TRUN(DEG)	RANGE(FT)	RRATE(FPS)
			INNER(DEG)	MIDDLE(DEG)	OUTER(DEG)	
CSM	LEM	69 72119 217.414114			746693.828	1
CSM	LEM	69 72119 7 2.098114			731503.539	2
CSM	LEM	69 72119 8 2.566114			728283.195	1
CSM	LEM	69 72119 9 4.617114			724941.336	2
CSM	LEM	69 72119 943.887 62	1.1096191 259.3762207	22.5576875	1.2080078	1
CSM	LEM	69 72119 946.906 62	1.0656738 259.1455078	22.6428316 1.5930176	3.1970215	2
CSM	LEM	69 7211910 5.555 62	.8898926 258.0139160	22.8378389 1.6259766	3.1640625	1
CSM	LEM	69 7211910 9.316114			721417.187	2
CSM	LEM	69 721191029.414 62	1.4282227 258.4094238	21.2393281 1.6040039	3.2629395	1
CSM	LEM	69 721191113.117114			717953.797	2
CSM	LEM	69 721191215.125114			714490.414	1
CSM	LEM	69 721191258.777 62	.2856445 249.4555664	22.6373384 2.5158691	4.0979004	2
CSM	LEM	69 7211913 .547 62	.2416992 249.3347168	22.6675508 2.5268555	4.0869141	1
CSM	LEM	69 721191320.387114			710844.742	2
CSM	LEM	69 721191352.465 62	359.3298340 246.7749023	22.5933931 3.0102539	4.1857910	1
CSM	LEM	69 721191357.098 62	359.3847656 246.3684082	22.7691743 3.0651855	4.3505859	2

CSM	LEM	69	121191752.375114		604743.0731		
CSM	LEM	69	721191853.535114		690915.086		
CSM	LEM	69	721191941.215 62	.6152344 229.9328613	22.2473238 .9997559	2.3291016	
CSM	LEM	69	721191948.887 62	.4724121 229.3945312	22.4121187 1.0327148	2.2961426	
CSM	LEM	69	7211920 8.625114			686054.195	
CSM	LEM	69	7211921 3.785 62	359.3957520 226.1096191	21.9946382 1.1645508	1.7907715	
CSM	LEM	69	721192125.965114			680889.492	
CSM	LEM	69	7211922 3.438 62	358.4948730 223.0224609	22.1621797 1.3842773	1.5380859	
CSM	LEM	69	721192226.598114			676636.211	
CSM	LEM	69	7211923 7.707 62	.7910156 219.1992187	22.8625581 1.0217285	2.6257324	
CSM	LEM	69	721192424.516 62	359.6594238 216.2438965	22.0660493 .6481934	1.3183594	
CSM	LEM	69	721192545.574114			662114.297	
CSM	LEM	69	721192548.605 62	358.6157227 212.1679687	22.0687959 .3845215	.2856445	
CSM	LEM	69	7211926 9.484 62	359.0002441 211.3549805	21.8655488 .3186035	.4504395	
CSM	LEM	69	721192933.285 62	358.7145996 201.4892578	21.8902681 .1538086	.0988770	
LEM	CSM	69	721192935.656 11	359.8461914 76.0144043	356.1877441 9.2724609	643993.273 3.3288574	-84.7531
LEM	CSM	69	721193041.336 11	354.1113281 78.5083008	2.3400879 .8789063	638290.234 357.0886230	-87.8921
CSM	LEM	69	721193052.586114			636837.656	
CSM	LEM	69	7211931 7.395 62	359.1979980 196.8200684	22.0193574 .0329590	.2636719	
CSM	LEM	69	721193142.527 62	358.8684082 195.0952148	22.0578096 .0109863	.0329590	

LEM	CSM	69	721193149.	117	11	359.0551758	359.9011230	632287.039	-90.4031
						70.4113770	7.6574707	359.4946289	2
CSM	LEM	69	7211932	1.266	62	358.6816406	22.0578096		1
						194.2053223	.0219727	359.9340820	2
CSM	LEM	69	7211932	2.215114				630700.781	1
									2
CSM	LEM	69	721193224.	527	62	358.4619141	22.0468233		1
						193.1066895	.0549316	359.8352051	2
LEM	CSM	69	721193256.	945	11	358.5717773	357.1875000	625983.672	-93.5421
						67.5878906	1.3293457	2.2851563	2
CSM	LEM	69	7211933	5.035114				624867.711	1
									2
LEM	CSM	69	7211934	4.824	11	1.0986328	359.3518066	619605.273	-96.0531
						61.8640137	7.3498535	.2966309	2
LEM	CSM	69	721193512.	375	11	357.2753906	2.5378418	613076.797	-98.5651
						62.3693848	355.5834961	357.1545410	2
LEM	CSM	69	721193617.	215	11	355.4956055	4.6252441	606623.359	-101.0761
						61.1718750	5.3063965	354.4299316	2
LEM	CSM	69	721193736.	617	11	356.5393066	354.8803711	598519.039	-104.8431
						56.3269043	4.1308594	4.3615723	2
LEM	CSM	69	721193842.	035	11	62307129	354.8474121	591540.312	-106.7261
						49.5922852	10.7226562	4.6691895	2
LEM	CSM	69	721194047.	637	11	353.04411621	357.3193359	577807.992	-111.7481
						50.3833008	3.9111328	1.7138672	2
LEM	CSM	69	7211941	6.355	11	1.7578125	356.2536621	575706.875	-112.3761
						41.2426758	9.5581055	3.5156250	2
LEM	CSM	69	721194125.	125	11	6.4284668	6.2526855	573680.797	-113.6321
						41.6491699	4.9438477	359.2749023	2
LEM	CSM	69	721194144.	145	11	358.5278320	4.3505859	571429.594	-114.2601
						42.6379395	.7910156	355.1220703	2
LEM	CSM	69	7211942	4.105	11	356.6601562	4.6472168	569103.359	-114.2601
						43.5168457	359.3627930	354.8583984	2
LEM	CSM	69	721194227.	074	11	355.2209473	3.77792969	566551.992	-115.5151
						43.9343262	1.7578125	355.5285645	2
LEM	CSM	69	721194246.	027	11	354.0454102	3.2409668	564375.836	-116.1431
						44.2199707	2.8564453	355.9130859	2
LEM	CSM	69	7211943	5.457	11	353.3203125	2.4938965	562124.633	-116.7711
						44.0222168	2.5927734	356.6601562	2
LEM	CSM	69	721194324.	848	11	357.0336914	1.5380859	559873.437	-118.0261
						39.4189453	2.8454590	357.7917480	2

LEM	CSM	69	721194347	•367	11	2.8564453	.4614258	557171.992	-118.0261
						32.5195313	.0988770	359.0332031	2
LEM	CSM	69	7211944	7.426	11	2.4279785	359.2199707	554770.719	-118.6541
						32.0141602	4.4384766	.4504395	2

## CDH TO TPI

VEH1	VEH2	YYMMDDHHMMSS.SSS	XFSHAFT(DEG)	TRUN(DEG)	RANGE(FT)	RRATE(FPS)
			INNER(DEG)	MIDDLE(DEG)	OUTER(DEG)	
LEM	CSM	69 721195358.598	11 358.5058594	353.4082031	481156.477	-124.3041
			7.8552246	353.7487793	6.3281250	2
LEM	CSM	69 7211955 3.687	11 1.5380859	3.2629395	473127.199	-123.6771
			1.6259766	348.9807129	356.0339355	2
CSM	LEM	69 721195535.055114			468954.590	1
						2
LEM	CSM	69 7211956 9.316	11 355.4626465	355.8471680	465097.918	-123.0491
			4.6472168	356.1328125	4.0649414	2
CSM	LEM	69 721195635.664114			461420.207	1
						2
LEM	CSM	69 721195717.098	11 359.6923828	355.6384277	456768.477	-123.0491
			357.1545410	356.3635254	3.9770508	2
CSM	LEM	69 721195738.605114			453764.301	1
						2
LEM	CSM	69 721195824.957	11 354.8254395	3.9111328	448439.039	-122.4211
			358.7475586	358.4838867	355.8361816	2
LEM	CSM	69 721195926.266	11 .3076172	.5932617	441010.078	-122.4211
			350.3430176	357.9345703	359.0441895	2
CSM	LEM	69 721195945.348114			438209.445	1
						2
LEM	CSM	69 72120 031.117	11 359.9121094		433055.836	-121.7931
			347.7282715	15.1281738	359.6154785	2
LEM	CSM	69 72120 236.715	11 357.7368164	357.8356934	417822.719	-121.1651
			343.8171387	357.7807617	1.9665527	2
LEM	CSM	69 72120 318.117	11 359.7143555	.0329590	412870.078	-121.1651
			339.9060059	7.4157715	359.6484375	2
LEM	CSM	69 72120 336.746	11 1.6589355	358.7915039	410543.836	-120.5381
			337.0605469	5.4272461	1.0766602	2
CSM	LEM	69 72120 348.926114			408740.285	1
						2
LEM	CSM	69 72120 412.254	11 1.7138672	355.8691406	406266.559	-120.5381
			335.3356934	4.0209961	3.9880371	2

CSM	LEM	69	72120	450.437114		401327.426		1
LEM	CSM	69	72120	520.215 11	355.5834961 338.2470703	2.8564453 5.0207520	398087.199 356.5173340	2 2
LEM	CSM	69	72120	628.125 11	357.2424316 333.4460449	358.3850098 9.8327637	389982.879 .9228516	2 2
CSM	LEM	69	72120	655.426114			386380.180	1 2
CSM	LEM	69	72120	7 6.906 62	359.4506836 93.6364746	22.5467012 1.0876465		1 2
CSM	LEM	69	72120	713.957 62	359.3408203 93.2739258	22.5851533 1.1755371	1.2304688 1.2744141	1 2
LEM	CSM	69	72120	735.625 11	.0659180 327.3706055	359.3737793 .7690430	381878.559 .4724121	2 2
CSM	LEM	69	72120	756.324114			379149.602	1 2
CSM	LEM	69	72120	813.984 62	359.7692871 90.1977539	22.8350923 1.3732910		1 2
LEM	CSM	69	72120	842.707 11	358.5498047 325.7336426	2.4499512 .7800293	373999.359 357.4072266	-118.6541 2
CSM	LEM	69	72120	844.977 62	359.2858887 89.1979980	22.3791597 1.4721680	1.5820313 370825.324	1 2
CSM	LEM	69	72120	9 6.414114				1 2
CSM	LEM	69	72120	917.125 62	358.7145996 88.2751465	21.8023775 1.5930176		1 2
LEM	CSM	69	72120	951.086 11	355.8581543 325.2392578	3.9550781 1.0546875	365895.039 355.8691406	-118.6541 2
CSM	LEM	69	72120	954.586 62	358.5607910 86.2866211	22.0330904 1.5930176	1.1975098 362379.523	1 2
CSM	LEM	69	721201017.637114					1 2
LEM	CSM	69	721201059.355 11	358.5827637 319.3395996	4.0759277 1.4392090	357865.758 355.8471680	-118.0261 2	
CSM	LEM	69	72120111	5.098 62	.1318359 82.2106934	22.8433321 1.0546875	1.4172363 354055.246	1 2
CSM	LEM	69	721201128.637114					1 2
LEM	CSM	69	721201310.047 11	357.1655273 314.7033691	358.9453125 359.3627930	342482.559 1.1206055	-116.7711 2	

C-11

LEM	CSM	69	721201328.746	11	353.8366699	357.7258301	340306.398	-116.7711
					317.1752930	359.6923828	2.3620605	2
CSM	LEM	69	721201339.566	62	359.7802734	22.7746675		1
					75.1464844	1.1425781	1.1425781	2
LEM	CSM	69	721201347.437	11	354.5178223	356.2097168	338130.238	-117.3991
					315.6152344	.3845215	3.8342285	2
CSM	LEM	69	721201434.098	62	.1318359	22.5192354		1
					72.8723145	1.6149902	1.9555664	2
CSM	LEM	69	721201436.617114				332059.707	1
								2
CSM	LEM	69	721201447.098	62	359.6594238	22.7499483		1
					72.0703125	1.7687988	1.8786621	2
LEM	CSM	69	721201452.555	11	357.4951172	2.7136230	330551.199	-116.7711
					309.6826172	357.1325684	357.5280762	2
LEM	CSM	69	7212016 .547	11	356.8249512	358.4838867	322596.957	-115.5151
					307.2436523	1.9885254	1.5600586	2
LEM	CSM	69	7212017 8.656	11	2.0764160	359.4177246	314792.797	-115.5151
					298.8830566	3.8122559	.9228516	2
LEM	CSM	69	721201816.816	11	354.5068359	3.9770508	306876.078	-114.8871
					303.3984375	357.4401855	356.5173340	2
LEM	CSM	69	7212020 9.406	11	.3186035	358.9892578	294006.719	-114.2601
					292.5878906	358.3410645	1.3732910	2
LEM	CSM	69	721202038.305	11	356.2426758	.5383301	290695.578	-113.6321
					295.4223633	355.3527832	.1538086	2
LEM	CSM	69	721202145.957	11	358.0554199	.1867676	283032.117	-113.6321
					290.5883789	359.6154785	.2636719	2
LEM	CSM	69	721202251.035	11	357.6928711	359.9670410	275678.199	-113.0041
					288.0944824	1.6259766	.4504395	2
LEM	CSM	69	721202424.887	11	359.3078613	.0549316	265125.699	-112.3761
					282.3706055	6.7016602	.4394531	2
LEM	CSM	69	721202454.926	11	359.8681641	359.7692871	261748.898	-111.7481
					280.5578613	3.4167480	.8239746	2
LEM	CSM	69	721202513.324	11	359.7473145	359.5056152	259694.680	-112.3761
					279.9755859	358.0883789	1.1315918	2
LEM	CSM	69	721202532.207	11	358.6486816	358.7255859	257593.559	-111.7481
					280.2832031	357.3303223	1.9775391	2
LEM	CSM	69	721202550.605	11	356.8029785	357.6379395	255558.100	-111.7481
					281.3049316	359.8242187	3.0432129	2
LEM	CSM	69	7212026 9.004	11	354.1333008	356.2536621	253513.260	-111.7481
					283.1616211	2.8674316	4.1638184	2

LEM	CSM	69	721202627.586	11	350.5078125	354.3969727	251440.279	-111.1211
					285.9741211	6.4270020	5.3063965	2
LEM	CSM	69	721202646.504	11	346.2451172	351.9360352	249329.779	-111.1211
					289.4567871	10.7666016	6.4050293	2
LEM	CSM	69	7212027 5.555	11	343.1799316	354.0563965	247209.898	-111.1211
					291.6979980	6.6467285	4.9768066	2
LEM	CSM	69	721202724.695	11	350.3430176	.4724121	245099.398	-111.1211
					283.8208008	1.8237305	359.9890137	2
LEM	CSM	69	721202743.746	11	359.8352051	.0109863	242998.279	-110.4931
					273.5266113	359.9890137	.7470703	2
LEM	CSM	69	7212028 2.785	11	.3186035	357.4731445	240906.539	-110.4931
					272.2961426	358.0773926	3.2958984	2
LEM	CSM	69	721202821.785	11	359.7912598	354.8913574	238814.799	-109.8651
					272.0874023	356.7041016	5.9216309	2
LEM	CSM	69	721202840.785	11	359.3188477	356.2316895	236732.439	-110.4931
					271.7578125	359.0332031	4.6032715	2
LEM	CSM	69	721202859.797	11	358.8574219	357.6818848	234640.699	-109.8651
					271.4172363	.1757813	3.1530762	2
LEM	CSM	69	721202918.816	11	.1428223	358.9892578	232548.959	-109.8651
					269.3408203	1.0546875	1.8786621	2
LEM	CSM	69	721202937.816	11	358.6816406	.2526855	230466.600	-109.2371
					270.0439453	.9777832	.6042480	2

## APPENDIX D

### Apollo 11 Landing Radar Data

The LM landing radar data that was used in the analysis is listed in the two card format of the HOPE orbit determination program. The first card specifies the vehicle, the time of the observation (year (mod 1900), month, day, hour, minute, and second), three code numbers,  $V_{XA}$  measurement,  $V_{YA}$  measurement,  $V_{ZA}$  measurement, and the slant range measurement ( $\rho$ ). The second card specifies the inner, middle, and the outer gimbal angles. The units are feet and feet per second.

D-2

## LANDING RADAR OBSERVATIONS

VEHI	YYMMDDHHMMSS.SSS	XFVX(FPS)	VY(FPS)	VZ(FPS)	RANGE(FT)
			INNER(DEG)	MIDDLE(DEG)	OUTER(DEG)
LEM	69 72020 953.164125	79.1564941	.2746582	28.0261233	43753.4501
LEM	69 72020 955.164125	78.9147949	359.7583008	20.3796387	41897.5701
LEM	69 72020 957.164125	78.3654785	359.9450684	12.7001953	41144.1951
LEM	69 72020 959.164125	77.9589844	.6701660	4.9328613	39329.5501
LEM	69 7202010 1.164125	77.8401211	1.2744141	1.2524414	39005.8501
LEM	69 7202010 3.164125	78.0468750	1.1865234	3.0541992	39671.3601
LEM	69 7202010 5.164125	78.1457520	.1867676	3.6694336	38520.3001
LEM	69 7202010 7.164125	77.9919434	358.9782715	3.9221191	38444.7701
LEM	69 7202010 9.164125	77.7502441	353.8793945	4.5503262	37781.1851
LEM	69 720201011.164125	77.2558594	359.9352051	5.2294922	37473.6601
LEM	69 720201013.164125	77.9040527	.3569336	4.7680664	37295.6351
LEM	69 720201015.164125	77.8491211	1.2634277	3.8891602	37284.8451
LEM	69 720201017.164125	77.2448730	.6921387	4.2187500	36594.2851
LEM	69 720201019.164125	77.4645996	.5603027	5.0207520	36480.9901
LEM	69 720201021.164125	77.3657227	1.3732910	4.9987793	36480.9901
LEM	69 720201025.164125	77.1780551	359.558594	3.1201172	35666.3451
LEM	69 720201027.164125				35785.0351

LEM	69 720201025.164125	76.8933105 359.34.8203	2.9663086	35191.5841
LEM	69 720201031.164125	76.1692129 .8789063	3.186 352	34262.491
LEM	69 720201033.164125	76.7724609 .7910156	3.2849121	34967.8851
LEM	69 720201035.164125	77.1130371 359.9890137	3.2629395	34511.9141
LEM	69 720201037.164125	77.0031738 359.9340820	3.1061309	34290.6201
LEM	69 720201039.164125	75.8056641 .5493164	3.0212402	33195.4351
LEM	69 720201041.164125	74.2895508 .6811523	2.9223633	33119.9151
LEM	69 720201043.164125	75.3272656 .2307129	2.8894043	33087.5351
LEM	69 720201045.164125	76.5197754 .0878906	2.9443359	32245.9151
LEM	69 720201047.164125	74.0039062 359.6484375	2.9553223	31733.3901
LEM	69 720201049.164125	73.9160156 1.4721680	2.9553223	31560.7501
LEM	69 720201051.164125	73.4436035 .7031250	2.8344727	30800.0551
LEM	69 720201053.164125	72.6635742 359.6704102	2.7355957	30514.1201
LEM	69 720201054.086125	72.9492188 359.8022461	1.1206055 1204.332	2 1
LEM	69 720201055.164125	72.0931641 359.8352051 359.2968750		2
LEM	69 720201057.164125	73.2128906 359.8022461 358.6596680		30449.3801
LEM	69 720201058.176125	72.0373535 359.6044922 359.0551758 -94.0511999		30109.4951 1
LEM	69 720201059.164125	71.7077637 .1310359 359.3408293		29311.0351
LEM	69 72020111 .246125	70.6640625 .5273438 359.4726562 1232.243		2 1
LEM	69 72020111 1.164125	69.8510742 .9008789 359.6813965		28884.8301
		77.1626777 1.1206055 359.8352051		2

LEM	69 72020111 3.164125	71.1584473	.8349609	.1098633	27573.8451
LEM	69 72020111 5.164125	70.9277344	.3076172	.2746582	26388.4001
LEM	69 72020111 6.277125	70.0048828	-46.0559998	.3186035	1
LEM	69 72020111 7.164125	69.8270996	359.9450684	.3735352	2
LEM	69 72020111 7.934125	68.9941406	.3076172	1176.941	1
LEM	69 72020111 9.164125	68.7963867	.5712891	.3955078	2
LEM	69 720201111.164125	69.5324707	.9997559	.4394531	27325.6751
LEM	69 720201111.957125	68.8293457	-04.7783995	.4394531	27309.4951
LEM	69 720201113.164125	68.3459473	359.4177246	.3186035	2
LEM	69 720201113.957125	67.9174805	359.4836426	1138.975	1
LEM	69 720201115.164125	67.9284668	.4284668	.3295898	2
LEM	69 720201117.164125	66.8627930	.9008789	.2526855	26726.8301
LEM	69 720201117.957125	66.4562988	-59.6303992	.1318359	2
LEM	69 720201119.164125	65.9729004	.8569336	.0549316	26273.6501
LEM	69 720201119.957125	65.6872559	.6811523	359.9340820	2
LEM	69 720201121.164125	66.4233398	1.0107422	1136.895	1
LEM	69 720201123.164125	67.1044922	.5383301	359.7692871	2
LEM	69 720201124.086125	67.1923828	.8239746	25707.1751	
LEM	69 720201125.164125	66.7639160	-81.4463987	359.2419434	2
LEM	69 720201126.086125	67.7636719	.2966309	358.9892578	1
LEM	69 720201127.164125	66.7639160	359.5275879	25307.9451	
			358.9123535	1038.426	2
			.2526855	358.9782715	1
				25361.8951	2

5

LEM	69 72020112 <sup>c</sup> .164125	68.4228516	.9887695	358.9672852	2
LFM	69 72020113 <sup>c</sup> .055125	67.5439453	.4064941	358.9233358	2
LEM	69 720201131.164125	66.6870117	-95.5056000	359.0022461	1
LEM	69 720201131.926125	66.5441895	359.7253418	358.9782715	2
LEM	69 720201133.164125	66.1816406	359.5275879	359.0332031	1
LEM	69 720201135.164125	66.7095844	359.6594238	359.0002441	2
LEM	69 720201135.887125	67.3022461	359.9670410	359.0112305	1
LEM	69 720201137.164125	66.9177246	-73.6806000	.0439453	2
LEM	69 720201137.995125	67.2363281	.7250977	358.9782715	2
LEM	69 720201139.164125	66.4562988	.2526955	359.0112305	1
LEM	69 720201139.887125	66.1486816	359.9340820	359.0441895	2
LEM	69 720201139.887125-979.4935837	65.6652832	359.5605469	359.0332031	1
LEM	69 720201141.164125	65.7212148	359.9340820	359.1101074	2
LEM	69 720201141.887125	65.5554190	-74.4167995	.4943848	1
LEM	69 720201143.164125	65.3796387	1.3513184	359.1540527	2
LEM	69 720201143.965125	64.7534180	1.3732910	359.1870117	1
LEM	69 720201145.164125	63.5888672	960.588	359.2529297	2
LEM	69 720201145.875125-912.5479889	63.2702637	.6591797	359.1979980	1
LEM	69 720201147.164125	63.5559082	.5053711	359.2309570	2
LEM	69 720201147.895125	62.9077148	.1423223	359.1760254	1
LEM	69 720201149.164125	63.5559082	-80.2343988	.7141113	2
LEM	69 720201149.164125	64.0283203	1.1755371	359.1760254	1
				22383.8551	
				22383.8551	

D-6

LEM	69 720201149.926125	64.3469238	.1.4282227	359.6991211	920.542	1
LEM	69 720201151.164125	63.509766	.6811523	359.6771484	22254.3751	2
LEM	69 720201151.895125-891.4247894	63.3471680	.4064941	359.0441895		1
LEM	69 720201153.164125	62.5451660	359.7473145	359.2529207		2
LEM	69 720201153.897125	-93.323994				1
LEM	69 720201155.164125	62.4572754	359.5935059	359.3627930		2
LEM	69 720201155.887125	62.1057129	359.7692671	359.5715332	21202.3501	2
LFM	69 720201155.887125	911.180				1
LEM	69 720201157.164125	62.0617676	359.9121094	359.7143555		2
LEM	69 720201157.164125	62.0577812	.6262207	359.9711230	2921.81	1
LEM	69 720201157.895125-845.0567856	61.9519043	.8459473	.0549316		2
LEM	69 720201159.164125	61.5628906	1.5930176	.1757813	20835.4901	2
LEM	69 720201159.895125	-40.7231994				1
LEM	69 7202012 1.164125	61.2817383	1.2854004	.2856445		2
LEM	69 7202012 1.887125	60.8312988	1.3842773	.3845215	20376.9151	2
LEM	69 7202012 3.164125	60.2050781	.9997559	.4284668		1
LEM	69 7202012 3.164125	60.2929687	.9997559	.5383311	20139.5351	2
LEM	69 7202012 3.895125-791.4759903	59.9633789	.6701660	.5383301		1
LEM	69 7202012 5.164125	60.5346680	.6152344	.6262207	19923.7351	2
LEM	69 7202012 5.887125	60.5017090	-62.5391994			1
LEM	69 7202012 7.164125	.4614258	.6262207			2
LEM	69 7202012 7.887125	61.2268066	.3735352	.6491934	19643.1951	2
LEM	69 7202012 7.887125	846.517				1
LEM	69 7202012 9.164125	61.2597656	.4724121	.6591797		2
LEM	69 7202012 9.164125	61.4355469	.4284668	.6152344	19443.9751	2
LEM	69 7202012 9.897125-787.2255859					1

LEM	69 720201211.164125	61.3476562	.8239746	.6481934	19048.3001	2
LEM	69 720201211.895125	60.8982031	.8789063	.5932617		2
LEM	69 720201213.164125	60.7653809	-40.2655995	1.4941406		1
LEM	69 720201213.164125	59.8235566	1.7468262	.5493164		2
LFM	69 720201213.895125	59.7436523	2.3510742	835.422		1
LFM	69 720201215.164125	58.9196777	1.3073730	.4943848		2
LEM	69 720201215.957125-734.4175873	59.1833496	1.0217285	.2856445		2
LEM	69 720201217.164125	58.7878418	.0549316	.1538086	17981.5351	2
LEM	69 720201217.937125	59.6118164	-68.5991993	.3405762	.0219727	1
LEM	69 720201219.164125	59.9743652	.8020020	359.8681641		2
LEM	69 720201219.895125	60.6445313	1.2634277	783.587		1
LEM	69 720201221.164125	59.6777344	1.0107422	359.7473145		2
LEM	69 720201221.895125-713.8095856	59.4140625	.5822754	359.4067383		2
LEM	69 720201223.164125	58.5681152	.3625488	359.3078613	17103.8651	2
LEM	69 720201223.895125	58.4033203	-74.1743094	359.3670410	359.3847656	1
LEM	69 720201225.164125	58.2495117	.3405762	359.4396973		2
LEM	69 720201225.926125	58.2385254	.2197266	766.945		1
LEM	69 720201227.164125	58.6560059	1.0766602	359.5385742		2
LEM	69 720201227.895125-679.8063812	58.7219238	1.1425781	359.5385742		1
LEM	69 720201229.164125	59.1833496	1.8896484	359.5605469	16422.3901	2
LEM	69 720201229.895125	58.4912109	-49.9647999	1.4611816	359.5495605	1

D-8

LEM	69 720201231.164125	58.1945801	1.1755371	359.5166016	16023.1501
LEM	69 720201231.895125	57.4914551	.9118652	359.4726562	2
LEM	69 720201233.164125	57.5463967	.7800293	359.3957520	1
LEM	69 720201233.897125	57.0849609	.9228516	359.4506836	2
LEM	69 720201235.164125	57.5024414	1.0327146	359.5166016	1
LEM	69 720201235.897125		-46.5407996		2
LEM	69 720201237.164125	57.2827148	1.4501953	359.5825195	1
LEM	69 720201237.895125	57.7993723	1.5161133	359.6264648	2
LEM	69 720201239.164125	57.8979492	1.9445801	359.6264648	1
LEM	69 720201239.937125	58.6120605	1.6040039	359.6594238	2
LEM	69 720201239.937125	58.7438965	1.6149902	359.6154785	1
LEM	69 720201241.164125	58.5351562	.4064941	359.6154785	2
LEM	69 720201242.055125		-51.8736000		1
LEM	69 720201243.164125	57.9748535	.6591797	359.5495605	2
LEM	69 720201243.895125	56.9860840	.5603027	359.5605469	1
LEM	69 720201243.895125	56.8762207	.9887695	359.5385742	2
LEM	69 720201245.164125	56.6674805	.8459473	359.4616699	1
LEM	69 720201245.957125	591.8359909			2
LEM	69 720201245.957125	57.5573730	.7141113	359.4177246	1
LEM	69 720201247.164125	57.9199219	.2746582	359.4067383	2
LEM	69 720201247.895125		-56.4791994		1
LEM	69 720201249.164125	58.3593750	.3295898	359.5275879	2
LEM	69 720201249.895125	56.9531250	1.2963867	359.7253418	1
LEM	69 720201249.895125			632.071	2
LEM	69 720201251.164125	56.5026855	1.5930176	359.8681641	1
					12910.2351

LEM		55.6457520	1.7248535	.0000000	2
LEM	69 720201251.895125-549.9455948	55.9643555	1.0107422	.0769043	1
LEM	69 720201253.164125	56.0961914	.5053711	.1428223	2
LEM	69 720201253.937125	56.6674805	-48.9647999		1
LEM	69 720201255.164125	56.7553711	1.4062500	.3186035	2
LEM	69 720201255.887125	56.6784668	1.7358398	.3845215	1
LEM	69 720201257.164125	56.4477539	2.6916504	.4943848	2
LEM	69 720201257.895125-526.9277916	56.3598633	1.7578125	.5053711	1
LEM	69 720201259.164125	56.5686035	.7360840	.5163574	2
LEM	69 720201259.895125	-45.3287997			1
LEM	69 7202013 1.164125	56.5026855	359.9450684	.5053711	2
LEM	69 7202013 1.887125	56.9750977	.6701660	.5383301	2
LEM	69 7202013 3.164125	56.7224121	1.1096191	.5712891	1
LEM	69 7202013 3.164125	56.8212891	2.0324707	.5932617	2
LEM	69 7202013 3.895125-501.8047905	56.4697266	2.2631836	.6042480	1
LEM	69 7202013 5.164125	57.1179199	1.7138672	.5493164	2
LEM	69 7202013 5.895125	-25.4519999			1
LEM	69 7202013 7.164125	57.0959473	1.3073730	.5053711	2
LEM	69 7202013 7.895125	57.3815918	.4174805	.4284668	1
LEM	69 7202013 9.164125	56.7663574	.5603027	.3845215	2
LEM	69 7202013 9.926125-469.6047897	56.2280273	.1977539	.3295898	2
LEM	69 720201311.164125	55.7446289	.4064941	.2526855	1
LEM	69 720201311.164125	55.6677246	.0109863	.1647949	2

8-10

LEM	69 720201311.895125	-44.8439999		1	
LEM	69 720201313.164125	55.7446289	.2526855	.0769043	2
LEM	69 720201314.055125	56.1071777	359.9450684	359.9670410	2
LEM	69 720201315.164125	56.5466309	.2307129	359.8242187	2
LEM	69 720201315.926125-454.4063911	56.9421387	.1757813	359.7253418	2
LEM	69 720201317.164125	57.1728516	.7690430	359.6154785	2
LEM	69 720201317.957125	56.6125488	1.9116211	359.7253418	2
LEM	69 720201317.957125	56.6125488	-12.8471999		1
LEM	69 720201319.164125	55.8984375	2.5598145	.0878996	2
LEM	69 720201319.895125	56.1730957	2.0104980	.1977539	2
LEM	69 720201321.164125	55.9753418	1.5490723	.2966309	2
LEM	69 720201321.895125-418.7287903	56.2390137	1.0437012	.4174805	2
LEM	69 720201323.164125	56.0522461	1.0986328	.4833984	2
LEM	69 720201323.895125	56.1950684	-26.6639998		1
LEM	69 720201325.164125	55.9863281	1.1315918	.6701660	2
LEM	69 720201325.895125	55.8544922	.9777832	.402.369	1
LEM	69 720201327.164125	55.6347656	.7250977		2
LEM	69 720201327.895125-386.7863922	1.1315918	.8239746	7795.7751	2
LEM	69 720201329.164125	55.2572441	1.0656738	.8349609	2
LEM	69 720201329.895125	55.0964355	.9448242	.7504.4451	2
LEM	69 720201331.164125	54.6240234	-15.0287999	.9118652	1
LEM	69 720201331.164125	55.0305176	.9338379	.7250.8801	2
LEM	69 720201341.164125	55.0305176	.5493164	.9448242	2
				6538.7401	

LEM	69 720201341.754125	46.3623047	1.7029809	.8893926	2
				217.567	1
LEM	69 720201343.164125	46.3952637	2.2302246	.8569336	2
		45.3955078	2.0544434	.7910156	6177.2751
LEM	69 720201343.895125-375.5807915	45.7690430	1.5270996	.7141113	2
					1
LEM	69 720201345.164125	45.3186035	.7360840	.5383301	2
			-25.9368000		1
LEM	69 720201345.937125	45.6481934	.3515625	.4614258	2
					5653.9601
LEM	69 720201347.164125	44.3957520	1.1975098	.3186035	2
				206.992	1
LEM	69 720201347.965125	44.0112305	1.5930176	.2746582	2
					5395.0001
LEM	69 720201349.164125	43.3959961	2.4389648	.1533086	2
		43.4399414	2.0874023	.0219727	1
LEM	69 720201351.164125	44.1101074	1.8566895	359.7912598	2
			-18.6647999		1
LEM	69 720201351.926125	43.9782715	1.4062500	359.7692871	2
					4979.5851
LEM	69 720201353.164125	44.3078613	1.1096191	359.8681641	2
				190.869	1
LEM	69 720201353.887125	43.3959961	1.1865234	359.9560547	2
					4758.3901
LEM	69 720201355.164125	42.6269531	1.7797852	.0988770	2
		42.4291992	3.2629395	.2526955	1
LEM	69 720201355.957125-296.6263962	43.2531738	3.3618164	.3076172	2
			-15.5136000		1
LEM	69 720201357.957125	43.0773926	1.9676758	.2636719	2
					4564.1701
LEM	69 720201359.164125	42.7697754	359.7692871	.2856445	2
				173.013	1
LEM	69 720201359.945125	42.7697754	359.3518066	.2856445	2
		39.7595215	359.8352051	.3625488	4094.0151
					2

D-12

LEM	69 7202014 2.164125-259.2743950	39.657123	359.5495605	.4504395	1
LEM	69 7202014 3.164125	38.9245605	359.7253418	.4394531	2
LEM	69 7202014 4.164125		-21.0988000		1
LEM	69 7202014 5.164125	39.0563965	359.4646289	.5603027	2
LEM	69 7202014 6.164125	38.5621117	359.3298340	.5163574	2
LEM	69 7202014 7.164125	38.2953398	359.4177246	.5493164	2
LEM	69 7202014 8.164125	37.8369141	359.3408203	.6262207	2
LEM	69 7202014 7.994125-226.0430968	36.7712402	359.9670410	.5603027	2
LEM	69 7202014 9.164125	36.1010742	.3845215	.6921387	2
LEM	69 720201410.145125		-19.6343999		1
LEM	69 720201411.164125	35.1123047	.9129883	.6811523	2
LEM	69 720201412.027125	35.4090355	.7693430	.6481934	2
LEM	69 720201412.027125	35.9344434	.3295898	.6921387	2
LEM	69 720201413.164125	36.0900879	.3295898	.5603027	2
LEM	69 720201414.164125-202.4735985	36.8811035	.0549316	.5712891	2
LEM	69 720201415.164125	36.2548828	.6042480	.5712891	2
LEM	69 720201416.047125		-14.7864000		1
LEM	69 720201417.164125	36.0131836	1.3293457	.5053711	2
LEM	69 720201418.055125	35.4969262	1.6699219	.6701660	2
LEM	69 720201418.055125	34.7937012	2.1423340	.7250977	2
LEM	69 720201419.164125	34.5300293	2.0764160	.7580566	2
LEM	69 720201420.066125-173.6223965	33.7609863	1.9017578	.8459473	2
LEM	69 720201421.875125		-12.1199009		1
LEM	69 720201423.164125	33.3984375	.5493164	.5008780	2
					2316.6131

LEM	69 720201423.984125	32.5085449	359.3188477	1.5051270	2
				140.248	1
LEM	69 720201425.164125	32.5085449	358.5058594	1.8566895	2
		32.2998047	358.6706543	2.5158691	2177.4221
LEM	69 720201426.164125-152.8855972	32.4865723	359.5385742	3.0102539	1
LEM	69 720201427.164125	32.8820801	359.9230957	3.2209805	2
LEM	69 720201428.027125		-9.9383998		1
		32.4316406	.1208496	3.3618164	2
LEM	69 720201429.164125	32.1020508	.1428223	3.4616934	1960.5431
LEM	69 720201430.176125	30.9045410	359.4726562	3.2189941	2
LEM	69 720201431.164125	29.4104004	358.2529297	3.0432129	2
LEM	69 720201432.277125-125.5799980	28.9940430	359.3298340	2.7905273	1
LEM	69 720201433.164125	28.0371094	359.4836426	2.5598145	2
LEM	69 720201433.965125		-10.1807998		1
		27.7954102	.0439453	2.4609375	2
LEM	69 720201435.164125	27.8723145	.3295898	2.1862703	1664.8971
LEM	69 720201435.957125	27.4328613	.4174805	1.9775391	2
LEM	69 720201437.176125	27.6416016	.7470703	1.7578125	1573.1821
LEM	69 720201437.957125-108.5783987	27.7075195	.5932617	1.5380859	2
LEM	69 720201439.176125	27.4548340	.6921387	1.1645508	1460.5681
LEM	69 720201440.055125		-11.3927999		1
		27.9272461	.8020620	1.2084961	2
LEM	69 720201441.176125	28.8171387	359.9890137	1.1975098	1401.6211
LEM	69 720201442.156125			101.589	2
		30.7177734	.2307129	1.1975098	1
LEM	69 720201444.387125-93.2511078			27.6153809	2
				.2307129	1.3403320

LEM	69 720201445.207125	25.4013906	.2356445	1.3623047	1229.0911
LEM	69 720201446.437125	24.5214844	-1.9179999	1.5390859	2
LEM	69 720201447.207125	24.6972656	.3955078	1.4831543	1
LEM	69 720201448.047125	25.1417051	.8459473	1.4721680	2
LEM	69 720201449.207125	25.8947754	1.0217285	1.6479492	1
LEM	69 720201450.066125	-81.4015989	26.2353516	1.1535645	2
LEM	69 720201451.215125	26.0925293	.8459473	1.5161133	1
LEM	69 720201452.098125	-9.9383998	25.5981445	.4833984	2
LEM	69 720201453.215125	24.7302246	.7250977	1.5380859	978.6531
LEM	69 720201453.977125	24.2248535	.9777832	1.4611816	2
LEM	69 720201455.215125	23.1811523	.9997559	1.5710449	2
LEM	69 720201453.977125	24.2248535	.9777832	1.4611816	1
LEM	69 720201457.215125	21.8078613	1.2034961	1.3952637	2
LEM	69 720201457.824125	-60.5359993	21.4892578	1.0217285	1
LEM	69 720201459.215125	21.0278320	.8789063	1.4282227	2
LEM	69 720201459.977125	20.8630371	-6.0599999	1.3183594	1
LEM	69 7202015 1.215125	20.2038574	.5712891	1.1975098	2
LEM	69 7202015 1.977125	19.8083496	.1209496	1.1865234	2
LEM	69 7202015 3.215125	19.3139648	.2197266	74.545	1
LEM	69 7202015 3.977125	-49.0423994	18.9624023	.9229516	2
LEM	69 7202015 5.215125	19.3139648	.0878906	1.0986329	1
					705.6661
					662.5'61

D-15

LEM	69	7202015	5.977125	18.6987305	.0549316	1.3293457	2
					-7.7568000		1
LEM	69	7202015	7.215125	18.5668945	359.9121094	1.3952637	2
							625.8201
LEM	69	7202015	7.977125	18.1054687	359.6484375	1.6918945	2
						66.570	1
LEM	69	7202015	9.215125	17.9626465	359.8022461	1.8237305	2
							581.5811
LEM	69	7202015	9.906125	17.6110840	359.3791504	1.9555664	2
				-38.6399994			1
LEM	69	720201511.	215125	17.3144531	359.8461914	2.0654297	2
							551.3691
LEM	69	720201511.	945125	17.1606445	.3515625	2.3291016	2
					-5.8176000		1
LEM	69	720201513.	215125	17.0507812	.5603027	2.3840332	2
							512.5251
LEM	69	720201514.	016125	16.6223145	.7250977	2.5598145	2
						58.596	1
LEM	69	720201515.	215125	16.5344238	.9667969	2.6916504	2
							486.6291
LEM	69	720201515.	984125	15.4687500	.9997559	2.8125003	2
				-27.9495997			1
LEM	69	720201517.	215125	12.0739746	.6811523	2.9333496	2
							461.8121
LEM	69	720201518.	004125	9.3383789	.7031250	3.2080078	2
					-4.3631999		1
LEM	69	720201519.	215125	6.3061523	.4394531	3.3398438	2
							448.8641
LEM	69	720201519.	937125	4.9768066	.1647949	3.5156250	2
						61.369	1
LEM	69	720201521.	215125	5.1196289	.2087402	3.6804199	2
							420.4421
LEM	69	720201521.	937125	5.1086426	.1647949	3.8671875	2
				-15.3271998			1
LEM	69	720201523.	215125	5.5500820	.0219727	3.9990234	2
							405.7041
LEM	69	720201524.	277125	5.0436035	.4504395	4.2187500	2
					-3.6360000		1
LEM	69	720201525.	215125	5.4931641	.3955078	4.4165039	2
							389.5191
				5.7238770	.3295899	4.5493309	2

LEM	69 720201526.437125	5.7348633	.4294668	57.729	1
LEM	69 720201527.215125	5.5371794	.3945215	4.8669434	2
LEM	69 720201528.445125	-12.1071998			367.9391
LEM	69 720201529.215125	5.9545898	.2956445	5.207520	1
LEM	69 720201530.437125	6.0424805	.3405762	5.1196289	2
LEM	69 720201531.215125	5.7897949	-1.9392000		1
LEM	69 720201531.215125	5.7897949	.2856445	5.2075195	2
LEM	69 720201532.437125	6.1093984	.2087402	5.1745605	343.1221
LEM	69 720201532.437125	6.3391113	.1867676	5.0537109	2
LEM	69 720201533.215125	6.1523438	.1098633	5.0097656	2
LEM	69 720201534.437125	-9.2735999			1
LEM	69 720201535.215125	6.4919336	359.8791504	4.9108887	2
LEM	69 720201536.437125	6.8334961	359.7912598	4.8229980	332.3321
LEM	69 720201537.215125	6.8334961	-3.8784000		1
LEM	69 720201537.215125	6.8334961	359.5275879	4.6911621	2
LEM	69 720201538.437125	7.0642090	359.2639160	4.6362305	2
LEM	69 720201539.215125	7.8222656	358.8903809	4.5043945	1
LEM	69 720201540.496125	7.6464844	358.6816406	4.3835449	2
LEM	69 720201541.215125	-9.1447998			1
LEM	69 720201541.215125	7.2619629	358.5278320	4.2626953	2
LEM	69 720201542.445125	7.2839355	358.3520508	4.1967773	316.1471
LEM	69 720201542.445125		-3.6360000		2
LEM	69 720201543.215125	6.9114004	358.4399414	4.0100098	1
LEM	69 720201543.215125	8.3935547	358.6047363	3.9660645	312.9101
LEM	69 720201544.477125	11.0632324	358.7585449	47.154	2
LEM	69 720201545.215125	11.3488770	358.8244629	3.9660645	2
LEM	69 720201546.477125	-11.9783998		302.1201	1

LEM	69 720201547.215125	11.7333984	359.0112305	3.7573242	2
LEM	69 720201548.47125	12.3266602	359.0332031	3.7243652	2
		-5.8176000			1
LEM	69 720201549.215125	13.6669922	359.2419434	3.6254893	2
LEM	69 720201550.437125	14.8425293	359.4726562	3.5705566	2
		-41.433			1
LEM	69 720201551.215125	14.934199	359.5605469	3.4826660	2
LEM	69 720201552.445125	15.1611328	359.6813965	3.4387207	2
		-11.3343998			1
LEM	69 720201553.215125	15.3588867	359.9780273	3.2958984	2
LEM	69 720201554.426125	15.368730	.0659180	3.2080078	2
		-4.3631999			1
LEM	69 720201555.215125	15.7104492	.2526855	3.1091309	2
LEM	69 720201556.437125	15.7983398	.3515625	2.9882813	2
		-30.858			1
LEM	69 720201557.215125	15.6225586	.3735352	2.8125000	2
LEM	69 720201558.437125	15.605859	.3625488	2.7136230	2
		-9.1447998			1
LEM	69 720201559.215125	15.6555176	.4394531	2.5488281	2
LEM	69 7202016 .438125	15.5236816	.5273438	2.4060059	2
		-4.8480000			1
LEM	69 7202016 1.215125	15.4138184	.5822754	2.2192383	2
LEM	69 7202016 2.437125	15.4907227	.6591797	2.1093750	2
		-22.537			1
LEM	69 7202016 3.215125	15.4907227	.8129893	1.9006349	2
LEM	69 7202016 4.437125	15.4687500	.8789063	1.7468262	2
		-7.2127999			1
LEM	69 7202016 5.215125	15.6774902	1.0107422	1.5380859	2
LEM	69 7202016 6.496125	15.7653809	1.1425781	1.3952637	2
		-4.3631999			1
		15.7653809	1.3623047	1.1865234	2

D-18

LEM	69 7202016 7.215125	15.4797363	1.4062500	1.1755371	244.9331
LEM	69 7202016 8.496125	10.5468750	1.2414551	1.2524414	2
LEM	69 7202016 9.215125	9.3493652	1.2414551	1.2963867	1
LEM	69 720201626.195125	5.6689453	1.0546875	2.2412109	2
LEM	69 720201627.215125	5.5480957	.9558105	2.2521973	1
LEM	69 720201628.484125	-6.1823999	.9777832	2.3291016	2
LEM	69 720201629.215125	.9008789	.6042480	2.3620605	2
LEM	69 720201630.477125	359.2749023	.5932617	2.4499512	1
LEM	69 720201631.215125	359.2309570	.8459473	2.4829102	2
LEM	69 720201632.516125	359.7583008	2.1203613	2.6916504	1
LEM	69 720201633.215125	359.4726562	2.9003906	2.7905273	2
LEM	69 720201634.477125	-4.6367999	358.6047363	2.9333496	1
LEM	69 720201635.215125	359.7583008	3.1311035	2.9333496	2
LEM	69 720201636.477125	.0329590	.7272000	3.0541992	1
LEM	69 720201637.215125	359.7143555	3.1970215	3.1091309	2
LEM	69 720201638.445125	359.5605469	2.9882813	6.761	1
LEM	69 720201639.215125	.0219727	1.9665527	3.1420893	2
LEM	69 720201640.445125	-3.7352000	359.7912598	3.1530762	1
LEM	69 720201641.215125	.4614258	.6042480	3.2739258	2
LEM	69 720201642.484125	.0000000	.4943848	3.3178711	1
LEM	69 720201643.215125	3.0990234	.0020020	3.4606934	2

LEM	69 720201644.477125	3.3178711	.7690430	3.5705566	2
		2.6477051	.5163574	6.934	1
LEM	69 720201645.215125	2.6696777	.3845215	3.7133789	2
		-3.9927999		98.1891	
LEM	69 720201646.484125	3.0322266	.1538086	3.8122559	2
				1	
LEM	69 720201647.215125	2.9663086	359.5495605	3.9770508	2
			2.6664000	84.1621	
LEM	69 720201648.484125	3.4497070	358.2861328	4.1748047	2
				1	
LEM	69 720201649.215125	2.9223633	356.7810059	4.1748047	2
			7.281	86.9251	
LEM	69 720201650.477125	3.0871582	356.7810059	4.3835449	2
				1	
LEM	69 720201651.215125	5.3173828	356.8798828	4.6582031	2
		-1.2880000		1	
LEM	69 720201652.445125	5.0756836	356.7910922	4.8339844	2
				78.7671	
LEM	69 720201653.215125	4.7680664	356.8359375	4.9548340	2
			.0000000	1	
LEM	69 720201654.316125	4.6142578	356.7150979	5.1525879	2
				76.6091	
LEM	69 720201655.215125	4.4934082	356.4843750	5.2954102	2
			5.548	1	
LEM	69 720201656.387125	4.1748047	356.3635254	5.4162598	2
				77.6881	
LEM	69 720201657.215125	4.5373535	356.4074707	5.5920410	2
				55.0291	
LEM	69 7202017 7.215125	6.0534668	2.0983887	8.0310059	2
				1	
LEM	69 7202017 7.848125	6.0314941	2.2631836	8.1848145	2
				57.1871	
LEM	69 7202017 9.215125	4.1528320	1.8017578	8.6132813	2
		-1.5456700		1	
LEM	69 7202017 9.996125	1.4831543	1.5490723	8.8330078	2
				56.1481	
LEM	69 720201711.215125	354.9902344	.3405762	9.2504883	2
			-1.9392000	1	
LEM	69 720201712.176125	355.5944824	.5493164	9.6130371	2

LEM	69 720201713.215125	355.7502773	1.5490723	9.9865723	45.3181
LEM	69 720201714.437125	356.1437988	2.6257324	10.3710937	2
LEM	69 720201715.215125	356.8469238	2.9003906	10.6567383	1
LEM	69 720201716.477125	-2.4472000			2
LEM	69 720201717.215125	357.4291992	3.3268848	11.0632324	2
LEM	69 720201718.484125	357.4051172	3.5375977	11.2719727	34.5281
LEM	69 720201719.215125	358.2971191	3.7243652	11.6125488	2
LEM	69 720201720.324125	358.8354492	2.9663086	11.8103027	2
LEM	69 720201721.215125	358.7915039	1.1535645	12.0849609	1
LEM	69 720201722.324125	358.6926270	1.1315918	12.3706055	2
LEM	69 720201723.215125	-1.4168000	1.4721680	12.7770996	2
LEM	69 720201724.395125	1.7138672	.7141113	13.1066895	1
LEM	69 720201725.215125	2.1093750	11.8775998		2
LEM	69 720201726.324125	3.1420898	.1428223	13.4912109	2
LEM	69 720201727.215125	2.6586914	358.8024902	13.7988281	22.6591
LEM	69 720201728.316125	.9016000		15.429	1
LEM	69 720201729.215125	2.9333496	357.2863770	14.1613770	2
LEM	69 720201730.336125	3.0651855	357.3413086	14.2163086	22.6591
LEM	69 720201731.215125	.9016000		14.2712402	2
LEM	69 720201732.324125	3.5815430	355.5285645	14.3481445	1
LEM	69 720201733.215125	-7.2720000			2
LEM	69 720201734.336125	4.6472168	355.9240723	14.5019531	2
LEM	69 720201735.215125	4.8999023	356.0339355	14.5788574	24.8171
LEM	69 720201736.324125	5.3833008	356.1437988	14.7216797	1
LEM	69 720201737.316125				2
LEM	69 720201738.215125				29.1331

LEM	69	720201734.316125	5.5151367	356.2866211	14.8205566	2
			7.5991999			1
			5.2075195	356.4514160	14.8205566	2
LEM	69	720201735.215125	4.7680664	356.5502930	14.8095703	2
			-9.6960000			1
LEM	69	720201736.324125	4.3615723	358.1323242	14.9084473	2
LEM	69	720201737.215125	3.5046387	359.9230957	15.0952149	2
LEM	69	720201738.348125	1.5710449	.4504395	15.6225586	2
LEM	69	720201739.215125	.3515625	2.6037598	15.6555176	2
LEM	69	720201740.387125	.5152000			1
			4.5483399	.5053711	14.0185547	2